Microwave Electronics

DEVELOPMENT AND ANALYSIS OF A COMPACT COPLANAR ANTENNA WITH FLARED MONOPOLE FOR DUAL BAND APPLICATIONS

A thesis submitted by

GIJO AUGUSTIN

in partial fulfillment of the requirements for the degree of

DOCTOR OF PHILOSOPHY

Under the guidance of

Prof. K. Vasudevan

**DEPARTMENT OF ELECTRONICS
FACULTY OF TECHNOLOGY
COCHIN UNIVERSTIY OF SCIENCE AND TECHNOLOGY
COCHIN-22, INDIA**

JANUARY 2009

Dedicated

to

The Almighty

CERTIFICATE

Certified that this thesis entitled **"DEVELOPMENT AND ANALYSIS OF A COMPACT COPLANAR ANTENNA WITH FLARED MONOPOLE FOR DUAL BAND APPLICATIONS"** is a bona fide record of the research work carried by Mr. Gijo Augustin under my supervision in the Centre for Research in ElectroMagnetics and Antennas, Department of Electronics, Cochin University of Science and Technology. The results presented in this thesis or parts of it have not been presented for the award of any other degree.

Cochin - 22   **Dr. K. Vasudevan**
26th January 2009   Supervising Teacher.

DECLARATION

I hereby declare that the work presented in this thesis entitled "Development and analysis of a compact coplanar antenna with flared monopole for dual band applications" is a bona fide record of the research work done by me under the supervision of Prof. K. Vasudevan, Department of Electronics, Cochin University of Science and Technology, India and that no part there of has been presented for the award of any other degree.

Cochin-22   GIJO AUGUSTIN
26th January 2009

Acknowledgement

CONTENTS

Chapter 4

Development of a Flared Monopole Antenna from the Coplanar Waveguide Fed Strip Monopole 85

Development of a Flared Monopole Antenna with V-Shaped Element for Dual Band Applications 117

Chapter **6**

INTRODUCTION

"The Antenna serves to a communication system the same purpose that eyes and eyeglasses serve to a Human"

- Constantine A Balanis

Wireless communication is the fastest growing field of technology which has captured the attention of social life in the present century. Modern wireless local area networks are implemented in many homes, business centres and campuses which focus many applications including wireless sensor networks, automated highways and factories. The cellular systems have experienced exponential growth over the last decade and there are currently around two billion users worldwide. The explosive growth of wireless systems coupled with the development of laptop and palmtop computers indicates a bright future for wireless networks, both as stand-alone systems and as part of the larger networking infrastructure. For the successful implementation of any wireless communication system, the antenna technology plays one of the important role. A good design of the antenna can reduce the system requirements and improve the overall system performance.

This chapter provides history of wireless communication with a special attention towards the development of modern antenna technology. The descriptions in this chapter include the classification of antennas in general, advances in printed antenna technology, a brief description about CAD packages for antenna research. This chapter concludes with the motivation of the work along with the thesis organization.

1.1 A short History of wireless communication

The history of wireless communication starts with the prediction of James Clerk Maxwell about the existence of Electromagnetic waves in 1873[1]. He postulated that light is electromagnetic in nature and that electromagnetic radiation of other wavelengths should be possible. In 1888, the physical existence of these waves was demonstrated by Heinrich Hertz with the help of first spark-gap generator

In 1896 Guglielmo Marconi demonstrated wireless telegraph to English telegraph office [2]. In the preceding years, 1894-1900, J.C. Bose performed research with electromagnetic waves with the first Horn antenna [3]. During the year 1901, Guglielmo Marconi opened the way for modern wireless communications by transmitting the three dot morse code for the letter 'S' over a distance of three kilometres[4]. The transmitting antenna used in this experiment consists of 50 vertical wires in the form of a fan connected to ground through a spark transmitter. The receiving antenna was a 200m wire pulled and supported by a kite. This was the beginning of antenna era. The shortwave radio is developed during 1921 which enabled radio transmission to the other side of the world[5]. During 1933 Edwin Armstrong demonstrates frequency modulation (FM) to David Sarnoff and in 1940, Daniel Noble, a professor of electrical engineering at the University of Connecticut, designed an FM mobile-radio system for the State Police[6]. FM is a key to the transmission of digital information carried over RF. In 1982 Global System for Mobiles(GSM) group is formed which laid the foundation of the modern wireless mobile networks. The demonstration of L band digital radio and the release of first GSM specification were the key events in wireless communication history in the beginning of the 19th century. The first GSM call is made in the year 1991 in Finland and six years later the IEEE

802.11 standard also known as Wi-Fi was created[7]. In the preceding year Bluetooth Special interest group was formed and the first Bluetooth product was released by Ericcson in the year 2000[8]. It was a wireless headset and phone adapter meant for cell phones. During July 2005 iFiber Wire Linked two points which are apart by 125 mile using standard 802.11b routers while not amplifying the signal. The wireless communication research is now progressing rapidly which enabled easy of communication for the Mankind. Wireless technology is creating a huge appeal for sophisticated voice and data services such as Wi-Fi, 3G, in addition to GSM, CDMA and UMTS.[9]. An overview of the frequency band allocated for modern wireless communication standards are summarized in Table 1.1

System	Description	Frequency Band
GSM-900	Global System for mobile communication	880-960 MHz
GPS	Global Position Systems	1208 - 1248 MHz 1556 – 1595 MHz
DCS-1800	Digital Communication System	1710-1795 MHz
PCS-1900	Personal Communication System	1850-1990 MHz
PHS	Personal Handy-Phone Systems	1905-1920 MHz
UMTS	Universal Mobile Telecommunications Systems	1920-2170 MHz
Wi-Bro	Wireless Broadband	2300-2390 MHz
ISM	Industrial, Scientific and Medical	2400-2484 MHz 5150-5350 MHz 5725-5825 MHz
DVB-H	Digital Video Broadcasting	470-890 MHz
RFID	Radio Frequency Identification Systems	30 – 2400 MHz
UWB	Ultra Wide Band	3100 -10600 MHz

Table 1.1 Frequency band allocations

1.2 Timelines in Communications History

Wireless communication history [10] is summarized in the Table 1.2,

1865	Prediction of electromagnetic wave propagation by Maxwell
1887	Heinrich Hertz proved the existence of electromagnetic waves
1895	5 – 6mm wavelength transmission from J.C. Bose
1901	Guglielmo Marconi sends first wireless signals
1905	Marconi Patents his directive horizontal antenna.
1906	First Radio Broadcasting by Fessenden.
1914	Production of 170KHz radio by AT&T company
1924	Directive short wave antenna is developed by Prof.Hidetsugu Yagi
1929	600 MHz radio link in Italy by Marconi
1933	FM technique developed by Armstrong
1934	AM mobile communication systems implemented
1935	Invention of Radar by Watson Watt
1943	Digital Modulation and Transmission
1968	Development of a Cellular Telephone
1981	First Cellular mobile telephone is offered
1982	Color two way video teleconferencing service is offered
1986	Integrated Service Digital Network is
1995	CDMA is introduced
2000	3G standard finalized

Table 1.2 Milestones in communication History

1.3 The role of Antennas in wireless communication systems

Antenna serves as one of the critical component in any wireless communication system. In general, the antenna behaves as a transducer between guided wave and a free space. The IEEE standard Definition of terms for Antennas defines the antenna or aerial as "a means for radiating or receiving radio waves"[11]. All antennas operate on the same basic principles of electromagnetic theory. The word antenna is derived from the Latin word *antemna* which became, in Latin language, antenna. The term antenna was first used by Marconi in a lecture in 1909[12].

The evolution of antennas begins, soon after James Clerk Maxwell unified the theories of electricity and magnetism. In nineteen forty antenna technology was primarily related on wire type radiating elements which operates in frequencies up to about in UHF. The II World War launched a new era in modern antenna technology with elements such as waveguide, apertures horn antennas and reflectors [13]. The invention of microwave sources such as klystron and magnetron accelerated this new era of microwave communication.

The II World War also made developments in computer architecture and technology and it has a major impact on the advance of modern antenna technology. The numerical methods were introduced that allowed ease of analysis for complex antenna systems [14].

In the middle years of nineteenth century, antenna technology witnessed drastic improvement in its impedance bandwidth as great as 40:1 or more. These wideband antennas had the geometries specified by angles instead of linear dimensions and they are referred to as frequency independent antennas.

The major applications of these wideband antennas include TV reception, point to point communication, and feed for reflects and lenses.

Roughly 20 years later, a new radiating element, patch antenna, was introduced which find many applications with much ease of fabrication compared to the earlier antenna designs. These antennas can provide easy integration with active components and various antenna characteristics such as gain, radiation pattern etc can be controlled electronically. Major advances in millimetre wave antennas have been made in recent years including integrated antennas where active and passive circuits are combined with the radiating elements in one compact unit. Smart antennas, also known as adaptive arrays, were introduced during the recent years which incorporate signal processing algorithms embedded with the antennas. These antennas provide easy integration with the advanced digital systems [15].

1.4 Antenna Classification in General

A broad classification of Antennas are (1) Wire Antennas (2) Aperture Antennas (3) Array antennas (4) Reflector antennas (5) Lens Antennas (6) Printed Antennas.

The wire antennas are very common in nature and are seen in auto mobiles, buildings, ships, and aircraft and so on. This broad category includes classical antenna type's dipole, loop and helix. The circular loop is more common because of its simple constriction. Aperture antenna are very useful for aircraft and space craft applications because they can be flush mounted on the skin of large spacecrafts. Horn antenna is a classical example for aperture antenna. Many applications require radiation characteristics that may not be possible with a single antenna element but in such cases an array of

antennas results the desired radiation behaviour. A broad classification of classical antennas are depicted in Fig.1.1
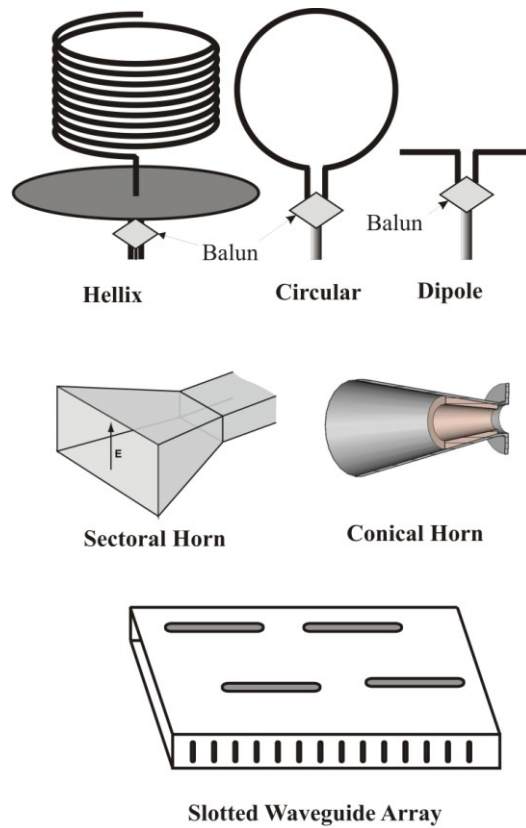
Fig.1.1: A Broad Classification of Antennas

Recent developments in array antennas [16,17,18] include adaptive arrays that are capable of beam forming. Reflector antennas are commonly used to commutate over great distances. A very common antenna form for communication over millions of miles is a parabolic reflector antenna. Antennas of this type are built with diameter as large as 300 m. Lens antennas are used to collimate incident energy by using geometrical configuration of appropriate material. They can be used in most of the applications like that of parabolic reflectors, especially at higher frequencies. As the name implies,

printed antennas are simple and inexpensive to fabricate using modern printed circuit technology. They are low profile and conformable to planar and non planar surfaces and compatible with MMIC designs. One among the most popular printed antenna is Microstrip patch antenna.

1.5 Planar Antennas

Rapid developments in wireless communication systems resulted in drastic growth of compact handheld devices such as mobile phones and PDAs. [19, 20] In order to meet the miniaturization requirements, the antennas employed in communication terminals must be compact antenna such as microstrip patches and printed monopoles. Printed antennas are very attractive for applications in communication devices such as wireless local area networks (WLAN). They can be easily integrated on the circuit board of a communication device to reduce the packaging cost.

The origin of printed antennas begins from the use of planar microwave technologies such as microstrip, slot lines, coplanar lines, etc.[21, 22]Even though, the possibility of radiation from these printed structures was suggested as early as 1950, the first practical printed antenna appeared in the mid- nineteen seventies. These antennas were fabricated with printed circuit technology, and the miniaturization trend started. The different types of printed antennas are listed in the following sessions. The printed antennas have the key features such as,

- Light weight and small overall dimensions.
- Ease of fabrication using printed circuit technology
- Easy integration with electronic components
- Integrable to array systems.

And one of the important drawbacks of these antennas is its degradation of efficiency due to the dielectric loss.

1.5.1 Microstrip Antenna

In its simplest form, a Microstrip patch antenna consists of a radiating patch on one side of a dielectric substrate, which has a ground plane on the other side as shown in Fig.1.2
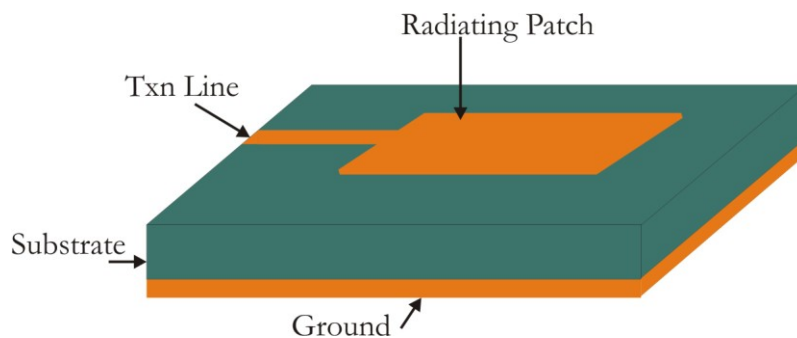
Fig.1.2 The basic geometry of microstrip radiator.

This patch is fed with a microstrip transmission line. The patch will radiate effectively if the length of the patch is typically about a half guide-wavelength in size. This radiation arises from the fringing of electromagnetic fields between the patch edge and the ground plane. These fringing region act as a small two- element array and give rise to small degree of directivity seen with microstrip patches.

Microstrip patch antennas are increasing in popularity for use in many modern systems because of

- Light weight and low volume.
- Low profile planar configuration which can be easily made conformal to host surface.
- Low fabrication cost, hence can be manufactured in large quantities.

- Supports both, linear as well as circular polarization.

- Can be easily integrated with microwave integrated circuits (MICs).

- Capable of dual and triple frequency operations.

- Mechanically robust when mounted on rigid surfaces.

Microstrip patch antennas suffer from a number of disadvantages as compared to conventional antennas. Following are few of them,

- Narrow bandwidth

- Low efficiency

- Low Gain

- Extraneous radiation from feeds and junctions

- Poor end fire radiator except tapered slot antennas

- Low power handling capacity.

- Surface wave excitation

The large antenna quality factor (Q) of the microstrip antenna leads to narrow bandwidth and low efficiency. Q can be reduced by increasing the thickness of the dielectric substrate. But as the thickness increases, an increasing fraction of the total power delivered by the source goes into a surface wave. This surface wave contribution can be counted as an unwanted power loss since it is ultimately scattered at the dielectric bends and causes degradation of the antenna characteristics [23].

The shape of the patch is not restricted to rectangles. The patch is generally square, rectangular, circular, triangular and elliptical or some other common shape as shown in Fig.1.3
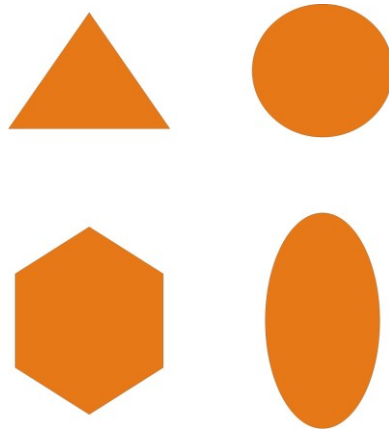
Fig. 1.3 Various radiator patch geometries for the microstrip Antenna.

1.5.2 Planar inverted F antenna

As the name implies, the planar inverted F antenna is distinguished by the loop formed by the short right angle elements of the letter 'F'[24] as shown in the Fig.1.4
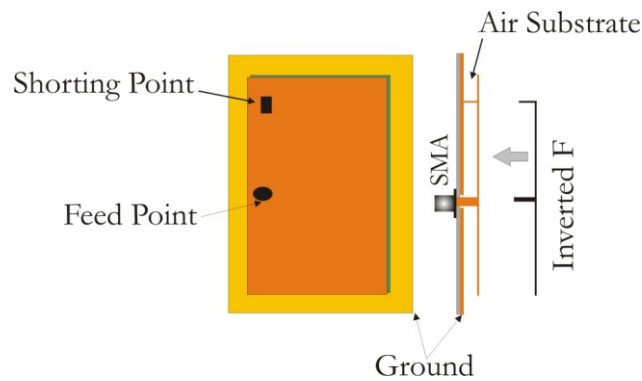
Fig. 1.4 Inverted 'F' Antenna Geometry.

Basically the Inverted F Antenna is a type of monopole in which the top section is folded down so as to be in parallel with the ground plane. They typically consist of a rectangular planar element with a ground plane and a feeding mechanism with a short circuiting plate or pin.

Planar Inverted F-Antennas(PIFA) are good candidates as internal antennas and they have important features like compactness, good bandwidth, moderate gain and are less prone for breakage. The Planar inverted F antennas are famous for multiband applications in handheld devices such as mobile handsets, notebook PCs, PDAs. This intern results reduction in the height of the antenna while maintaining the resonant length.

1.5.3 Planar monopole/dipole antennas.

Planar monopole antennas are popular for their large bandwidth, moderate gain with nearly onmidirectional radiation characteristics and are attractive for wireless communication applications[25,26]. The major limitations of these antennas are the ground plane size and orientation of the radiator. The geometry of a monopole antenna is depicted in fig.1.5
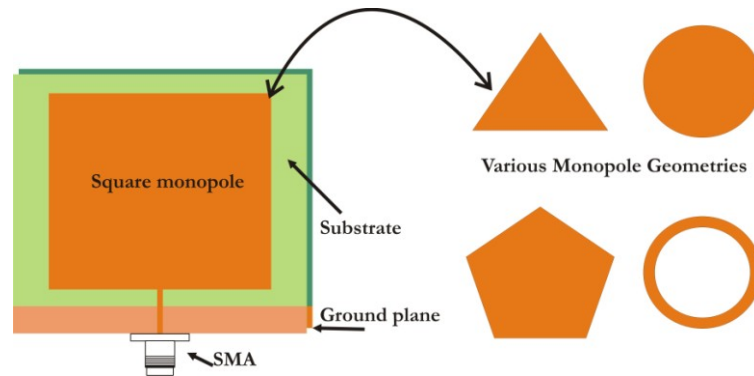
Fig.1.5 Printed Square Monopole Antenna.

Generally, a monopole antenna consists of a thin vertical wire mounted over the ground plane, whose bandwidth increases with increase in its diameter [27]. A planar monopole antenna can be treated as a cylindrical monopole antenna with large effective diameter.

A printed dipole antenna is the most popular element for the base station antennas of the cellular system because a half wave length dipole antenna has a wide frequency bandwidth, more than 15 % for VSWR less than 2. Printed dipole antenna is also used as the feeding source of aperture antenna. The printed dipole antenna has many advantages like planar structure, small volume, light weight and low cost.

1.6 Excitation Techniques for printed antennas

The printed monopole antennas can be fed by different methods. The popular feed techniques used are the coaxial probe, microstrip line and coplanar feed line. [28]

In the case of a coaxial probe feed, the inner conductor of the coaxial connector is soldered to the radiating monopole, while the outer conductor is grounded. In this case the entire system is not planar in nature since the radiating structure is perpendicular to the ground plane.

In microstrip line feed technique the feed line is directly connected to the edge of the monopole –radiator shown in Fig 1.6 Here the patch and the feed line are etched on the same substrate to provide a planar structure. It provides easy integration with RF circuit boards but, creates spurious feed radiation.
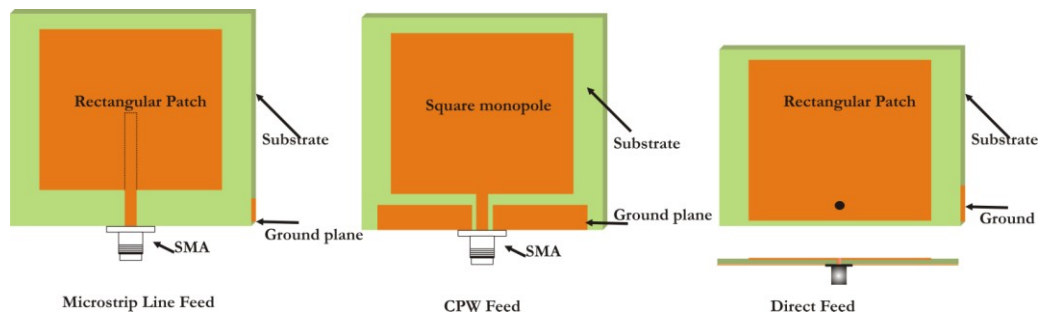
Fig.1.6 Different Feeding Techniques

1.7 Coplanar wave guide and its application in antennas

The coplanar waveguide was invented by C.P. Wen in 1969[29]. A conventional CPW consists of a centre strip conductor with semi-infinite ground planes on either side on a dielectric substrate. Compared to a microstrip line the CPW provides many advantages like simplicity in fabrication, easy shunt as well as series surface mounting of active and passive devices, eliminating the need for wraparound and via holes [30], and reduction in radiation loss[31]. In addition the ratio of a/b determines the characteristic impedance so size reduction is possible. Moreover a ground plane exists between any two adjacent lines; hence cross talk effects between adjacent lines are very week [32,33]. Therefore, CPW circuits can be made denser than conventional microstrip circuits. These, as well as several other advantages, make CPW ideally suited for MIC as well as MMIC applications.

1.7.1 TYPES OF COPLANAR WAVEGUIDES

Generally coplanar waveguides can be classified as,

(1) Conventional CPW
(2) Conductor backed CPW
(3) Micro-machined CPW

In a conventional CPW, the ground planes are of semi-infinite extent on either side. However, in a practical circuit the ground planes are made of finite extent. The conductor-backed CPW has an additional ground plane at the bottom surface of the substrate. This lower ground plane provides mechanical support to the substrate and acts as a heat sink for circuits with active devices. A conductor backed CPW is shown in Fig.1.7
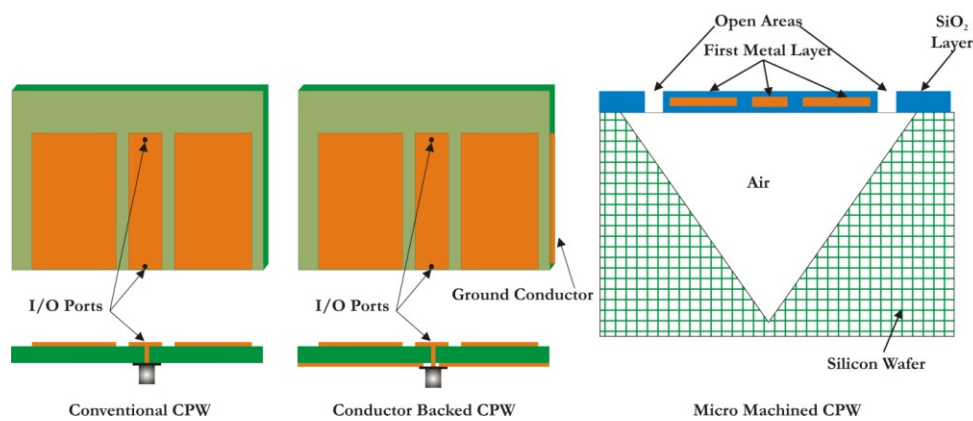
Fig.1.7 Different types of CPW Configurations.

The micro machined CPWs are of two types, namely, the micro shield line [34, 35] and the CPW suspended by a silicon dioxide membrane above a micro machined groove[36,37]

1.7.2 Coplanar wave guide antennas

Nowadays Coplanar Wave guide fed monopoles are increasingly popular for dual band and wideband applications due to their attractive features such as low radiation loss, less dispersion, wide bandwidth, simple uni-planar structure and easy integration with active devices without via holes. Recently asymmetric coplanar strip line and slot line are also used to feed the monopole antenna. The main advantage of using coplanar waveguide in the feed includes the capability of CPW to mount components without via holes.

At the same time it helps integration of MMIC circuits such as phase shifters using solder bumps and flip chip techniques.

Broadly we can classify the CPW antennas to (1) Grounded Coplanar Waveguide Patch Antennas. (2) Electromagnetically Coupled Coplanar Fed Antenna and (3) Aperture Coupled Patch Antenna. In grounded coplanar waveguide patch antenna, the patch is formed by widening the center strip conductor of the CPW. The outer conductor of the connector is integrated to the grounded CPW lower ground plane and this results the launcher efficiently provide transition from Co-axial to grounded CPW[38]. In the case of Electromagnetically coupled CPW feed, the CPW and the patch antenna are located on opposite sides of a dielectric substrate [39,40] and the electromagnetic energy from the CPW is coupled to the patch antenna. The aperture coupled CPW patch antenna [41] consists of patch and grounded CPW feed structure with a gap in the conductor and are fabricated on separate substrates and the aperture is etched in the common ground plane.

1.8 Design concepts – Printed Monopoles.

There are a number of printed monopole antenna designs can be find in the present literature ranging from single band monopoles, multiband monopoles and ultra wideband antennas. The very basic design is in the form of a straight metallic conductor usually operated with one-quarter wavelength. But this design results large antenna height and it is impossible to integrate such an antenna in a compact communication gadget such as mobile phone. In order to reduce the height of the monopole a number of techniques such as bending, folding or wrapping [42, 43, 44] two-dimensional planar monopoles to three-dimensional structures. These techniques reduce the total antenna height up to a large extent. Few typical designs are shown in the fig.1.8
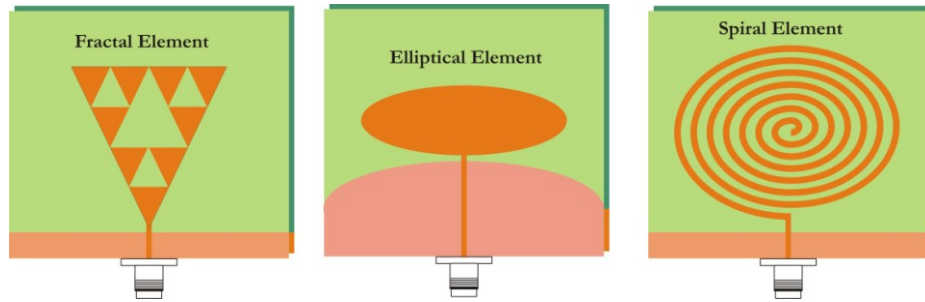
Fig.1.8 Different Printed Monopole antenna designs.

Most of the multiband techniques used in the printed monopoles are the excitation of two or more modes with different current paths. These techniques includes, loading a meandered wire, which is generating the 900MHz resonance, to an inverter-L geometry with resonance at 1.8GHz[45,46].

1.9 Challenges in Antenna Design

The modern wireless communication industry is advancing rapidly that all the communication systems are integrating many applications such as WLAN, Bluetooth etc to the hand held devices. In the near future, most of the wireless protocols will be employed in the mobile devices. Antenna isolation is very difficult problem to solve because of close proximity between antennas in space limited devices particularly in MIMO devices.

Another challenge is small space available in most of the mobile devices. In order to overcome this challenge, we need multiband designs with consistent radiation pattern, efficiency and polarization over the wide frequency band. Generally, most of the multiband antennas meet the return loss requirements, but the radiation performance is degrading at upper frequencies. Electronically tunable antennas are potential solution for few cases such as DVB-H.

Antenna planning and placement is another challenge, which help to select and place the antenna efficiently in a system by considering both electrical and mechanical requirements. For example the UWB antennas used for short range applications will not be highly efficient like WiMax and WLAN antennas and they can be fabricated as a low-efficient chip antenna. The WiMax and WLAN antennas should provide much higher efficiency since they have long range application and in most of the cases they are used to get certification from the carrier. In the case of GPS antenna circular polarization is desired. In the case of DVB-H a narrow band antenna with tuner element will be a good selection since we do not watch every TV channels at the same time.

The miniaturization of the handheld communication devices demands small antennas with stringent specifications in bandwidth, pattern characteristics including polarization, less sensitivity to the environment etc. The miniaturization has theoretical limitations to the achievable gain and efficiency of the radiator.

Ground plane of the antenna plays an important role in its design. The ground plane is generally symbolised as the return path for the current in the patch. Conventional antenna design uses image technique to provide the infinite ground plane. This theory is not possible while designing electrically small ground plane antennas. In the case of whip antennas, the ground plane can be treated as the other half of the dipole to the antenna. The characteristics of small antennas mounted on the handheld devices get affected by the antenna position on the terminal chassis and the dimensions of the chassis due to the existence of radiating surface currents on the terminal ground plane induced by the antenna element. All these factors make the design of an antenna with less ground plane effect, a major challenge.

In the case of large antennas, the challenges in design are mainly to realize ultra-low side-lobes, reduce Electromagnetic Interference. The modelling of the large antennas to predict its performance is another difficult task. Currently, commercial software's are quite limited in their ability to handle the structures which require a problem description with a very large number of meshes because of their complexity, multi-scale characteristics and homogeneous nature.

1.10   Motivation of present research

Multiband Printed Monopole antennas have aroused widespread applications, especially in low power wireless communication gadgets. In the era of modern wireless communication systems, multiband antennas with omni-directional radiation characteristics play a vital role. The Ultra wideband antenna can attain broad bandwidth and is a good candidate for wideband applications. But the use of UWB antenna for narrowband applications results out-of-band spurious emission in the transmission mode. Therefore, for narrow band applications in multiple frequencies, multiband antenna is preferably an excellent choice. Moreover, multiband antenna can sustain reasonable gain and stable radiation pattern throughout the application band.

The key idea behind the work presented in this thesis is that by flaring the strip monopole fed by coplanar waveguide results resonance at a low frequency region compared to the strip monopole antenna and by loading the strip monopole with a 'v' shaped element results a new resonance at a high frequency region. The position of the 'v' shaped element is very critical to achieve the desired performance. The compact dual band monopole antenna thus obtained meets all criteria required to use in modern wireless gadget applications as an internal antenna. The optimized ground plane required for the antenna is very small.

1.11 Organization of the Thesis

Chapter 1 presents the introduction of the research topic by describing an overview of antenna research, classical antennas like printed monopoles and other planar antennas and important feeding techniques for printed antennas. The motivation of the work is also included in this introductory chapter.

Chapter 2 provides review of literatures concerning the present work. Recent developments in the field of printed antennas like monopole antennas and other broadband and dual band antennas, modified coplanar waveguide antennas and important feeding techniques are referred in detail. The printed uniplanar antennas are promising candidates for modern wireless communication systems due to their low profile, light weight and nearly omni-directional radiation characteristics. Finally, an overview of the progress in Numerical Analysis using FDTD is also referred.

Chapter 3 covers the experimental and theoretical analysis methodology employed for the characterization of the antenna. Simulation and parametric analysis using commercial package Ansoft-HFSS is incorporated. Theoretical modeling of the antenna using FDTD technique is also included.

In Chapter 4 the experimental and theoretical analysis of the flared strip monopole antenna is discussed in detail. The development of flared monopole antenna from the coplanar waveguide fed strip monopole is depicted first. Parametric analysis of various antenna elements and the conclusions derived from the studies are also included.

In chapter 5, experimental as well as theoretical results are outlined. The conventional Finite ground coplanar waveguide is modified to form a dual band efficient radiator. The Characterization of a Finite Ground Coplanar waveguide fed flared monopole antenna and the integration of an additional element for dual

band performance without affecting the first resonant band is illustrated. The major part of this chapter includes the effect of ground plane parameters and parametric analysis of the antenna.

Chapter 6 is the concluding section of this Thesis. It describes important inferences based on results and salient features of the proposed dual band antenna and its applications. The scope of future work is also discussed in this chapter.

Appendix 'A' provides a strip monopole fed triangular patch antenna for wireless access point.

A microstrip leaky-wave antenna for low cost beam steering applications is provided in Appendix B.

Appendix C presents a novel electronically scannable log-periodic leaky wave antenna.

References

[1] J.C Maxwell, "A Treatise on Electricity and Magnetism". London, England: Oxford University Press, 1873, 1904.

[2] W.J.G Beynon," Marconi, radio waves and the ionosphere", radio science, vol.10, no.7, pp 657-664, July 1975.

[3] John D. Kraus, "Antennas since Hertz and Marconi", IEEE Trans. Antennas and Propagat. vol.33, no.2, pp 131-136, February 1985.

[4] Garratt, G.R.M. The Early History of Radio from Faraday to Marconi (London: Institution of Electrical Engineers, 1994).

[5] "Events in Telecommunications History", AT&T Archives, 1992

[6] The Story of Telecommunications, George P. Oslin, Mercer University Press, 1992.

[7] Blake, G. G. History of Radio Telegraphy and Telephony. London: Chapman & Hall, 1928 (reprinted by Arno Press, 1974).

[8] Bowers, Raymond, Alfred M. Lee, and Cary Hershey. Communications for a Mobile Society: An Assessment of New Technology. Beverly Hills, CA: Sage Publications, 1978.

[9] Modern Wireless Communications, Simon Haykin, Michael Moher, Prentice Hall, 2005.

[10] IEEE "Timeline of Milestones in Communications history" http://www.ieee.org/web/aboutus/history_center/conferences/comsoc/1940.html

[11] IEEE standard definitions of terms for antennas, IEEE Std 145-1983, June 1983.

[12] Garratt, G.R.M. The Early History of Radio from Faraday to Marconi (London: Institution of Electrical Engineers, 1994).

[13] Sterling, Christopher and George Shiers (Eds). History of Telecommunications Technology: An Annotated Bibliography (Lanham, MD: Scarecrow, 2000).

[14] Branko M. Kolundzija and Antonije R. Djordjevic, "Electromagnetic modeling of composite metallic and dielectric structures," Artechhouse, Inc., Norwood, MA, 2002.

[15] History of Wireless, Tapan K. Sarkar ,Wiley-IEEE Press, 2006.

[16] Chen, W.H.; Sun, J.W.; Wang, X.; Feng, Z.H.; Chen, F.L.; Furuya, Y.; Kuramoto, A., "A Novel Planar Switched Parasitic Array Antenna With Steered Conical Pattern", IEEE Transactions on Antennas and Propagation, Vol. 55, pp.1883-1887, 2007.

[17] Kin-Lu Wong; Fu-Ren Hsiao; Tzung-Wern Chiou, Omnidirectional planar dipole array antenna, IEE Transactions on Antennas and Propagation, Vol.52, pp. 624-628, 2004

[18]Keizer, W.P.M.N., " Fast Low-Sidelobe Synthesis for Large Planar Array Antennas Utilizing Successive Fast Fourier Transforms of the Array Factor", IEE E Transactions on Antennas and Propagation, Vol.55, pp. 715-722, 2007.

[19] Frigon, J.-F.; Eltawil, A.M.; Grayver, E.; Tarighat, A.; Zou, H., Design and Implementation of a Baseband WCDMA Dual-Antenna Mobile Terminal, IEEE Circuits and Systems Transactions, Vol.54, pp.518-529, 2007.

[20] Row, J.-S., Dual-frequency triangular planar inverted-F antenna, IEEE Transactions on Antennas and propagation, Vol.53, pp.874-876, 2005.

[21] J.R. James and P.S. hall, "Handbook of microstrip antennas-vol.1", edited , peter Peregrinus Ltd., U.K.

[22] David M.Pozar, "Microstrip Antennas", Proc. IEEE, Vol.80, No.1, pp.79-91, January 1992.

[23] Kin-Lu Wong, "Planar Antennas for Wireless Communications", John Wiley and Sons, 2002.

[24] Zhi Ning Chen and Michael Yan Wah Chia, Broadband Planar Antennas: Design and Applications, John Wiley and Sons, 2006.

[25] Kuo, J.-S.; Huang, C.-Y., Triple-frequency planar monopole antenna for side-feed communication device on GSM/DCS/PCS operation, IEE Electronics Letters, Vol.42, pp. 268-270, 2006.

[26] Liang, X.-L.; Zhong, S.-S.; Wang, W., Elliptical planar monopole antenna with extremely wide bandwidth, IEE Electronics Letters, Vol.42, No.8, pp.441-442, 2006

[27] Constantine A Balanis, Antenna Theory Analysis and Design, John Wiley & Sons, 2005

[28] Rainee N. Simons, Coplanar Waveguide Circuits, Components, and Systems, Wiley-Interscience, 2001.

[29] C. P. Wen,"Coplanar Waveguide: A Surface Strip Transmission Line Suitable for Nonreciprocal Gyromagnetic Device Applications," IEEE Trans. Microwave Theory Tech.,Vol. 17, No. 12, pp. 1087—1090, 1969.

[30] J. Browne, "Coplanar Circuits Arm Limiting Amp with 100-dB Gain," Microwaves RF, Vol. 29, No. 4, pp. 213—220, April 1990.

[31] J. Browne, "Coplanar Waveguide Supports Integrated Multiplier Systems," Microwaves RF, Vol. 28, No. 3, pp.137—138, March 1989.

[32] Technology Close-Up, Microwaves RF, Vol. 27, No. 4, p. 79, April 1988.

[33] J. Browne, "Broadband Amps Sport Coplanar Waveguide," Microwaves RF, Vol. 26, No. 2, pp. 131—134, Feb. 1987.

[34] J. Browne, "Broadband Amp Drops through Noise Floor," Microwaves RF, Vol. 31, No. 2, pp. 141—144, Feb. 1992.

[35] V. Milanovic, M. Gaitan, E. D. Bowen, and M. E. Zaghloul, Micromachined Microwave Transmission Lines in CMOSTechnology," IEEE Trans. Microwave T heory Tech., Vol. 45, No. 5, pp. 630—635, May 1997.

[36] J. Browne, "Coplanar MIC Amplifier Bridges 0.5 To 18.0 GHz," Microwaves RF, Vol. 26, No. 6, pp. 194—195, June 1987.

[37] T. M. Weller, L. P. B. Katehi, and G. M. Rebeiz, "High Performance Microshield Line Components," IEEE Trans. Microwave T heory Tech., Vol. 43, No. 3, pp.534—543, March 1995.

[38] J. W. Greiser, "Coplanar Stripline Antenna," Microwave J., Vol. 19, No. 10, pp. 47—49, October 1976.

[39] W. Menzel and W. Grabherr, "A Microstrip Patch Antenna with Coplanar Feed Line," IEEE Microwave and Guided Wave L ett., Vol. 1, No. 11, pp. 340—342, November 1991.

[40] L. Giauffret and J.-M. Laheurte, "Parameteric Study of the Coupling Aperture in CPW-Fed Microstrip Antennas," IEE Proc. Microw. Antennas Propag., Vol. 146, No. 3, pp. 169—174, June 1999.

[41] R. Q. Lee and R. N. Simons, "Coplanar Waveguide Aperture-Coupled Microstrip Patch Antenna," IEEE Microwave and Guided Wave L ett., Vol. 2, No. 4, pp. 138—139, April 1992.

[42] Seong-Youp Suh; Stutzman, W.L.; Davis, W.A., "A new ultrawideband printed monopole antenna: the planar inverted cone antenna (PICA)", IEEE Transactions on Antennas and Propagation, Vol.52, No.5, pp.1361-1364, 2004.

[43] I-Fong Chen; Chia-Mei Peng, "Microstrip-fed dual-U-shaped printed monopole antenna for dual-band wireless communication applications", Electronics Letters, Vol.39, No.13, pp.955-956, 2003.

[44] Hanhua Yang, Shu Yan, "A novel P-shaped printed monopole antenna for RFID applications" ,Microwave and Optical Technology Letters, Vol.51, No.2, pp.554-556, 2009.

[45] Wen-Shan Chen, Yu-Chen Chang, "CPW-fed printed monopole antenna with branch slits for WiMAX applications", Microwave and Optical Technology Letters, Vol.50, No.4, pp.952-954, 2008

[46] Shun-Yun Lin, Kuang-Chih Huang , "Printed pentagon monopole antenna with a band-notched function", Microwave and Optical Technology Letters, Vol. 48, No. 10,pp. 2016-2018, 2006.

Literature Review

This chapter provides a brief review of the past work in the Antenna field. The theoretical and experimental work in different types of printed antennas around the world is illustrated. The first section briefly describes various developments in the printed antenna technology with emphasis to printed monopole antennas. The second section deals with recent trends in dual band printed monopole antenna design while the third part describes various CPW antenna designs employed recently in modern communication and military systems. This chapter also illustrates analytical and full wave solutions of monopole antennas with special emphasis on Finite difference time domain(FDTD) analysis of various antennas.

2.1 Recent developments in Printed Antenna Technologies.

The present research in printed antenna technology points to the development of antennas which cater the need of low profile, compact communication gadgets. The antenna designers around the world are concentrated in the design of compact antennas with efficient radiation characteristics. The following modules provide a comprehensive survey about the developments in the state of art printed antenna technology around the world.

L.Economou et al. presents circular microstrip patch antennas on glass for vehicle applications[1].Circular patches printed on RT Duroid were used, with glass laminated superstrates which excited surface waves of between 10% and 20% of the input power. Patches and microwave circuits within the glass laminate will introduce even more uncertainty into the resonant frequency and bandwidth. Overall, this could be a significant problem for microstrip antennas on automotive glass where communication bands demand bandwidths of 5% and above. Dual-frequency planar antenna for handsets is presented by Chiba et al.[2].The proposed dual-band antenna consists of an outer quarter-wavelength annular-ring with a short-circuited plane for a low resonance frequency, and an inner quarter-wave length rectangular patch for a high resonance frequency inside the outer antenna. This dual-band antenna, with omnidirectional radiation patterns is suitable for both cellular and personal communication systems.

A quarter-wavelength diversity patch configuration for the 2.4-GHz ISM band PC card application is presented by Laurent Desclos et al.[3]. The structure is based on partly interdigitation of two quarter wavelength separated patches through a set of fingers for achieving the required space diversity on single side printed substrate with good impedance matching and high cross polarization. This antenna has been incorporated in a high-speed wireless LAN PC card system. A Wide-Band Single-Layer Patch Antenna is presented by Naftali Herscovici in [4].

A new type of patch element is presented. The patch is suspended over the ground plane and supported by a nonconductive pin. It is fed by a three-dimensional (3-D) transition connecting the patch to a perpendicular connector. For many applications, this geometry eliminates the need for the parasitic elements and the dielectric substrate necessary to support them.

Design and Performance of Small Printed Antennas are presented by Waterhouse et al. in [5]. In this paper, electrically small microstrip patches incorporating shorting posts are thoroughly investigated. These antennas are suitable for mobile communications handsets where limited antenna size is a premium. Techniques to enhance the bandwidth of these antennas are presented and performance trends are established. From these trends, valuable insight to the optimum design, namely broad bandwidth, small size, and ease of manufacturing, is given.

A wideband electromagnetic-coupled single-layer microstrip patch antenna is studied experimentally by Mark et al. in [6]. A notable structure in the feeding design is that an inverted L-shaped strip is connected to the end of the microstrip line and no matching network is required. The remarkable feature of the antenna is that a small step is introduced at the end of the feed line. Moreover the noncontact structure facilitates the fabrication of antenna arrays.

Lafond et al. presents aperture coupled microstrip patch antenna with thick ground plane[7].The thickness has a strong effect on impedance matching at high frequencies owing to the ratio between the thickness and the wavelength, which increases with frequency. The ground plane thickness is a critical parameter in aperture coupled patch antennas at millimeter wave frequencies due to the reduction of the input impedance when the slot thickness becomes significant with respect to the wavelength. Finally, it appears that it is possible to design a slot fed

patch on a thick ground plane which exhibits good impedance matching owing to the proper choice of slot length and patch size for a given ground plane thickness.

A U-slot circular patch antenna with L-probe feeding is presented by Guo et al. in [8]. The authors have described the combination of the L-probe and U-slot broad banding techniques, in the design of a broadband single-layer circular patch antenna. For a foam substrate of thickness, the bandwidth of the resulting antenna was 15% wider than that using the U-slot alone and 14% wider than that using the L-probe alone.

Patch Antennas on Externally Perforated High Dielectric Constant Substrates are presented by Colburn et al.[9]. The idea of external substrate perforation was introduced in this paper and applied to a patch antenna to help mitigate the drawbacks of thick high dielectric constant substrates without sacrificing the patch element miniaturization or bandwidth. The introduction of the external perforation improved the far-field radiation pattern of a patch antenna on a relatively thick substrate without any reduction in bandwidth or increase in patch size. The authors found that the perforation must not be located too close to the patch due to fringing fields, or the resonant frequency would shift up. It was also seen that the position where the perforation is started or terminated does have some affect on the far-field radiation pattern.

R.Leclaratne et al. presents a novel microstrip patch antenna suitable for satellite communications[10]. It is designed by using two semi-discs with single feeding. The antenna is circularly polarized and suitable for mobile satellite communications and if fed as individual semi-rings as a dual band orthogonally polarized antenna.

Small circularly polarized printed antenna is proposed by H.Kan et al. in [11].The antenna consists of a synchronous sub array of shorted patches with the required feed network etched on a high dielectric constant substrate located below

the ground-plane of the antenna. The circularly polarized antenna has a return loss bandwidth of 8.5%, an axial ratio bandwidth of 11.3% and is relatively compact, with dimensions of 0.195 x 0.195 x 0.052 wave length.

The basic rules about electrically small antennas, and gave clues and guidelines about efficient antenna miniaturization are presented by Skrivervik A.K et al. in [12] and compact antenna designs using fractal antennas are presented by Gianvittorio J.P et al. in [13]. Azadegan R et al. in [14] states that with the virtual enforcement of the required boundary condition at the end of a slot antenna, the area occupied by the resonant antenna can be reduced. The two short circuits at the end of the resonant slot are replaced by some reactive boundary, including inductive or capacitive loadings.

The effect of inserting an array of series inductors to a resonant slot antenna on size, bandwidth and gain of the antenna is presented by Behdad N et al. [15]. The antenna size can be reduced efficiently without adverse effect on the impedance matching and gain and as it is expected that the antenna bandwidth is reduced as a result of this miniaturization technique.

A novel design technique for small resonant slot antenna has been demonstrated by Sarabandi K et al. in [16]. The compactness is achieved by generating a virtual open circuit at one end of the slot and bending the slot into three pieces in order to use the area of the board more efficiently.

Xuan Chen et al. discusses the dependence of the resonant frequency and input impedance of printed Hilbert antenna in [17]. A multi-band planar inverted-F antenna (PIFA) at UHF band is developed by adding lumped load and employing fractal concept and is presented by Hala Elsadek et al. in [18]. The authors achieved up to 68%-82% size reduction.

A symmetrical feed is utilized to enlarge the input impedance and to connect the compact PIFA for mobile devices by Schulteis S et al. [19]. They discovered that the size of a PIFA for integration in mobile devices can be reduced by inductive or capacitive loading.

Jin-Sen Chen et al. presents a triangular-ring slot antenna fed by coplanar waveguide feed line with protruded tuning stub and a back-patch at the bottom of the substrate for miniaturization in [20] and it is found that the resonant frequency can be significantly reduced as compared with CPW fed conventional ring-slot antennas. A novel reactive impedance substrate for antenna miniaturization with enhanced bandwidth performance is presented by Mosallaei H et al. [21]

The methods for miniaturizing spirals and other antennas using dielectric loading, artificial lumped loads, textured dielectrics and other approaches is presented by Volakis J.L et al. [22]. They achieved miniaturization without much distortion in gain and bandwidth.

The downsizing technique of antennas for handsets is presented by Kawano Y et al. in [23]. The authors utilized a magnetic material at 900MHz and 2GHz band. A Planar Inverted-F Antenna (PIFA), which is the popular built-in antenna for handset was used for the investigation.

Hung Tien et al presents the effect of slot loading on microstrip patch antennas in [24]. The Koch island fractal and H-shape slots are introduced to microstrip patch antennas and their effect on reduction of the resonant frequency is determined. Additional slots of more complex geometry are implemented on the H-shaped patch to further bring down its resonance frequency.

A substantial reduction in antenna size was achieved due to the use of the inverted-F antenna concept combined with a capacitive feeding system presented by Robert Borowiec et al. in [25]. A miniaturized printed monopole antenna

suitable for cellular handset terminals is presented which operates in three frequency bands, that is, GSM 1800, PCS 1900, and UMTS.

A compact printed hook-shaped monopole antenna for 2.4/5-GHz WLAN applications is presented by Chi-Hun Lee et al. [26]. The proposed antenna is compact and the radiation patterns are nearly omni-directional in nature. Peng Sun et al. presents a novel compact antenna operating at GSM, DCS, PCS and IMT2000 bands in [27]. A loosely coupled ground branch is used in the antenna, which covers all 2G and 3G wireless communication bands. A coplanar waveguide (CPW)-fed monopole antenna with dual folded strips for the radio frequency identification (RFID) application is presented by Wen-Chung Liu et al. [28] and the antenna has a very compact size including ground plane.

Cheng-Jung Lee Leong et al. presents a novel approach for the realization of compact antennas in [29]. The antenna utilizes left handed mode of propagation of the composite right/left-handed transmission line. The propagation constant approaches infinity at frequencies near the cutoff and electrically large, small sized antenna can be realized depending on the unit cell optimization and miniaturization.

Spence T. G et al. presents a new variation of the conventional open-sleeve dipole antenna in [30]. The proposed geometry provides miniaturization while retaining a comparable bandwidth in terms of the VSWR response to that of conventional open-sleeve dipoles. A miniaturization scheme for a square circularly polarized cavity-backed antenna using textured dielectric loading is proposed by Psychoudakis D et al. in [31]

Broadband microstrip patch antennas for MMICs is presented by Rowe et al.[32]. The stacked antenna consists of a 50Ω microstrip feed line and a patch element fabricated on alumina substrate which emulates the high dielectric constant materials used in MMICs. The parasitic patch elements are etched in

Rogers RT/duroid 58880 laminates and are separated by form dielectrics. Good efficiency, a broad impedance bandwidth and large front to back ratio eliminates the need for cavities or other structures to reduce back radiation. The proposed antenna structure exhibits an improved over the stacked patch antenna.

High directivity fractal boundary microstrip fractal boundary microstrip patch antenna presented by Borja et al.[33] shows that a patch antenna with a fractal boundary exhibits localized modes. The localization effect produces an electric current density that is mainly concentrated in certain regions at the boundary. The result is that the microstrip fractal boundary antenna behaves as an array of antennas. When the localized modes are properly in phase, a broadside pattern is obtained and the directivity increases in comparison with the directivity of the antenna at the fundamental mode frequency.

Clasen et al. [34] investigates the performance of a microstrip patch antenna integrated into a laminated glass windscreen of a vehicle. The antenna is fed using a coplanar waveguide feed printed on the innermost layer of the glass avoiding the need for a contacting feed. The patch and ground plane are meshed for manufacturing in the glass. Creating the patch from a mesh structure allows the antenna to be printed onto the glass and gives a degree of transparency

A broad band U-slot rectangular patch antenna on a microwave substrate is presented by Tong et al.[35]. It is found that the crucial step to design a broad-band -slot patch antenna printed on a microwave substrate is to use a larger thickness than the case with a foam material. The foam material in the previous studies is replaced by a dielectric substrate of relative permittivity 2.33. This substitution can ease the fabrication of the antennas especially in an array environment. The computed resonant frequencies and far-field patterns agree well with measured data. The measured gain of each antenna is about 6.5 dB.

Mark et al. presents the experimental study of a microstrip patch antenna with an L-shaped probe[36]. The L shaped probe is shown to be an attractive feed for the thick microstrip antenna. A parametric study on the rectangular patch antenna is presented and the antenna attains 36% impedance bandwidth and about 7-dBi average gain. The array design with the same configuration can substantially suppress the cross polarization of the proposed antenna. Both the antennas have stable radiation patterns throughout the pass band.

Small square dual spiral printed antennas are presented by kan et al. in [37].The antenna consists of two interleaved shorted spiral radiators and a feed network etched on a high dielectric material below the ground plane. A 10dB return loss bandwidth of 9.2% has been achieved with an omni directional radiation pattern. The proposed antenna is 28% smaller than a conventional shorted patch antenna, making it very desirable for mobile communication handset terminals.

A novel single-layer rectangular patch antenna using a coupled line feed is described by Van et al. in [38]. This coupled line matching technique increases the bandwidth of the patch antenna by a factor more than 2.5 as compared to the normal edge fed patch with the same geometrical dimension. The primary advantage of this technique over previously available options is its compact physical dimensions.

Shackelford et al. presents U-slot patch antenna with shorting pin[39] which describes patch antenna loaded with U-slots and shorting pin for bandwidth enhancement. The measured results agree that the radiation characteristics are desirable for indoor wireless networking applications.

A broadband two-layer shorted patch antenna with low cross-polarization is presented by Baligar[40]The antenna has a bandwidth of 11% centered around 1.975GHz with a gain of 8.6dB, and exhibits better than -13dB cross-polarization levels in the H-plane. The computed and measured results of the co-planar configuration of the structure are compared with its new two-layer stacked configuration. The stacked geometry is found to reduce radiated cross-polarization levels significantly and offers a larger impedance bandwidth, a higher gain and radiation efficiency compared to the co-planar structure as well as the patch antenna structure.

A simple low-cost planar antenna for indoor communication under the Bluetooth protocol is presented by G.Vermeeren et al.[41]. A simple low-cost rectangular ring antenna is developed and the dimensions of the same were optimized by commercially available simulation packages. The transmission characteristics of a transmitter receiver pair proved to be sufficient in a realistic indoor environment and can be utilized for Bluetooth protocol in the 2.5GHz ISM-band.

The combination of a microstrip patch antenna at 900 MHz and a folded reflector antenna in the 60GHz frequency range integrated in a common aperture is described by Menzel et al.[42].The 900MH antenna is based on a resonator-backed microstrip patch antenna, while the mm-wave antenna consists of a folded reflector antenna with a polarizing grid integrated into the antenna patch and a twisting and focusing planar reflector placed on the bottom of the 900 MHz antenna box. Both antennas show excellent performance.

Bandwidth enhancement technique for Quarter wave patch antennas are depicted in [43] by Chiu et al.. They present a novel technique that improves the performance of a conventional quarter-wave patch antenna. Two different geometries of U-slot and L-slit are investigated experimentally with the inclusion

of a folded inner small patch and achieved the impedance bandwidths of 53% and 45. Radiation patterns are found to be stable across the whole operating frequency bands.

A Thin Internal GSM/DCS Patch Antenna for portable mobile terminal applications is presented by K.L. Wong et al. [44] The antenna incorporates a small portion of the top patch beyond the top edge of the system ground plane of the mobile terminal, which results enhanced bandwidths of the two resonant modes for covering the GSM and DCS bands. Kin Lu Wong et al. [45] presents a shorted internal patch antenna which is mounted at the bottom end of the lower ground plane of the mobile phone, and can generate a wide operating band for UMTS operation. A novel Compact Wide-Band Planar Antenna for Mobile Handsets is presented by Zhengwei Du et al. in [46]. It is capable of covering the major wireless communication and navigation systems bands like GSM, GPS, DCS, PCS, UMTS, and WLAN. The radiating patch is jointly designed with the shape of the ground plane to optimize its performance.

P. Ciais et al. [47] presents a planar inverted-F antenna (PIFA) operates in penta-band suitable for handheld terminals. This antenna consists of capacitively loaded shorted patches, a slot, and an efficient antenna-chassis combination to achieve multiband and wideband performances to operate in the 850 MHz, 900 MHz, 1800 MHz, 1900 MHz, and UMTS bands. A wideband monopole antenna integrated within the front-end module package is proposed by Saou-Wen Su et al. [48]. The antenna is a good candidate for WLAN / WiMax applications and is integrated within the frond-end module package of the system.

Juha Villanen et al presents a Coupling Element Based Mobile Terminal Antenna Structure in [49]. The work concentrates on the possibilities to reduce the volume of mobile terminal antenna by efficiently utilizing the radiation of the currents on the mobile terminal chassis. The non resonant coupling elements are

used to optimally couple the dominating characteristic wave modes to the chassis. The design of a miniature mobile handset antenna using Genetic Algorithm and MoM is presented by Tieming Xiang et al. [50]. It can provide wide bandwidth to cover the operating bands for modern mobile communications, including GSM, DCS, PCS, and UMTS bands. Kati Sulonen et al. discussed the variations in antenna radiation pattern on the performance of the mobile handset in [51]. The different antenna radiation pattern characteristics on the performance of the antenna in different environments at 2 GHz are investigated.

A Folded Meandered-Patch Monopole Antenna for Triple-Band Operation is presented by Fa-Shian Chang et al. [52]. The proposed antenna is suitable for applications in mobile phones for GSM, DCS and PCS triple-band operations.K.L. Wong et al. developed an Internal GSM/DCS Antenna Backed by a Step-Shaped Ground Plane for a PDA Phones[53].

The antenna consists of two radiating strips to operate at about 900 and 1800 MHz for GSM/DCS operation, and is backed by a short circuited to a step-shaped ground plane. With the use of the step-shaped ground plane, which is to be placed at the top edge of the system ground plane of a PDA phone, the antenna can be employed in very close proximity to the possible RF shielding metal cases for battery and associated RF module/circuitry, with almost no degradation in the antenna performances.

An Internal Shorted Patch Antenna for UMTS Phone is presented by Saou-wen Su et al. [54]. This internal mobile phone antenna design eliminate the required isolation distance between the antenna and the RF shielding metal box, thus providing a promising alternative for integrating various elements inside a mobile gadget.

2.2 Dual Band Printed Monopole Antennas:

The interest in dual frequency printed monopole antennas attracted many researchers around the world which helps to improve the design of modern communication systems such as PDAs and other mobile communication gadgets. This part of the literature review depicts the recent research on dual band antennas with special attention to printed monopoles.

A.Serrano et al. reported dual band GSM/DCS 1800 printed antenna[55] made with bow-tie radiating element. The antenna is excited by a vertical SMA connector with the outer conductor connected to the ground plane of the antenna. The radiation characteristics of the antenna are similar to those of conventional microstrip patches.

Dual-band patch antenna for mobile satellite systems is presented by R.Lelaratne and R.J. Langley[56]. The antenna excites two separate modes which results dual linear polarization on each bands. The dual frequency band design, based on a rectangular patch, has a single feed point, suppresses unwanted mode interference and produces acceptable radiation patterns.

D.Viratelle and R.J. Langley illustrates a Dual band printed antenna for mobile telephone applications [57]. The compact, lightweight, low-cost, dual-band antenna, printed on a flexible printed circuit material and conductor area. The basic Inverted F antenna is simply modified by separating part of the upper plate to create a second resonance. A single coaxial feed connected to the inner patch excites both frequency bands. Shorting pins are replaced by strip conductors.

Dual band slot-loaded short-circuited patch antenna presented by Y.X. Guo et al.[58] presents a technique for size reduction with slot-loading. By controlling the short-plane width, the two resonant frequencies can be significantly reduced and the frequency radio is tunable.

F.Yang et al. presents a switchable dual band circularly polarized patch antenna with single feeding [59]. The antenna utilizes two diode controlled slots in the patch for dual band operation and pair of tuning stubs are used to tune the CP performance. The structure has the advantage of low profile, small and is suitable for GPS, satellite links and other wireless communication applications.

A wide-band Dual polarization patch antenna with Directional Coupler is presented by K.L. Lau et al. in [60].A coupled line directional coupler mounted at the back of the ground plane is used to enhance the isolation between the L-probes to a large extent. The antenna appears to have high input isolation and simple in structure. This antenna can be used in the base stations of cellular communication systems.

Kin-Lu Wong et al. presents Broadband Dual-polarized Aperture Coupled patch antennas with modified H-Shaped Coupling slots [61]. The new design of aperture coupled patch antenna with modified H-Shaped coupling slots for achieving dual polarization radiation with high isolation over a wide bandwidth. By using the proposed coupling slots, whose two upper side arms are bent inward with a proper angle, the isolation between the two feeding ports of the patch antenna can greatly be improved. At the same time when using a pair of modified H Shaped coupling slots for each feeding port, the isolation can be further be improved.

Broad-band dual polarized patch antenna fed by capacitive coupled feed and slot coupled feed is presented by wong et al. [62]. Several promising feeding structures for achieving broad band dual polarized patch antennas with high isolation and low cross polarization have been proposed, and prototype antenna have been constructed and experimentally studied. Results demonstrate that with the proposed feeding structure, high isolation for the two polarizations in the entire impedance bandwidth can be obtained.

Broadband Dual frequency operation of circular patch antennas and arrays with a pair of L-shaped slots is presented by Jui Han Lu[63]. The proposed design consists of a circular patch antenna fed by an L-strip microstrip line for broadband dual frequency operation. The circular patch is loaded with L shaped slots which results an additional resonance other than the fundamental resonance. Measured gain for the two operational band is found to be about 4.7 dBi . The application of the antenna in a broadband patch antenna array is also demonstrated.

A Low-Profile Planar Monopole Antenna for Multiband Operation of Mobile Handsets is presented by K.L. Wong et al. [64]. The proposed antenna has a planar rectangular radiating patch in which a folded slit is inserted at the patch's bottom edge. The folded slit separates the rectangular patch into two sub patches, one smaller inner sub patch encircled by the larger outer one. The proposed antenna is then operated with the inner sub patch resonating as a quarter-wavelength structure and the outer one resonating as both a quarter-wavelength and a half-wavelength structure.

G.Jaworski et al. presents a broadband matching of dual-linear polarization stacked probe-fed micro strip patch antenna [65]. The authors present a novel approach for impedance matching of probe-fed stacked microstrip antenna elements. The matching structure is compact and enables more than doubling of the operational bandwidth. A circuit model for the feeding probes is also developed and its impact on antenna impedance is discussed. The matching circuit comprises coupled strip line structures and the antenna feeding probes are modeled carefully using an equivalent circuit model.

A planar meander-line antenna consisting of three branched strips for very-low-profile GSM/DCS/PCS/WLAN   triple-band operation of mobile phones proposed by Jeun-Wen Wu et al [66]. The branch strips are designed to operate as

quarter-wavelength structures at 900 and 1800 MHz, respectively, and covering above mentioned bands.

A multiband CPW-fed notched planar monopole using a genetic algorithm in conjunction with the method of moments (MoM) is proposed by Liu W.-C et al [67]. The introduction of a suitable notch to a rectangular CPW-fed patch, the desired multi-frequency resonant modes and broad impedance bandwidths can be obtained. Wang-Sang Lee et al. developed a Multiple Band-Notched Planar Monopole Antenna for Wireless Systems in [68]. The antenna consists of a wideband planar monopole antenna and the multiple U-shape slots, producing band-notched characteristics.

Amir Hossein Yamini et al. [69] presented a bow-tie printed antenna. The paper explains the experimental and simulation results based on dipole antenna concepts and compared with the theoretical results based on FDTD. Antennas for the applications for WLAN/HIPERLAN/ISM triple band are presented by Yu-Seng Liu et al. in [70]. The authors presents a mender line antenna excited with inverted planar L-shaped structure which results three resonant modes. Jingjing Huang et al. [71] proposed multiband fractal patch antenna for the mobile applications. The characteristics of the novel fractal patch antenna is described by means of experimental and computational results and self-similarity properties of the fractal shape are translated into its multiband behavior.

Integrated planar multiband antennas for personal communication handsets are presented by Martinez-Vazquez M et al. [72]. Triple band operation was achieved by combining spur-line techniques with parasitic patches, while the use of an additional slot introduces a fourth resonance with acceptable performance without increasing antenna volume so that a quad-band antenna is obtained.

Sanz-Izquierdo B et al. [73] proposed a PIFA for WLAN applications fabricated in multiple layers.   The antenna size was reduced by removing metallization in areas of low current density. The construction is simple with the metal etched from a thin layer sheet folded around a honeycomb former. A multiband printed dipole antennas using parasitic elements for multiple wireless services is presented by Jean-Marie et al. [74]. First, an elementary dipole antenna was studied and characterized at the operating frequency of 2.9 GHz. Next, two compact dual-band planar-antenna configurations are presented.

A novel modified T-shaped planar monopole antenna, with two asymmetric horizontal strips as additional resonators to produce the lower and upper resonant modes is presented by Sheng-Bing Chen et al. [75]. The authors implemented a dual-band antenna for covering 2.4- and 5-GHz wireless local area network (WLAN) bands.

A novel microstrip antenna applicable for multiband operation is proposed by Wen-Jiao Liao et al. [76]. The design was evolved from a conventional parallel stripline dipole with modifications in the dipole geometry and feeding structure. Circular polarized microstrip patch antennas for broadband and dual-band operation is presented by Y.J. sung et al.[77] in which Circular polarization can be flexibly controlled by adjusting the size and offset of the loaded holes on the antenna. The dual band operation of the hole loaded circular patch antenna with single feed is also proposed. The antennas are suitable for application in wireless communication and mobile satellite communication.

W.C.Liu et al. presents CPW-fed compact meandered patch antenna for dual-band operation[78] in which they propose a technique for dual band operation by inserting a meandering slit at the edge of the rectangular printed patch fed by coplanar waveguide. The antenna provide sufficient impedance bandwidth and suitable radiation characteristics for being applied in the UMTS

and 5.2GHz wireless gadgets. K. Ghorbani et al. presents wide-band aperture stacked patch antennas[79]. The dual polarized printed antenna is based upon an aperture stacked patch layout and incorporates a simple dual-layered feeding technique to achieve dual-polarized radiation. A cross shaped reflector patch ensures the front to back ratio of the antenna is greater than 20dB over the entire impedance bandwidth. The antenna is simple to manufacture and is suitable for mobile communications base station array.

Ka-Lam Lau et al. presents a dual band Vertical patch antenna for Dual-Band Operation [80]. A proximity coupling feeding technique is described for the recently invented vertical patch antenna. It reduces the projection area and remains simple in structure and wide in bandwidth. Moreover, it can be operated in dual bands by simply adding a smaller circular-VPA inside. The antenna is fed by a proximity-coupled probe, which maintains the advantages of the original single-band vertical patch antenna, such as small size, wide bandwidth and simple structure. The achieved bandwidths are 7% and 26%, respectively, at the lower and upper frequency bands.

A Compact circularly polarised microstrip antenna design for dual-band applications is presented by Yim et al. [81]It is realised by integrating a dual-band dual-fed patch antenna with a dual-band branch-line coupler in a compact multi-layer structure. The use of a dual-band hybrid and multi-layer structure allow both compact size and good isolation between the antenna and the feeding network to be realized. A quasi-omnidirectional dual-band back to- back E-shaped patch antenna for laptop applications is presented by J.Guterman et al.[82].In spite of the laptop's large ground plane size, the antenna radiates a quasi-omnidirectional total gain radiation pattern in both operating bands. The low profile antenna conformably embraces the ground plane edge and therefore can be integrated inside the plastic cover of a laptop display panel. Owing to its unique properties,

the proposed solution can be an alternative to popular flat-plate, inverted-F and slot laptop internal antennas.

A simple theoretical design method for maximizing the return-loss bandwidth of a circular microstrip patch antenna is presented by Abunjaileh et al. in [83] Theoretical bandwidth improvement of up to 3:1 is achieved when compared to a single-mode antenna. By considering a dual-mode antenna as a filter network, it is shown that a significant improvement in bandwidth may be obtained when compared with a single mode device, this can be achieved by adjusting the coupling values.

A Wide-Band Dual-Polarized Stacked Patch Antenna is proposed by serra et al.[84]. The dual polarization in the wide band is achived by stacking two square aluminium patches fed by two microstrip lines through a couple of crossed slots opened in copper ground plane. The microstrip lines feeding the slots terminate with radial stubs to improve impedance matching. The specific feeding technique is useful to reduce the cross polarization level and to increase the isolation between the two polarization ports.

Lau et al. presented a Dual-band stacked folded shorted patch antenna[85]suitable for the indoor wireless communication systems that are required to cover the operating bandwidths of three wireless communication systems, CDMA800, GSM900 and PCS, simultaneously. This antenna is mounted in the middle of a rectangular ground plane. It consists of two stacked rectangular patches with different sizes. The larger one is responsible for the lower band operation while the smaller is responsible for the upper band operation.

A Dual-band triangular patch antenna with modified ground plane is presented by L.Liu et al.[86]. The parasitic wire element around the main triangular patch provides a dual-frequency band antenna. Modifying the small ground plane

by introducing a rectangular slot allows tuning of the frequency bands and the band spacing ratio.

Yagi Patch Antenna With Dual-Band and Pattern Reconfigurable Characteristics is presented by Yang et al. in [87].The beam can scan in the E-plane by switching the modes of the antenna, which is implemented by changing the states of the switches installed in the slots etched on the parasitic patches. Different modes of the antenna have different radiation patterns and operating frequency bands. The antenna can be used in radar, satellite communications, etc.

A Novel Low-Profile Broadband Dual-Frequency Planar Antenna for Wireless Handsets is presented by Rong Lin Li et al.[88].The dominant antenna element for the 2-GHz band is a two-strip monopole which consists of an S-strip and a T-strip while a planar monopole is added for the 5-GHz operation. The mutual coupling between the two-strip monopole and the planar monopole leads to a bandwidth enhancement in both the 2-GHz band and the 5-GHz band. The dual-frequency planar antenna is realized on a thin substrate without via process, enabling its easy integration with RF front-end circuits.

A Novel Low-Profile Broadband Dual-Frequency Planar Antenna for Wireless Handsets is presented by RongLin et al.[89].The antenna features low profile due to the introduction of an S-strip and aT-strip which are separately printed on the two sides of a thin substrate (no via process is involved in the fabrication), forming the two-strip monopole. The bandwidth of the dual-frequency planar antenna is enhanced by taking advantage of the two-strip configuration and the mutual coupling between the planar monopole and the two-strip monopole.

A compact vertical patch antenna for dual band WLAN operation is presented by F.S. Change et al.[90].The antenna consists mainly of one driven patch and one shorted parasitic patch, both of which wind along two concentric

circles. The antenna can be quite practical in applications of ceiling-mount access points. A dual-band antenna design consists of two patch radiators suspended above a ground plane is presented by Toh et al. in [91].The performance in the lower and upper bands can be controlled with less mutual coupling effect. The antenna also features less beam squinting of the radiation patterns at boresight for both operating bands.

2.3 CPW Techniques in Antennas:

Coplanar wave guide has become an attractive feeding technique and can be effectively utilized in the design of compact printed antenna designs. The key features of Coplanar Wave Guide such as, availability of ground in the same plane and good transfer characteristics attracted many researchers and the following review illustrates most of the CPW antennas reported recently.

A nonleaky conducted-backed coplanar waveguide fed rectangular microstrip patch antenna is presented by D.R. Jahagirdar et al. [92]. The authors provides a new arrangement for exciting microstrip patch antenna which allows easier integration with monolithic microwave integrated circuits.. This structure can be utilized to feed a rectangular patch through an aperture in the back plane.

W.S.T. Rowe et al. [93] presents a broadband CPW fed stacked patch antenna for integration with monolithic and optical integrated circuits. A large aperture is used as resonator within the operating band. Thick slabs of rogers 5880 duroid and form are used as substrates. The high dielectric feed substrate caused an opposite effect on the coupling strength an also limited the maximum achievable bandwidth of the antenna.

A single layer CPW fed active patch antenna is presented by Kenneth H.Y.Ip. et al. [94]. The group presents a single-layer CPW fed active patch antenna at 2.75GHz. The patch antenna acts both as a resonator and a radiator.

Electromagnetic coupling is utilized for providing the appropriate closed-loop positive feedback. The structure leads to a layout with no via-holes, a reduced component count, and a simplified dc bias network. This type of antenna can find applications in low-cost proximity sensing. Collision avoidance, power communications.

The technique for the reduction of backward radiation for CPW fed Aperture stacked patch antennas on small ground planes is presented by W.S.T. Rowe et al.[95]. The proposed antenna is mounted on a finite sized ground plane that incorporates a reflector element to reduce backward radiated field. By altering the reflector element parameters, the rear field pattern can be adjusted to provide field cancellation in arbitrary directions

Jeen-Sheen Row in [96] presents a patch antenna fed by shorted coplanar microstrip line. By embedding a shorting pin in the microstrip feed line, the proposed antenna is capable of operating at two distinct modes with different radiation characteristics. In addition, the frequency radio of the two resonant frequencies is also tunable by loading an additional slot in the microstrip patch. The proposed antenna has the advantage of compact size and suitable for mobile communication applications.

A circularly polarized CPW fed antenna is presented by H.Aissat et al. in [97] which utilizes the combined excitation of the patch by an inclined slot and the CPW feed line termination. The asymmetrical characteristics of the excitation involve the excitation of both the odd and the even modes in the CPW line. Another CPW fed array is presented by I Jen Chen et al. [98] in which the array elements are placed in the direction transverse to the feeding CPW line and are excited by a couple of 100ohm slot lines, which are combined to form the 50ohm feeding CPW. The circularly polarized radiation is obtained by placing similar perturbation segments to each of the array elements.

Broadband designs of coplanar capacitive fed shorted patch antennas is presented by H.D. chen[99]. These antennas provide easy fabrication and very wide impedance bandwidth. By incorporating the feeding strip length of about one radiating patch length, the radiating patch width ranging about 2-2.6 times of the radiating patch length and the feeding strip placed close to the bottom edge of the radiating patch an impedance bandwidth in excess of 70% can be obtained. W.S.T. Rowe et al. presents a CPW fed antenna in [100] well suited for integration with monolithic and optical integrated circuits. The proposed design uses a CPW feed line on high dielectric constant substrate, and a stacked patch configurations for the enhanced impedance bandwidth.

A single layer CPW fed active patch antenna is presented by Kenneth H et al. [101]. This active antenna utilizes electromagnetic coupling for closing the feedback loop. The structure leads to a layout with no via-holes, a reduced component count, and a simplified dc bias network. The antenna find applications in low-cost proximity sensing, collision avoidance, power combining or communications.

A simple impedance matching technique for patch antennas fed by coplanar microstrip line is presented by Jeen-sheen Row[102]. By placing a shorting through hole at a proper position the resonant input resistance of the edge-fed patch antenna can be easily tuned to 50Ω. It is clear from the measured results that the position of the through hole is very much related to the length of the radiating edge of the patch antenna. The proposed technique is more flexible for designing the patch antenna in a limited area than the insert-microstrip line feed. And the required size is more compact than the use of the quarter wave length transformer or the shunt stub line.

Jeong Geum Kim et al. presents a CPW patch antenna using micromachining technology[103]. The radiating patch and the feed line network

can be optimized separately with a substrate. The antenna performance is improved by elevating the patch in the air. A patch antenna is also designed with simle feed network. Since the proposed antenna allows the integration with MMICs, it can be applied for the system on chip(SOC) including an antenna at mm-wave frequency.

2.4 FDTD Techniques:

The developments in the field of Finite Difference Time Domain(FDTD) analysis in the last few decades is illustrated in this session.

The Finite-Difference Time-Domain (FDTD) method is first proposed by Yee in 1966 in [104]. It is a simple method to discretize the differential form of Maxwell's equations. The technique used by Yee is a grid of electric field and an offset magnetic field to obtain the updated fields throughout the computational domain.

Yee proposed a non orthogonal grid scheme during 1987 and several attempts have been made to implement alternative orthogonal coordinate systems[105, 106].A.Teflove in [107] pointed out that Numerical-dispersion and grid-anisotropy errors can be kept small by having a sufficient number of grid spaces per wavelength. He is also presented the stability criteria for the Yee algorithm in [108]. The application of3D FDTD method for the analysis of microstrip antenna and other microstrip circuits is presented by D. M. Sheen et. al. in [109] Berenger in [110] provided the material-based Absorbing Boutray condition and is known as the Perfectly matched layer absorbing boundary condition. The technique found to be one of the best techniques for the reduction of boundary reflections compared to any ABC proposed earlier.

FDTD technique is implemented by Reineix and Jecko to analyze microstrip antennas and the work is presented in [111]. During 1992, Leveque et al. [112]

modeled frequency-dispersive microstrip antennas, while Wu et al. [113] used the FDTD method to accurately measure the reflection coefficient of various microstrip-patch configurations. An analysis of the mutual coupling between two microstrip antennas using FDTD technique is presented by Uehara et al. in [114]. Oonishi et al. [115] and Kashiwa et al. [116] used one of the conformal FDTD approaches to analyze microstrip antennas on a curved surface.

The FDTD technique is used to design twin-slot antennas during 1994, by Qian et al. and it is presented in [117]. Later, Reineix and co-workers [118, 119,120] have expanded their FDTD analysis to include the input impedance of microstrips with slots, to obtain the radar cross section of microstrip-patch antennas, and to model the radiation from microstrip patches with a ferrite substrate. The interaction of a hand held antenna and a human were also studied by Jensen and Rahmat- Samii [121]. Also in 1994, Chen and Wang [122] calculated the currents induced in the human head with a dipole-antenna model from a cellular phone. Martens et al. [123] have used a dipole model and a full model for a hand-held antenna to compute the fields induced in the human head.

Same year, Luebbers et al. [124] and Chen et al. [125] analyzed hand-held on a monopole antenna on a conducting or dielectric box using FDTD. Toftgird et al. [126] calculated the effect the presence of a person has on the radiation from such antennas. Jensen and Rahmat-Samii [127] presented results for the input impedance and gain of monopole, PIFA, and loop antennas on hand-held transceivers. The 3-D FDTD design analysis of a 2.4-GHz polarization-diversity printed dipole antenna with integrated balun and polarization-switching circuit for WLAN and wireless communication applications was carried out by Huey-Ru Chuang et al. [128]. Pattern reconfigurable leaky-wave antenna analysis using FDTD method was introduced by Shaoqiu Xiao et al. [129].

The Analysis of CPW-fed folded-slot and multiple-slot antennas on thin substrates were carried out using FDTD method [130]. M. Kar and P.F Wahid [131] described the FDTD analysis of dual-feed microstrip patch antennas. S. Dey et al. [132] proposed conformal FDTD analysis technique for modeling cylindrical DRs. FDTD analysis of radiation pattern of antenna on truncated ground plane was investigated by Yamamoto et al. [133].

References

[1] L.Economou and R.J. Langley, " Circular microstrip patch antennas on glass for vechicle applications", IEE Proc. Microwave Antennas and Propag. , Vol.345, No.5, pp. 416-421, 1998.

[2] N. Chiba, T. Amano and H. Iwasaki, "Dual-frequency planar antenna for handsets", IEE Electronics Letters, Vol.34, No.25, 1998.

[3] Laurent Desclos, Tomislav Drenski, and Mohammad Madihian, "An Interdigitated Printed Antenna for PC Card Applications", VOL. 46, NO. 9, pp.1388-1389. 1998.

[4] Naftali Herscovici, "A Wide-Band Single-Layer Patch Antenna", IEEE Transactions on Antennas and Propagation, Vol.46, No.4, pp.471-471, 1998.

[5] Rod B. Waterhouse, S. D. Targonski, and D. M. Kokotoff, "Design and Performance of Small Printed Antennas", VOL. 46, NO. 11,pp.1629-1633, 1998.

[6] C.L.Mak, K.M.Luk and K.F.Lee, "Microstrip line-fed L-strip patch antenna", IEE Proc. Microwave Antennas and Propagation, Vol.146, No.4, pp.282-284, 1999.

[7] Lafond, M. Himdi and J.P. .Daniel, "Aperture coupled microstrip patch antenna with thick ground plane in millimetre waves", IEE Electronics Letters, Vol.35, No.17, pp.1394-1395, 1999.

[8] Y.X. Guo, K.M. Luk and K.F. Lee, "U-slot circular patch antennas with L-probe feeding", IEE Electronics Letters, Vol.35, No.20, pp. 1694-1695, 1999.

[9] Joseph S. Colburn, and Yahya Rahmat-Samii, "Patch Antennas on Externally Perforated High Dielectric Constant Substrates", IEEE Transactions on Antennas and Propagation, Vol. 47, No.2, pp.1785-1794, 1999.

[10] R. Leclaratne and R.J. Langley, " Patch antenna for mobile satellite terminal", IEE Electronics Letters, Vol.36, No.6, pp. 489-490, 2000.

[11] H. Kan and R.B. Waterhouse, "Small circularly polarised printed antenna", IEE Electronics Letters, Vol.36, No.5, pp. 393-394, 2000.

[12] PCS antenna design: the challenge of miniaturization, Skrivervik A.K, Zurcher J.-F, Staub O, Mosig J.R, IEEE Antennas and Propagation Magazine, Vol. 43, Issue 4, Aug. 2001 pp.12 – 27

[13] Fractal antennas: a novel antenna miniaturization technique, and applications, Gianvittorio J.P, Rahmat-Samii Y, IEEE Antennas and Propagation Magazine, Vol. 44, Issue 1, Feb. 2002 pp.20 – 36

[14] A novel approach for miniaturization of slot antennas, Azadegan R, Sarabandi K, IEEE Transactions on Antennas and Propagation, , Vol. 51, Issue 3, March 2003 pp.421 – 429.

[15] Slot antenna miniaturization using distributed inductive loading, Behdad N, Sarabandi K, IEEE Antennas and Propagation Society International Symposium 2003, Vol. 1, 22-27 pp.308 - 311 vol.1

[16] Design of an efficient miniaturized UHF planar antenna, Sarabandi K, Azadegan R, IEEE Transactions on Antennas and Propagation, Vol. 51, Issue 6, June 2003 pp.1270 - 1276 .

[17] A down-sized printed Hilbert antenna for UHF band, Xuan Chen, Safieddin Safavi Naeini, Yaxin Liu, IEEE Antennas and Propagation Society International Symposium, 2003, Vol. 2, 22-27 June 2003 pp.581 – 584

[18] Multiband miniaturized PIFA for compact wireless-communication applications, Hala Elsadek, Dalia Nashaat, Hani Ghali, Microwave and optical technology letters, Vol. 42, Issue 3 , Jun 2004, pp. 230 – 234.

[19] A small planar inverted F antenna with capacitive and inductive loading, Schulteis S, Waldschmidt C, Sorgel W, Wiesbeck W, IEEE Antennas and Propagation Society International Symposium, 2004. Vol. 4, 20-25 June 2004 pp.4148 - 4151

[20] CPW-fed compact equilateral triangular-ring slot antenna, Jin-Sen Chen, IEEE Antennas and Propagation Society International Symposium, 2004, Vol. 3, 20-25 June 2004 pp.2416 – 2419.

[21] Antenna miniaturization and bandwidth enhancement using a reactive impedance substrate Mosallaei H, Sarabandi K, IEEE Transactions on Antennas and Propagation, Vol. 52, Issue 9, Sept. 2004 pp.2403 – 2414.

[22]Miniaturization methods for narrowband and ultrawideband antennas Volakis J.L, Chi-Chih-Chen Ming Lee, Kramer B, Psychoudakis D, IEEE International Workshop on Antenna Technology: Small Antennas and Novel Metamaterials, 2005. IWAT 2005. 7-9 March 2005 pp.119 – 121.

[23]A study on miniaturization of 900 MHz and 2 GHz band antennas utilizing magnetic material, Kawano Y, Hayashida S, Bae S, Koyanag Y, Morishita H, IEEE Antennas and Propagation Society International Symposium, 2005 Vol. 3B, 3-8 July 2005 pp.347 – 350.

[24]A compact printed hook-shaped monopole antenna for 2.4/5-GHz wlan applications, Chi-Hun Lee, Seong-Ook Park, Microwave and optical technology letters, Vol. 48, Issue 2 , Dec 2005, pp. 327 – 329.

[25]A miniaturized antenna for 2G/3G frequency-band applications, Robert Borowiec, Piotr M. Stobodzian, Microwave and optical technology letters, Vol. 48, Issue 2 , Dec 2005, pp. 399 – 402.

[26]A compact printed hook-shaped monopole antenna for 2.4/5-GHz wlan applications, Chi-Hun Lee, Seong-Ook Park, Microwave and optical technology letters, Vol. 48, Issue 2 , Dec 2005, pp. 327 – 329.

[27]Compact planar monopole antenna with ground branch for GSM/DCS/PCS/IMT2000 operation, Peng Sun, Zhenghe Feng, Microwave and optical technology letters, Vol. 48, Issue 4 , Feb 2006, pp. 719 – 721.

[28]Compact CPW-fed dual folded-strip monopole antenna for 5.8-GHz RFID application, Wen-Chung Liu 1, Ping-Chi Kao 2, Microwave and optical technology letters, Vol. 48, Issue 8 , May 2006, pp. 1614 – 1615.

[29]Composite right/left-handed transmission line based compact resonant antennas for RF module integration Cheng-Jung Lee Leong, K.M.K.H, Itoh T, IEEE Transactions on Antennas and Propagation Vol. 54, Issue 8, Aug. 2006 pp.2283 – 2291.

[30] A Novel Miniature Broadband/Multiband Antenna Based on an End-Loaded Planar Open- Sleeve Dipole, Spence T. G, Werner D. H, IEEE Transactions on Antennas and Propagation, Vol. 54, Issue 12, Dec. 2006 pp.3614 – 3620

[31]Cavity-Backed Miniature Wideband UHF Circular Polarized Antenna With Textured Dielectrics Psychoudakis D, Volakis J. L, Wing Z, Halloran J. H, IEEE

Transactions on Antennas and Propagation , vol. 54, Issue 12, Dec. 2006 pp.3586 – 3592

[32] W.S.T. Rowe and R.B. Waterhouse, " Broadband microstrip patch antennas for MMICs", IEE Electronics letters, vol.36, No.7, pp. 597-598, 2000.

[33] C. Borja, G. Font, S. Blanch and J. Romeu, "High directivity fractal boundary microstrip
patch antenna", IEE Electronics letters, vol.36, No.9, pp.778-779, 2000.

[34] G.Clasen and R.J. Langley, " Meshed patch antenna integrated into car windscreen", IEE Electronics Letters, Vol.36, No.9, pp. 781-782, 2000.

[35] Kin-Fai Tong, Kwai-Man Luk, Kai-Fong Lee, and Richard Q. Lee, " A broadband U slot rectangular patch antenna on a microwave substrate", IEEE Transactions on antennas and propagation, Vo.48, No.6, pp. 954-961, 2000.

[36] C. L. Mak, K. M. Luk, K. F. Lee, and Y. L. Chow, "Experimental Study of a Microstrip Patch Antenna
with an L-Shaped Probe", IEEE Transactions on antennas and propagation, Vo.48, No.5, May 2000.

[37] H.K. Kan and R.B. Waterhouse, "Small square dual spiral printed antennas", IEE Electronics Letters, Vol.37, No.8, pp.478-479, 2001.

[38] M.D. van Wyk and K.D. Palmer, "Bandwidth enhancement of microstrip patch antennas using coupled lines", IEE Electronics Letters, Vol.37, No.13, pp.806-807, 2001.

[39] A.K. Shackelford, K.F. Lee, K.M. Luk and R.C. Chair, "U-slot patch antenna with shorting pin", IEE Electronics Letters, vol.37, No.12,pp.729-730, 2001.

[40] J.S. Baligar, U.K. Revankar and K.V. Acharya, "Broadband two-layer shorted patch antenna with low cross-polarisation", IEE Electronics Letters, Vol.37, No.9, pp.547-548, 2001.

[41] G. Vermeeren, H. Rogier, F. Olyslager and D. De Zutter, "Simple low-cost planar antenna for indoor communication under the Bluetooth protocol", IEE Electronics Letters, Vol.37, No.19, pp.1153-1154, 2001.

[42] W. Menzel, M. AI-Tikriti and M.B. Espadas Lopez, "Common aperture, dual frequency printed antenna (900 MHz and 60 GHz)", IEE Electronics Letters, Vol.37, No.17, pp.1059-1060, 2001.

[43] Chi Yuk Chiu, Kam Man Shum, Chi Hou Chan, and Kwai Man Luk, "Bandwidth Enhancement Technique for Quarter-Wave Patch Antennas",IEEE Antennas and wireless propagation letters, Vol.2, pp.130-132, 2003.

[44] Kin-Lu Wong,, Yuan- Chih Lin, and Ting-Chih Tseng, "Thin Internal GSM/DCS Patch Antenna for a Portable Mobile Terminal" , IEEE Transactions on Antennas and Propagation, Vol. 54, No. 1, pp. 238-241, 2006

[45] Kin-Lu Wong, Chun-Yi Lin, Fa-Shian Chang, "Internal UMTS patch antenna for a sliding mobile phone" , Microwave and optical technology letters, Vol. 48, Issue 4 , pp. 726 – 729, 2006.

[46] Zhengwei Du, Ke Gong and Jeffrey Shiang Fu, "A Novel Compact Wide-Band Planar Antenna for Mobile Handsets" , IEEE Transactions on Antennas and Propagation, Vol. 54, No. 2, pp. 613-619, 2006.

[47] P. Ciais, C. Luxey, A. Diallo, R. Staraj, G. Kossiavas, "Pentaband internal antenna for handset communication devices" , Microwave and optical technology letters, Vol. 48, Issue 8 , , pp. 1509 – 1512, 2006.

[48] Saou-Wen Su, Kin-Lu Wong, Chia-Lun Tang, and Shih-Huang Yeh, "Wideband Monopole Antenna Integrated Within the Front-End Module Package" , IEEE Transactions on Antennas and Propagation, Vol. 54, No. 6, pp. 1888-189, 2006.

[49] Juha Villanen, Jani Ollikainen, Outi Kivekäs, and Pertti Vainikainen, "Coupling Element Based Mobile Terminal Antenna Structures" , IEEE Transactions on Antennas and Propagation, Vol. 54, No. 7, pp. 2142-2153, 2006.

[50] Tieming Xiang, K. F. Man, K. M. Luk, and C. H. Chan, "Design of Multiband Miniature Handset Antenna by MoM and HGA" , IEEE Antennas and Wireless Propagation Letters, Vol. 5, pp. 179-182, 2006

[51] Kati Sulonen, Pertti Vainkainen, "Effects of Antenna Radiation Pattern on the Performance of the Mobile Handset" , IEEE Antennas and Propagation International symposium pp. 354-357, 2005.

[52]Fa-Shian Chang,Wen-Kuan Su and Kin-Lu Wong, " Folded Meandered-Patch Monopole Antenna for Triple-Band Operation" , IEEE Antennas and Propagation International symposium pp. 278-281, 2005

[53]Kin-Lu Wong and Chun Lin, "Internal GSM/DCS Antenna Backed by a Step-Shaped Ground Plane for a PDA Phone" , IEEE Transactions on Antennas and Propagation, Vol. 54, No. 8, pp. 2408-2410, 2006.

[54] Saou-Wen Su, Kin-Lu Wong, Chia-Lun Tang, and Shih-Huang Yeh, "Internal Shorted Patch Antenna for UMTS Mobile Phone" , IEEE Antennas and Propagation International symposium, pp. 343-346, 2005.
[55] A.Serrano-Vaello and D.Sanchez-Hernandez, " Printed antennas for dual band GSM/DCS 1800 mobile handsents", Vol.34, No.2, pp.140-141,1998.

[56] R.Lelaratne and R.J. Langley, " Dual band patch antenna for monile satellite systems", IEE. Proc. Microwave and Antennas and Propagation, Vol.147, No.6, pp.427-428, 2000.

[57] D.Viratelle and R.J. Langley, " Dual-band printed antenna for mobile telephone applications", IEEE Proc. Microw. Antennas Propag., Vol.147, No.5, pp. 381-382, 2000.

[58] Y.X. Guo, K.M. Luk and K.F. Lee, " Dual-band slot loaded short circuited patch antenna" , Electronics Letters, Vol.36, No.4, pp. 289-290, 2000.

[59] F.Yang and Y.Rahmat-Samii, " Switchable dual band circularly polarized patch antenna with single feed", IEE Electronics Letters, Vol.37, No.16, pp. 1002-1003, 2001.

[60] K.L. Lau, K.M. Luk, and Deyum Lin," A wide-band Dual polarization patch antenna with directional coupler", IEEE Antennas and wireless propagation letters, Vol.1. , pp.186-189, 2002.

[61] Kin-Lu Wong, Hao-Chun Tung, and Tzung Wern Chiou, " Broadband Dual polarized aperture Coupled patch Antennas with modified H.Shaed Coupled Slots", IEEE Trasactions on ANtenans and Propagation, Vol.50, No.2, pp.188-192,2006.

[62] Kin-Lu Wong and Tzun-Wern Chiou, " Broad-Band dual polarized Patch antennas fed by capacitively coupled feed and slot-coupled feed", IEEE Trasactions on Antennas and Propagation, Vo.50, No.3, pp.346-400, 2002.

[63] Jui-Han Lu, " Broadband Dual-Frequency operation of circular patch antennas and arrays with a pair of L-Shaped Slots", IEEE Trasactions on antennas and propagation, Vol.51, No.5,pp1018-1024, 2003.

[64] Kin-Lu Wong, Gwo-Yun Lee, and Tzung-Wern Chiou , "A Low-Profile Planar Monopole Antenna for Multiband Operation of Mobile Handsets", IEEE Transactions on Antennas and Propagation, Vol. 51, No. 1, pp. 121-125, 2003

[65] G.Jaworski and V.Krozer, " Broadband matching of dual-linear polarisation stacked probe-fed microstrip patch antenna", IET Electronics Letters, vol.40, No.4, 2004

[66]Jeun-Wen Wu, Chun-Ren Lin , Jui-Han Lu, "A planar meander-line antenna for triple-band operation of mobile handsets", Microwave and optical technology letters, Vol. 41, Issue 5 , pp. 380 – 386, 2004.

[67] Design of a CPW-fed notched planar monopole antenna for multiband operations using a genetic algorithm Liu W.-C, IEE proceedings -Microwaves, Antennas and Propagation , Vol. 152, Issue 4, 5 Aug. 2005 pp. 273 – 277.

[68] Multiple band-notched planar monopole antenna for multiband wireless systems, Wang-Sang Lee, Lim W.-G Jong-Won Yu, IEEE Microwave and Wireless Components Letters, , Vol. 15, Issue 9, Sept. 2005 pp. 576 – 578.

[69] Multiband behavior of wideband Sierpinski fractal bow-tie antenna, Yamini A.H, Soleimani M., The European Conference on Wireless Technology 2005 , 3-4 Oct. 2005 pp. 503 – 506.

[70] New multiband printed meander antenna for wireless applications, Yu-Seng Liu 1, Jwo-Shiun Sun, Rui-Han Lu, Yi-Jay Lee , Microwave and optical technology letters, Vol. 47, Issue 6 , Oct 2005, pp. 539 – 543.

[71] A novel multiband fractal patch antenna, Jingjing Huang, Ning Li, Jingzhao She, Zhenghe Feng, Asia-Pacific Microwave Conference Proceedings, APMC 2005. , Vol.4, 4-7 Dec. 2005.

[72] Integrated planar multiband antennas for personal communication handsets, Martinez-Vazquez M., Litschke O, Geissler M., Heberling D, Martinez-Gonzalez A.M, Sanchez-Hernandez, IEEE Transactions on Antennas and Propagation Vol. 54, Issue 2, Part 1, Feb. 2006 pp. 384 – 391.

[73] Single and double layer planar multiband PIFAs, Sanz-Izquierdo B, Batchelor J.C, Langley R.J, Sobhy M.I, IEEE Transactions on Antennas and Propagation, Vol.54, Issue 5, May 2006 pp. 1416 – 1422.

[74] Design of multiband printed dipole antennas using parasitic elements, Jean-Marie Floc'h, Hatem Rmili, Microwave and optical technology letters, Vol. 48, Issue 8 , May 2006, pp. 1639 – 1645

[75] Modified T-shaped planar monopole antennas for multiband operation, Sheng-Bing Chen, Yong-Chang Jiao, Wei Wang, Fu-Shun Zhang, IEEE Transactions on Microwave Theory and Techniques, Vol.54, Issue 8, Aug. 2006 pp. 3267 – 3270

[76] A novel multiband dipole antenna with a microstrip loop feed, Wen-Jiao Liao, Yu-Cheng Lu, Hsi-Tseng Chou, Microwave and optical technology letters, Vol. 49, Issue 1 , Nov 2006, pp. 237 – 241

[77] Y.J.Sung and Y.-S. Kim, " Circular polarized microstrip patch antennas for broadband and dual-band operation", IEE Electronics Letters, Vol.40, No.9, 2004.

[78] W.C. Liu and W.R. Chen, " CPW-fed compact meandered patch antenna for dual-band operation", IEE Electronics Letters, Vol.40, No.18, 2004.

[79] K.Ghorbani and R.B.Waterhouse, "Dual polarized wide-band aperture stacked patch antennas", IEEE Trasactions on antennas and propagation, Vol.52, No.8, pp.2171-2175, 2004.

[80] Ka-Lam Lau, Hang Wong, Chi-Lun Mak, Kwai-man Luk, and Kai-Fong Lee, "A Vertical Patch Antenna for Dual-Band Operation", IEEE ANTENNAS AND WIRELESS PROPAGATION LETTERS, VOL. 5, pp.95-98, 2006

[81] H.-Y.A. Yim, C.-P. Kong and K.-K.M. Cheng, "Compact circularly polarised microstrip antenna design for dual-band applications", IEE Electronics Letters, Vo.42, No.7, 2006.

[82] J. Guterman, Y. Rahmat-Samii, A.A. Moreira and C. Peixeiro, "Quasi-omnidirectional dual-band backto-back E-shaped patch antenna for laptop applications", IEE Electronics Letters, Vol.42, No. 15, 2006.

[83] A.I. Abunjaileh, I.C. Hunter and A.H. Kem, "Application of dual-mode filter techniques to the broadband matching of microstrip patch antennas", IET Microwave Antennas and propagation, Vol.1, No.2, pp.273-276, 2007.

[84] A. A. Serra, P. Nepa, G. Manara, G. Tribellini, and S. Cioci, "A Wide-Band Dual-Polarized Stacked Patch Antenna", IEEE ANTENNAS AND WIRELESS PROPAGATION LETTERS, VOL. 6, pp.141-144,2007.

[85] K.L. Lau, K.C. Kong and K.M. Luk, "Dual-band stacked folded shorted patch antenna ", IEE Electronics Letters, Vol.43, No.15, 2007.

[86] L. Liu, S. Zhu and R. Langley, "Dual-band triangular patch antenna with modified ground plane", IEE Electronics Letters, Vol.43, No.3, 2007.

[87] Xue-Song Yang, Bing-Zhong Wang, Weixia Wu, and Shaoqiu Xiao, "Yagi Patch Antenna With Dual-Band and Pattern Reconfigurable Characteristics", IEEE Antennas and Wireless propagation letters, Vol.6, pp.168-172, 2007.

[88] RongLin Li, Bo Pan, Joy Laskar, IEEE, and Manos M. Tentzeris, "A Novel Low-Profile Broadband Dual-FrequencyPlanar Antenna for Wireless Handsets", IEEE TRANSACTIONS ON ANTENNAS AND PROPAGATION, Vol. 56, No. 4,pp.1155-1163, 2008.

[89] RongLin Li, Bo Pan, Joy Laskar, and Manos M. Tentzeris, "IEEE Transactions on Antennas and Propagation, Vo.56, No.4, pp.1155-1162, 2008.

[90] F.-S. Chang, K.-C. Chao, C.-H. Lu and S.-W. Su, Compact vertical patch antenna for dual-band WLAN operation, IEE Electronics Letters, Vo.44, No.10, 2008.

[91] W.K. Toh and Z.N. Chen, "Tunable dual-band planar antenna", IEE Electronics Letters, Vol.44, No.1, 2008.

[92] Nonleaky conductor backed coplanar waveguide fed rectangular microstrip patch antenna is presented by D.R. Jahagirdar et al., March 1998.

[93] Broadband CPW fed Stacked Patch Antenna, W.S.T. Rowe and R.B. Waterhouse, IEE Electronics Letters, Vol.35, No.9, April 1999.

[94] Kenneth H.Y. IP, Tommy M.Y. Kan and George V. Eleftheriades, " A single – Layer CPW FED active patch antenna", IEEE Microwave and Guided Wave Letters, Vol.10, No.2, pp.64-66, 2000

[95] W.S.T. Rowe and R.B. Waterhouse, "Reduction of Backward Radiation for CPW fed Aperture stacked patch Antenna on Small ground Planes", IEEE Transactions on Antennas and propagation, Vol.51, No.6, pp.1411-1413, 2003.

[96] Jeen-Sheen Row, " Patch antenna fed by shorted coplanar microstrip line", IET Electronics Letters, Vol.39, No.13,pp.958-959, 2003.

[97] H.Aissat, L.Cirio, M.Grzekowiak, J.-M Laheurte and O.Picon, " Circularly polarized planar antenna excited by coplanar waveguide feedline", IEE Electronics Letters, Vol.40, No.7, 2004.

[98] I-Jen Chen, Chung Shao Huang and Powen Hsu, " Cicularly polarized patch antenna array fed by coplanar waveguide", IEEE Trasactions on antennas and propagation, Vol.52, No.6, pp. 1607-1609, 2004.

[99] H.-D. Chen, " Broadband design of coplanar capacitively fed shorted patch antenna", IET Microwave and antennas propagation., Vol.2, No.6, pp.574-579, 2008.

[100] W.S.T. Rowe and R.B. Waterhouse, " Broadband CPW fed stacked patch antenna", IEE Electronics Letters, vol.35, No.9, pp.681-682, 1999.

[101] Kenneth H. Y. Ip, Tommy M.Y. Kan, and George V. Eleftheriades, " A single layer CPW fed active patch antenna", IEEE Microwave and guided wave letters, Vol.10, No.2, pp. 64-66, 2000.

[102] Jeen-Sheen Row, " A simple impedance matching technique for patch antennas fed by coplanar microstrip line", IEEE Transactions on Antennas and Propagation, Vol.53, No.10, pp.3389-3391, 2005.

[103] Jeong-Geum Kim, Hyung Suk Lee, Ho-Seon Lee, Jun-Bo Yoon and Songcheol Hong, " 60-GHz CPW Fed post supported patch antenna using micromachining technology", IEEE Microwave and wireless components letters, Vol.15, No.10, pp.635-637,2005.

[104] K. S. Yee, "Numerical solution of initial boundary value problems involving Maxwell's equations in isotropic media," IEEE Transactions on Antennas and Propagation, 1966, AP-14, 4, pp. 302-307.

[105] A.C. Cangellaris and D.B. Wright, " Analysis of the numerical error caused by the stair stepped approximation of a conducting boundary in FDTD simulations of electromagnetic phenomena", IEEE Trans.Antennas propagate., Vol.39, pp.1518-1525, 1991.

[106] R.Holland, " Pitfalls in staircase meshing", IEEE transactions on Electromagnetic compatibility, vol. EMC-35, pp.434-439, 1993.

[107] Taflove, "Review of the formulation and applications of the finite-difference time-domain method for numerical modeling of electromagnetic wave interactions with arbitrary structures," Wave Motion, 1988, 10, 6, pp. 547-582.

[108] A. Taflove and M. E. Brodwin, "Numerical solution of steady state electromagnetic scattering problems using the time-dependent Maxwell's equations," IEEE Transactions on Microwave Theory Techniques, 1975, MTT-23, 8, pp, 623-630.

[109] D.M. Sheen, Sami. M. Ali, Mohamed D. Abouzahra and Jin Au Kong, "Application of the 3D FDTD method to the analysis of planar microstrip circuits", IEEE Transactions on Microwave Theory and Techniques, Vol. 38, No. 7, pp. 849-857, July 1990.

[110]J. P. Berenger, "A perfectly matched layer for the absorption of electromagnetics waves," Journal of Computational Physics, 1994,1 14, 1, pp. 185-200

[111] Reineix and B. Jecko, "Analysis of microstrip patch antennas using finite difference time domain method," IEEE Transaclions on Anlennas and Propagation, , 1989.AP-37, 1 1 , pp. 1361-1369.

[112] P. Leveque, A. Reineix, and B. Jecko, "Modelling dielectriclosses in microstrip patch antennas: Application of FDTD method," Electronics Letters, 1992, 28, 6, pp. 539-540

[113] C. Wu, K.-L. Wu, Z.-Q. Bi, and J. Litva, "Accurate characterization of planar printed antennas using finite-difference time domain method," IEEE Transactions on Antennas and Propagation, 1992, AP-40, 5, pp. 526-533.

64

[114] K. Uehara and K. Kagoshima, "FDTD method analysis of mutual coupling between microstrip antennas," IEICE Transactions on Commiinicatiotn, 1993, E76-B, 7, pp. 762-764.

[115] T. Oonishi, T. Kashiwa, and I. Fukai, "Analysis of microstrip antennas on a curved surface using the conformal grids FD-TD method," Electronics and Conimunications in Japan, Part 1, 1993, pp. 73-81

[116] T. Kashiwa, T. Onishi, and I. Fukai, "Analysis of microstrip antennas on a curved surface using the conformal grids FD-TD method," IEEE Transactions on Antennas and Propagation, AP-42, 3, 1994.pp. 423-427

[117] Y. Qian, S. Iwata, and E. Yamashita, "Optimal design of an offset-fed, twin-slot antenna element for millimeter-wave imaging arrays," IEEE Microumv aiid Guided Wave Letters, 4, 7, pp. 232-234, 1994.

[118] A. Reineix and B. Jecko, "A time domain theoretical method for the analysis of microstrip antennas composed by slots," Annales des Telecommunications, 48, 112, pp. 29-34, 1993.

[119] A. Reineix, J. Paillol, and B. Jecko, "FDTD method applied to the study of radar cross section of microstrip patch antennas," Annales des Telecommunications, 48, 11/12, pp. 589-593, 1993.

[120] A. Reineix, C. Melon, T. Monediere, and F. Jecko, "The FDTD method applied to the study of microstrip patch antennas with a biased ferrite substrate," Annales des Telecommunications, 49, 314, pp. 137-142, 1994

[121] M. A. Jensen and Y. Rahmat-Samii, "EM interaction of handset antennas and a human in personal communications," Proceedingsof the IEEE, 83, 1, pp, 7-17, 1995.

[122] H. Y . Chen and H. H. Wang, "Current and S A R induced in a human head model by electromagnetic fields irradiated from a cellular phone," IEEE Transactions on Microwave Theory Techniques, MTT-42, 12, pp. 2249-2254, 1994.

[123] L. Martens, J. De Moerloose, D. De Zutter, J. De Poorter, and C. De Wagter, "Calculation of the electromagnetic fields induced in the head of an operator of a cordless telephone," Radio Science, 30, 1, pp. 283-290, 1995

[124] R. Luebbers, L. Chen, T. Uno, and S. Adachi, "FDTD calculation of radiation patterns, impedance, and gain for a monopole antenna on a conducting box," IEEE Transactions on Antennas andpropagation, AP-40, 12, pp, 1577-1583, 1992.

[125] L. Chen, T. Uno, S. Adachi, and R. J. Luebbers, "FDTD analysis of a monopole antenna mounted on a conducting box covered with a layer of dielectric," IEICE Transactions on Communications, E76-B, 12, pp. 1583-1586, 1993.

[126] Toftgird, S. N. Hornsleth, and J. B. Andersen, "Effects on portable antennas of the presence of a person," IEEE Transactions on Antennas and Propagation, vol. 41, No.6, pp, 739-746, 1993.

[127] M. A. Jensen and Y. Rahmat-Samii, "Performance analysis of antennas for hand-held transceivers using FDTD," IEEE Transactions on Antennas and Propagation, vol. 42, No.8 , pp. 1106-1 113, 1994.

[128] 3-D FDTD design analysis of a 2.4-GHz polarization-diversity printed dipole antenna with integrated balun and polarization-switching circuit for WLAN and wireless communication applications, Huey-Ru Chuang, Liang-Chen Kuo, IEEE Transactions on Microwave Theory and Techniques, , Vol. 51, Issue 2, Part 1, Feb. 2003 pp. 374 – 381

[129] Pattern reconfigurable leaky-wave antenna design by FDTD method and Floquet's Theorem, Shaoqiu Xiao, Zhenhai Shao;, Fujise M, Bing-Zhong Wang, IEEE Transactions on Antennas and Propagation, Vol. 53, Issue 5, May 2005 pp. 1845 – 1848

[130] FDTD analysis of CPW-fed folded-slot and multiple-slot antennas on thin substrates Huan-Shang Tsai, York R.A., IEEE Transactions on Antennas and Propagation, Vol. 44, Issue 2, Feb. 1996, pp. 217 – 226

[131] M. Kar and P.F Wahid, " The FDTD analysis of a microstrip patch antenna with dual feed lines, "Proc. IEEE southeast conference, April 24-26, 1988.

[132] Supriyo Dey and Raj Mittra "A conformal Finite Difference Time Domain technique for modeling cylindrical dielectric resonators, "IEEE Trans. Microwave Theory and Tech., Vol. 47, no. 9, pp. 1737-1739, September 1999.

[133] FDTD analysis of radiation pattern of antenna on truncated ground plane, Yamamoto D, Arai H, Microwave Conference, 2000 Asia-Pacific, 3-6 Dec. 2000 pp. 378 – 381

Chapter 3

Methodology

This chapter provides the experimental and simulation methodology utilized for the analysis. The prototype of different antenna geometries were fabricated using photolithographic process and the antenna characterization is done with Vector Network Analyzer in the anechoic chamber. Parametric analysis of different antenna parameters are carried out using Ansoft HFSS and theoretical analysis in FDTD method is done in Matlab^{TM}.

3.1 Antenna Fabrication:

The accuracy of the antenna dimension is very critical in microwave frequencies. Therefore photolithographic technique is used to fabricate the antenna geometry. Photolithography is the process of transferring geometrical shapes from a photo-mask to a surface.

The various steps involved in the photolithographic technique are illustrated in fig.3.1
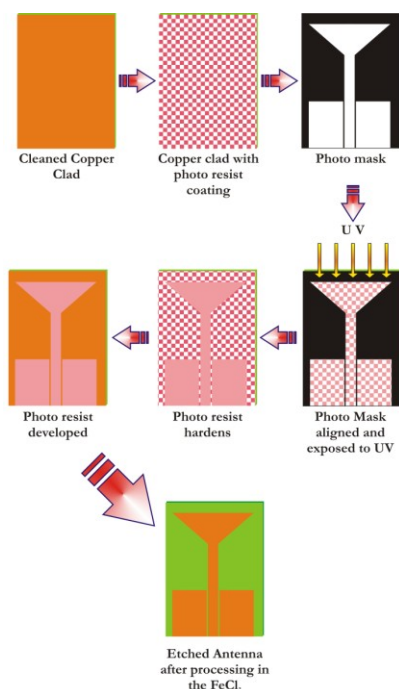
Fig.3.1 Different photolithographic steps.

The CAD drawing of the antenna is printed on a high quality butter paper with a high resolution laser printer. The copper clad of suitable dimension is cleaned with a suitable chemical like acetone to remove any chemical impurities. A thin layer of photo resist material is then applied over the copper clad using a high speed spinner. The antenna mask is carefully aligned over the photo resist coated

69

clad and exposed to UV. An extreme care must be taken to ensure that no dust or impurities are present in between the mask and copper clad. The layer of photo resist material in the exposed portions hardens, while the unexposed region remains the same and it can be removed by carefully rinsing with a suitable developer solution. The unwanted copper over the copper clad can be removed by processing the copper clad in a ferric chloride ($FeCl_3$) solution. The laminate is then cleaned to remove the hardened photo resist using acetone solution.

3.2 Antenna measurement facilities

A brief description of equipments and facilities used for the measurements of antenna characteristics is presented in this section.

3.2.1 Agilent E8362B PNA based measurement setup

The Agilent E8362B vector network analyzer is a member of the PNA Series network analyzer platform and provides the combination of speed and precision for the demanding needs of today's high frequency, high-performance component test requirements. The PNA Series meets these testing challenges by providing the right combination of fast sweep speeds, wide dynamic range, low trace noise and flexible connectivity. The operating frequency of the system is from 10 MHz to 20 GHz. It has 16, 001 points per channel with < 26 µsec/point measurement speed. The measurement setup along with the specifications of the VNA is depicted in fig.3.2[1,2]

Operating Band	10MHz to 10 GHz
IF Bandwidth	1Hz to 40KHz
RF Connector	3.5mm, 50 Ω
CPU	Intel Pentium 1.1 GHz
I/O ports	USB, LAN, GPIB
O/S	Windows XP
Measurement Automation Software	CREMA Soft
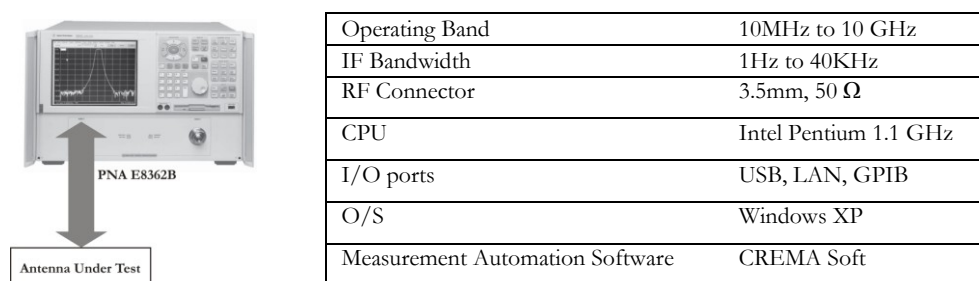
Fig.3.2 Measurement setup and PNA Specifications

3.2.1.1 Returnloss Measurement

Inorder to measure the returnloss characteristics of the antenna under test, the antenna is connected to any one of the network analyzer port and operating the VNA in S_{11} or S_{22} mode. The specific port of the analyzer should be calibrated for the frequency range of interest using the standard open, short and matched load, prior to the measurement. The S_{11} values of the antenna in the entire frequency band are then stored on a computer in Comma Separated Variable, 'CSV', format with the help of 'CREMA SOFT'-the measurement automation software. The frequency at which the returnloss value minimum is taken as the resonant frequency of the antenna. The range of frequency for which the returnloss value is within the -10dB points is usually treated as the band width of the antenna, usually expressed as the percentage of bandwidth.

3.2.1.2 Efficiency Measurement:

The antenna efficiency is estimated using wheeler cap method[3] by making two impedance measurements. The one is the input impedance before using the metallic cap over the antenna and the other one after putting the metallic cap. If the test antenna behaves like a series RLC circuit near its resonance, then the input resistance R should decrease after applying the cap, and the efficiency is calculated by the following expression.,

71

$$\eta = \frac{P_R}{P_R + P_L} = \frac{R_R}{R_R + R_L} = \frac{R_{nocap} - R_{cap}}{R_{nocap}}$$

3.2.2 HP 8510C VNA based Radiation pattern measurement Setup.

The diagram representation of the measurement setup is illustrated in fig.3.3,
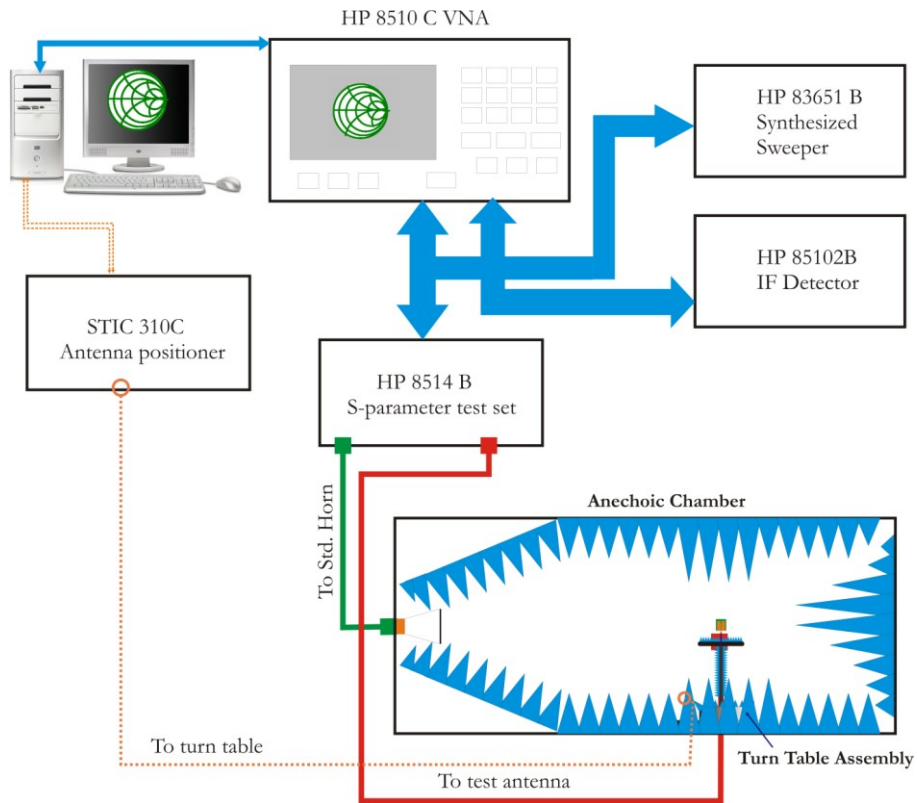
Fig.3.3 Radiation Pattern Measurement Setup

The major system components and measurement procedures are as follows,

3.2.2.1 Anechoic Chamber

The Anechoic chamber is an acoustic free room used to measure the antenna characteristics accurately [4]. The room consists of microwave absorbers fixed on the walls, roof and floor to avoid EM reflections. High quality low foam impregnated with dielectrically / magnetically lossy medium is used to make the microwave absorber. The tapered shapes of the absorber provide good impedance matching for the microwave power impinges upon it. Aluminium sheets are used to shield the chamber from electromagnetic interference from surroundings.

3.2.2.2 Turn table assembly for far field radiation pattern measurement

A turntable assembly consists of a microcontroller based antenna positioner, interfaced with an IBM pc for the radiation pattern measurement. The antenna under test (AUT) is mounted over the turntable assembly and a linearly polarized; wideband standard horn antenna is used as the transmitter for the radiation pattern measurement. The main lobe tracking for gain measurement as well as the polarization pattern measurement are carried out through this setup. The matlab based graphical user interface (GUI) manages the antenna characterization by synchronizing each component in the system.

3.2.2.3 Radiation Pattern Measurement.

The radiation pattern measurement is carried out in the anechoic chamber with the help of HP 8510c VNA. The antenna under test is mounted on a turntable assembly in the anechoic chamber and connected to one port of the network analyzer configured in the receiver mode. The other port of the network analyzer is connected to a wideband horn which act as the transmitter. The network analyzer and the turntable controller are interfaced to a computer which runs the measurement automation software "CREMA SOFT". The measurement

automation software requires *the measurement band*, *angular step size* and *file name* as input. The system automatically undergoes through calibration prior to the measurement and performs the transmission measurement for each step angle and records the angular transmission characteristics in a data file specified by the *file name*.

3.2.2.4 Antenna Gain Measurement

Gain transfer method is employed to measure the gain of the antenna [5]. The experimental setup for determining the gain is similar to the radiation pattern measurement setup. The gain of the AUT is measured relative to the power levels detected by a standard gain antenna. Inorder to measure the gain of AUT, the standard gain antenna is mounted on the turntable and a through calibration is performed at boresight direction. The AUT is carefully mounted over the turntable and extreme care is taken for the exact alignment. The relative power level is obtained from the analyzer and this provides the gain with respect to the standard antenna. The gain of the standard antenna is added to the relative gain to obtain the gain of the AUT.

3.3 The FDTD Method:

The Finite Difference Time Domain method is widely used for the theoretical analysis for microwave engineering. The technique provides a simple method for solving the Maxwell's equations by grid based differential time-domain numerical modeling method. The time dependent Maxwell equations in partial differential form are discretized using central –difference approximations to the space and time partial derivatives. K.S. Yee[6] proposed a modified form of Transmission Line Matrix(TLM) method, which formed the base of FDTD technique. This method solves the Maxwell's equations in a differential form discretized in space and time and tracks the time-varying fields throughout the volume of space.

74

3.3.1 Basic Concepts:

A function in time and space can be written as,

$$F^n(i, j, k) = F(i\Delta x, j\Delta y, k\Delta z, n\Delta t) \rightarrow (1)$$

The increment in time is represented by Δt, n is the time index and Δx, Δy, Δz are the space increments along the three coordinate,

The derivatives of the function F in eq. 1 can be written using central finite difference approximation as,

$$\frac{\partial F^n(i, j, k)}{\partial x} = \frac{F^n(i+1/2, j, k) - F^n(i-1/2, j, k)}{\Delta x} \rightarrow (2)$$

$$\frac{\partial F^n(i, j, k)}{\partial t} = \frac{F^{n+1/2}(i, j, k) - F^{n-1/2}(i, j, k)}{\Delta t} \rightarrow (3)$$

The basic formulation of FDTD method [7] is based on the differential formulation of Maxwell's Curl equations with piecewise, uniform, isotropic and homogeneous media.

$$\mu \frac{\partial H}{\partial y} = -\nabla \times E \rightarrow (4)$$

$$\varepsilon \frac{\partial E}{\partial t} = -\nabla \times H \rightarrow (5)$$

The above equations can be written in Cartesian coordinates as,

$$\frac{\partial \mathrm{H}x}{\partial t} = \frac{1}{\mu}\left(\frac{\partial \mathrm{E}y}{\partial z} - \frac{\partial \mathrm{E}z}{\partial y}\right) \rightarrow (6)$$

$$\frac{\partial \mathrm{H}y}{\partial t} = \frac{1}{\mu}\left(\frac{\partial \mathrm{E}z}{\partial x} - \frac{\partial \mathrm{E}x}{\partial z}\right) \rightarrow (7)$$

$$\frac{\partial \mathrm{H}z}{\partial t} = \frac{1}{\mu}\left(\frac{\partial \mathrm{E}x}{\partial y} - \frac{\partial \mathrm{E}y}{\partial x}\right) \rightarrow (8)$$

$$\frac{\partial \mathrm{E}x}{\partial t} = \frac{1}{\varepsilon}\left(\frac{\partial \mathrm{H}z}{\partial y} - \frac{\partial \mathrm{H}y}{\partial z} - \sigma \mathrm{E}x\right) \rightarrow (9)$$

$$\frac{\partial \mathrm{E}y}{\partial t} = \frac{1}{\varepsilon}\left(\frac{\partial \mathrm{H}x}{\partial z} - \frac{\partial \mathrm{H}z}{\partial x} - \sigma \mathrm{E}y\right) \rightarrow (10)$$

$$\frac{\partial \mathrm{E}z}{\partial t} = \frac{1}{\varepsilon}\left(\frac{\partial \mathrm{H}y}{\partial x} - \frac{\partial \mathrm{H}x}{\partial y} - \sigma \mathrm{E}z\right) \rightarrow (11)$$

By applying finite difference to the above scalar equations, the following equations can be derived,

$$
\begin{aligned}
H_y^{n+1/2}(i+1/2, j, k+1/2) = {} & H_y^{n-1/2}(i+1/2, j, k+1/2) \\
& + \left[\frac{\Delta t}{\mu.\Delta x}\right]\left(E_z^n(i+1, j, k+1/2) - E_z^n(i, j, k+1/2)\right) \\
& - \left[\frac{\Delta t}{\mu.\Delta z}\right]\left(E_x^n(i+1/2, j, k+1) - E_x^n(i+1/2, j, k)\right) \rightarrow (12)
\end{aligned}
$$

$$
\begin{aligned}
H_z^{n+1/2}(i+1/2, j+1/2, k) = {} & H_z^{n-1/2}(i+1/2, j+1/2, k) \\
& + \left[\frac{\Delta t}{\mu.\Delta y}\right]\left(E_x^n(i+1/2, j+1, k) - E_x^n(i+1/2, j, k)\right) \\
& - \left[\frac{\Delta t}{\mu.\Delta x}\right]\left(E_y^n(i+1, j+1/2, k) - E_y^n(i, j+1/2, k)\right) \rightarrow (13)
\end{aligned}
$$

$$
\begin{aligned}
E_x^{n+1}(i+1/2, j, k) = {} & E_x^n(i+1/2 j, k) \\
& + \left[\frac{\Delta t}{\varepsilon.\Delta y}\right]\left(H_z^{n+1/2}(i+1/2, j+1/2, k) - H_z^{n+1/2}(i+1/2, j-1/2, k)\right) \\
& - \left[\frac{\Delta t}{\varepsilon.\Delta z}\right]\left(H_y^{n+1/2}(i+1/2, j, k+1/2) - H_y^{n+1/2}(i+1/2, j, k-1/2)\right) \rightarrow (14)
\end{aligned}
$$

$$H_x^{n+1/2}(i,j+1/2,k+1/2) = H_x^{n-1/2}(i,j+1/2,k+1/2)$$
$$+\left[\frac{\Delta t}{\mu.\Delta z}\right]\left(E_y^n(i,j+1/2,k+1)-E_y^n(i,j+1/2,k)\right)$$
$$-\left[\frac{\Delta t}{\mu.\Delta y}\right]\left(E_z^n(i,j+1,k+1/2)-E_z^n(i,j,k+1/2)\right) \rightarrow (15)$$

$$E_z^{n+1}(i,j,k+1/2) = E_z^n(i,j,k+1/2)$$
$$+\left[\frac{\Delta t}{\varepsilon.\Delta x}\right]\left(H_y^{n+1/2}(i+1/2,j,k+1/2)-H_y^{n+1/2}(i-1/2,j,k+1/2)\right)$$
$$-\left[\frac{\Delta t}{\varepsilon.\Delta y}\right]\left(H_x^{n+1/2}(i,j+1/2,k+1/2)-H_x^{n+1/2}(i,j-1/2,k+1/2)\right) \rightarrow (16)$$

$$E_y^{n+1}(i,j+1/2,k) = E_y^n(i,j+1/2,k)$$
$$+\left[\frac{\Delta t}{\varepsilon.\Delta z}\right]\left(H_x^{n+1/2}(i,j+1/2,k+1/2)-H_x^{n+1/2}(i,j+1/2,k-1/2)\right)$$
$$-\left[\frac{\Delta t}{\varepsilon.\Delta x}\right]\left(H_z^{n+1/2}(i+1/2,j+1/2,k)-H_z^{n+1/2}(i-1/2,j+1/2,k)\right) \rightarrow (17)$$

Yee has proposed a three dimensional cell in which the electric fields lie along the midpoints of the cell edges and the magnetic fields are along the centre of the cell faces as depicted in fig.3.4
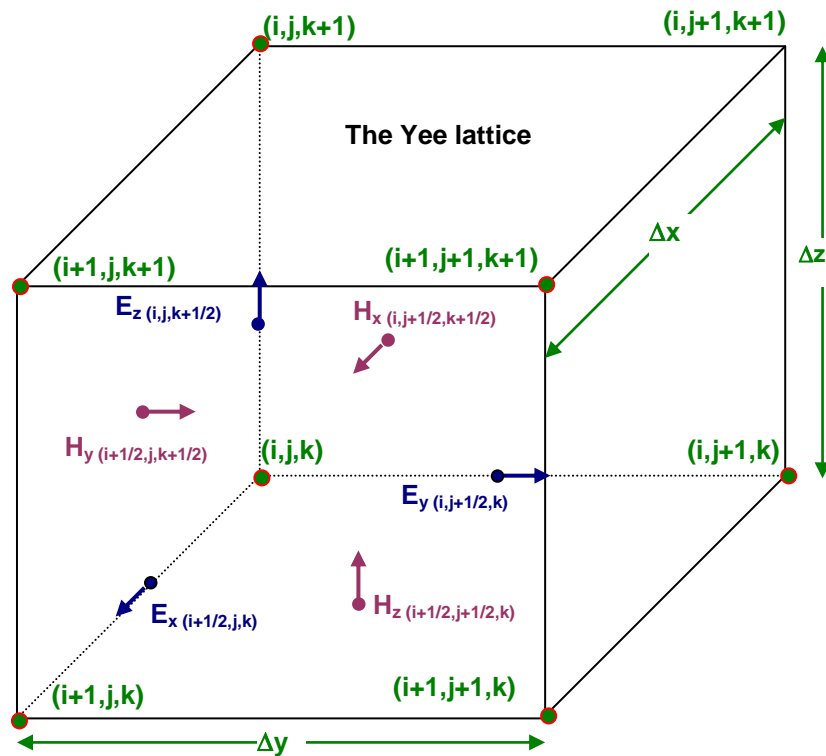
Fig. 3.4 Basic Yee Cell

Equations 12-17 are used to evaluate the Electric and Magnetic fields at alternate half time steps and each field components are computed in each time step, Δt. The filed equations are updated in each layer of the geometry and its value depend upon its value in the previous time step and the previous value of the other component at the adjacent special point. In order to make the coding in a programming language easier, Sheen et al.[8] renamed the indices of the field components, eliminating the ½ index notations. This provides the value of each field component to be stored in a three dimensional array, with the array indices corresponding to the spatial indices. The equations suggested by Sheen are,

78

$$H_{x,i,j,k}^{n+1/2} = H_{x,i,j,k}^{n-1/2} + \frac{\Delta t}{\mu \Delta z}\left(E_{y,i,j,k}^{n} - E_{y,i,j,k-1}^{n}\right) - \frac{\Delta t}{\mu \Delta y}\left(E_{z,i,j,k}^{n} - E_{z,i,j-1,k}^{n}\right) \rightarrow (18)$$

$$H_{y,i,j,k}^{n+1/2} = H_{y,i,j,k}^{n-1/2} + \frac{\Delta t}{\mu \Delta x}\left(E_{z,i,j,k}^{n} - E_{z,i-1,j,k}^{n}\right) - \frac{\Delta t}{\mu \Delta z}\left(E_{x,i,j,k}^{n} - E_{x,i,j,k-1}^{n}\right) \rightarrow (19)$$

$$H_{z,i,j,k}^{n+1/2} = H_{z,i,j,k}^{n-1/2} + \frac{\Delta t}{\mu \Delta y}\left(E_{x,i,j,k}^{n} - E_{x,i,j-1,k}^{n}\right) - \frac{\Delta t}{\mu \Delta x}\left(E_{y,i,j,k}^{n} - E_{y,i-1,j,k}^{n}\right) \rightarrow (20)$$

$$E_{x,i,j,k}^{n+1} = E_{x,i,j,k}^{n} + \frac{\Delta t}{\varepsilon \Delta y}\left(H_{z,i,j+1,k}^{n+1/2} - H_{z,i,j,k}^{n+1/2}\right) - \frac{\Delta t}{\varepsilon \Delta z}\left(H_{y,i,j,k+1}^{n+1/2} - H_{y,i,j,k}^{n+1/2}\right) \rightarrow (21)$$

$$E_{y,i,j,k}^{n+1} = E_{y,i,j,k}^{n} + \frac{\Delta t}{\varepsilon \Delta z}\left(H_{x,i,j,k+1}^{n+1/2} - H_{x,i,j,k}^{n+1/2}\right) - \frac{\Delta t}{\varepsilon \Delta x}\left(H_{z,i+1,j,k}^{n+1/2} - H_{z,i,j,k}^{n+1/2}\right) \rightarrow (22)$$

$$E_{z,i,j,k}^{n+1} = E_{z,i,j,k}^{n} + \frac{\Delta t}{\varepsilon \Delta x}\left(H_{y,i+1,j,k}^{n+1/2} - H_{y,i,j,k}^{n+1/2}\right) - \frac{\Delta t}{\varepsilon \Delta y}\left(H_{x,i,j+1,k}^{n+1/2} - H_{x,i,j,k}^{n+1/2}\right) \rightarrow (23)$$

The leaf-frog integration proposed by Yee is employed for the discretization in space and time and is shown in fig.3.5

Discretization in space and time

Leap frog time integration
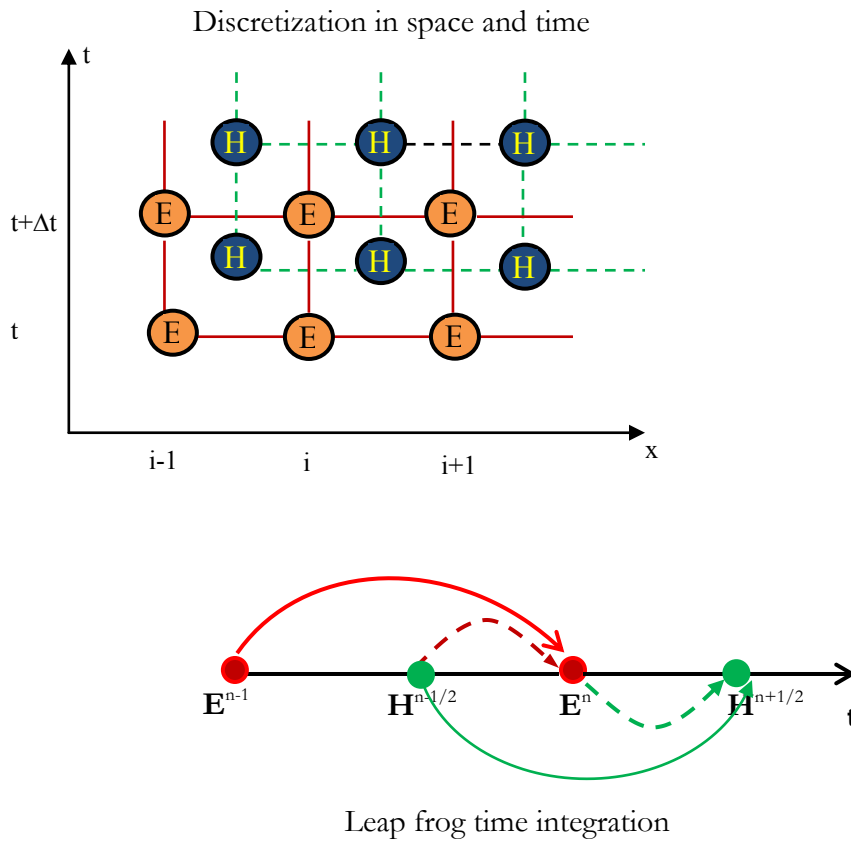
Fig.3.5 The FDTD technique by Yee.

3.3.2 Boundary conditions

As in the case of any computational electromagnetic method, FDTD technique requires complicated computational efforts and unlimited computational resources. In order to minimize the computational resources, the simulation domain is truncated and this results spurious fields from the boundaries unless appropriate techniques are employed to minimize this effects. The boundary condition should ensure that the outgoing wave is completely absorbed at the boundary, making domain appear infinite in extend with minimum numerical back reflection.

Perfectly matched layer (PML) boundary condition [9] is employed in theoretical modeling used in this thesis. In PML an artificial layer of absorbing material is placed around the outer boundary of the computational domain. The plane wave incident from the FDTD free space to the PML region at an arbitrary angle is completely absorbed.

3.3.3 The Nyquist Criterion

The Nyquist sampling theorem states that there must be at least two samples per spatial period for adequate sampling [10]. In most cases the sampling is not exact and the smallest wavelength is not precisely determined and more than two samples per wavelength is suggested.

3.3.4 Stair case approximation for the source modeling.

The feeding point is modeled using Lubber's[11] stair case approach. The mesh transition from the electric field source location to the full width of the coplanar wave guide is modeled as shown in the fig. 3.6
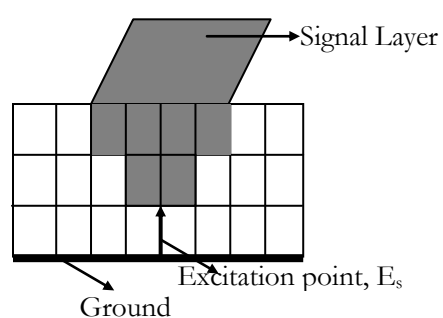
Fig. 3.6   Stair cased approach for the Feed modeling

It is seen from the stair cased transition in feed line that the substrate is discretized in order to incorporate more than one Yee cell. A gap feed model can

be obtained by applying the excitation field between the microstrip line and the ground plane using a stair cased mesh transition

3.3.5   The FDTD Flowchart:

The FDTD flow chart is illustrated in fig. 3.7.
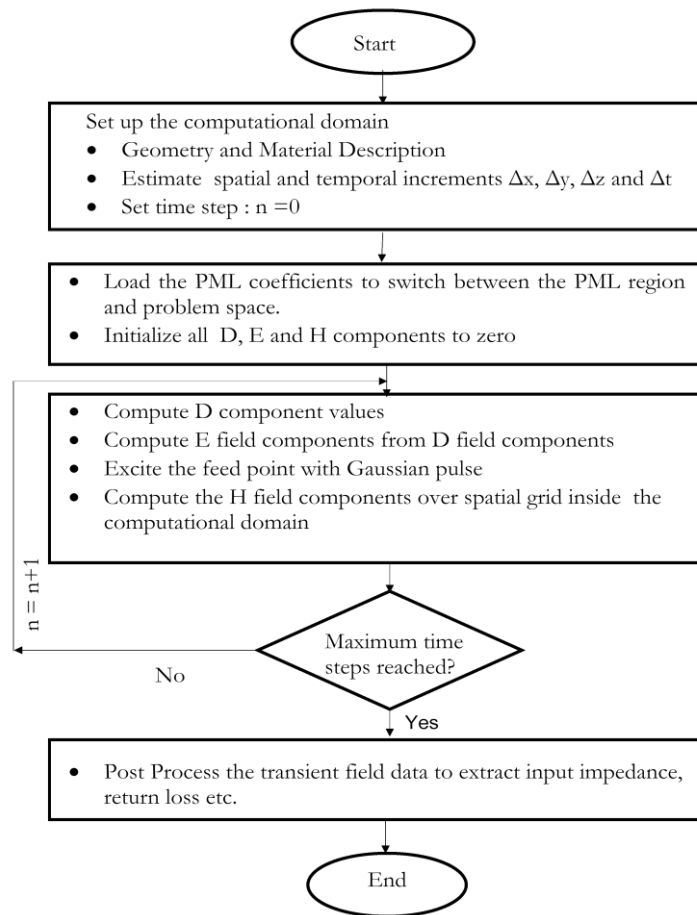
Fig. 3.7 The FDTD flowchart.

3.4 Simulation tool – Ansoft HFSS.

High Frequency Structure Simulator is a commercial Finite Element Method(FEM) solver for electromagnetic structures from Ansoft Corporation[12]. It is one of the most popular and powerful applications used for the complex RF electronic circuit elements and filters.

The simulations in this thesis is done with the help of Ansoft HFSS. The optimization tool available with HFSS is very useful for antenna engineers to optimize the antenna parameters very accurately. There are many kinds of boundary schemes and excitation techniques available in HFSS. Radiation boundary and PEC boundary are widely used in this work. The vector as well as scalar representation of E,H and J values of the device under simulation gives a good insight in to the problem under simulation.

References:

[1] Agilent PNA Microwave Network Analyzers Data Sheet.

[2] New Network Analyzer methodologies in Antenna/ RCS measurements, White Paper, Agilent Technologies.

[3] Hosung Choo; Rogers, R.; Hao Ling, "On the Wheeler cap measurement of the efficiency of microstrip antennas", IEEE Transactions on Antennas and Propagation, Vol.53, No.7,2005.

[4] Chung, B.K.; Chuah, H.T., "Design and construction of a multipurpose wideband anechoic chamber", IEEE Antennas and Propagation Magazine,Vol.45, No.6, 2003.

[5] Constantine A Balanis, Antenna Theory analysis and design, John Wiley & Sons, 2005.

[6] K.S.Yee, "Numerical solution of initial boundary value problems involving Maxwell's equations in isotropic media," IEEE Trans. Antennas Propagat. Vol.14, no.4, pp.302-307, May 1966.

[7] Andrew F Peterson, Scott L Ray and Raj Mittra, " Computational methods for electromagnetic, " University press, India, 2001.

[8] David M. Sheen, Sami M.Ali, Mohamed D. Abouzahra and Jin Au Kong, "Application of the three dimensional finite difference time domain method to the analysis of planar Microstrip circuits, " IEEE Trans. Microwave Theory and Tech., Vol. 38, pp. 849-857.

[9] Jean Pierre Berenger, " A perfectly matched layer for the absorption of electromagnetic waves", Journal of Computational physics, 114, pp.185-200, 1994.
[10] Allen Taflov, " Computational electromagnetic: The Finite Difference Time Domain method", Artech house publishers, London, 1995.

[11] R.J. Luebbers and H.S. Langdon, " A Simple feed model that reduces time steps needed for FDTD antenna and Microstrip calculatons", IEEE Trans. Antennas Propagat., Vol.44, pp.1000-1005, July 1996.

[12] HFSS User manual, Ansoft Corporation, USA.

Development of a Flared Monopole Antenna from the Coplanar Wave Guide Fed Strip Monopole

The wireless communication industry is integrating a number of services like Bluetooth, WLAN etc to the hand held communication devices. Therefore, in the present scenario, the bandwidth requirement of the antenna while maintaining the compactness becomes more critical.

Transmission lines are energy guiding devices that can be used to transfer electromagnetic signal from one part of the system to another. The coplanar waveguide has made much attention in the high frequency researchers because of its attractive features. This chapter presents the results of the investigations carried out to find the radiations characteristics or resonance phenomena in a finite ground coplanar waveguide fed strip monopole.

The first part of this chapter includes results of investigations carried out to study the behavior of a finite ground coplanar wave guide fed strip monopole while the second part of the chapter provides the development of a flared monopole antenna from the strip monopole. A parametric study which depicts the effect of various antenna parameters is carried out and conclusions are made from the results. The analysis includes simulation studies using Ansoft HFSS and measured results with Vector Network Analyzer.

The analysis carried out in this chapter is summarized in Table 4.1

Parameter	Measurements Conducted
Finite ground dimensions (L_g, W_g)	Returnloss, Radiation Pattern, Current density plots, Gain and Efficiency
Substrate parameters (ε_r, h)	
Monopole Length(L_m)	
Effect of flaring (W_f, L_f)	

Table 4.1 : Summary of the Analysis

4 – I. Finite Ground Coplanar Waveguide(FGCPW) fed Strip Monopole Antenna

4.1 Antenna Geometry

The analysis of finite ground coplanar waveguide fed monopole antenna is presented in this session. The antenna consists of a coplanar wave guide designed for 50Ω input impedance, fed with an SMA connector. The center conductor of the FGCPW is extended to form a strip monopole of dimension 'L_m'. The initial design parameters for the FGCPW fed strip monopole antenna are, L_g = 15mm, W_g = 10mm, g = 0.35mm, W_c = 3mm and L_m = 20mm. The geometry of the strip monopole antenna is depicted in fig 4.1
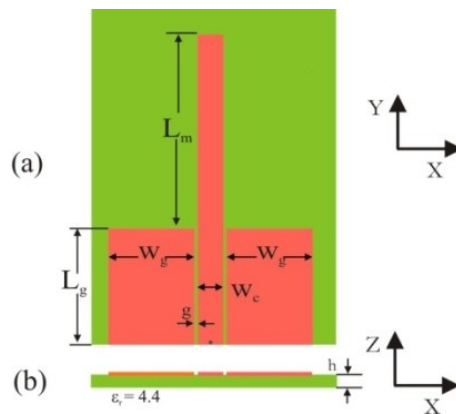
Fig.4.1 Geometry of the Finite Ground Coplanar Waveguide Fed Strip Monopole Antenna.(L_g = 15mm, W_g = 10mm, g = 0.35mm, W_c = 3mm, L_m = 20mm, h=1.6mm and ε_r=4.4).

4.2 Resonance in FGCPW fed Strip monopole:

The current variation at the surface of the FGCPW fed strip monopole is plotted in fig. 4.2 at the resonant frequency and analyzed. A better understanding about the resonance and radiation behavior of the strip monopole is obtained from the analysis.
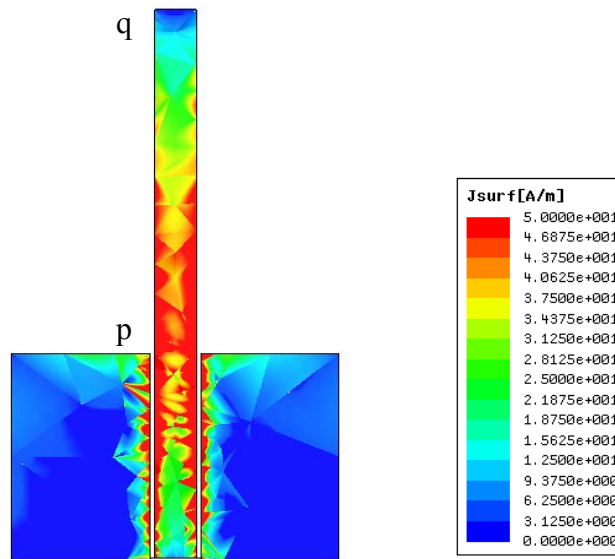
Fig.4.2 computed surface current density of the FGCPW fed strip monopole antenna at 2.53 GHz.(L_g = 15mm, W_g = 10mm, g = 0.35mm, W_c = 3mm, L_m = 20mm, h=1.6mm and ε_r=4.4)

It can be found from the surface current density plot drawn at the resonant frequency of the finite ground CPW strip monopole antenna that, the current at the position 'p' is maximum and a minima is observed at the tip 'q' of the monopole. That is nearly a quarter wave variations along the length of the strip monopole which corresponds to the resonant frequency. A strong interaction between the ground plane and strip monopole is observed at the interface. It is also observed that the current variation along the ground plane dimension is feeble.

4.3 Return loss Characteristics of FGCPW fed Monopole

The measured and simulated returnloss characteristics of the FGCPW strip monopole is illustrated in fig. 4.3
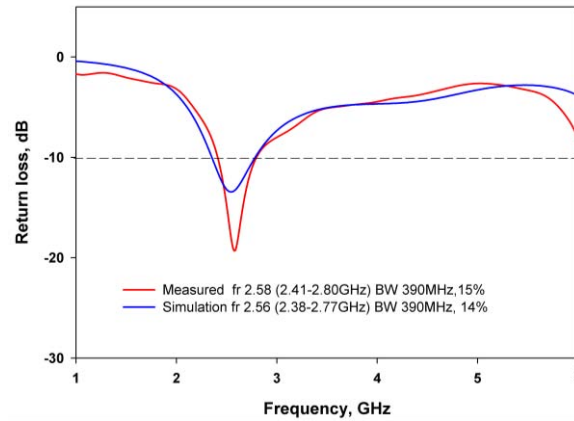
(a)
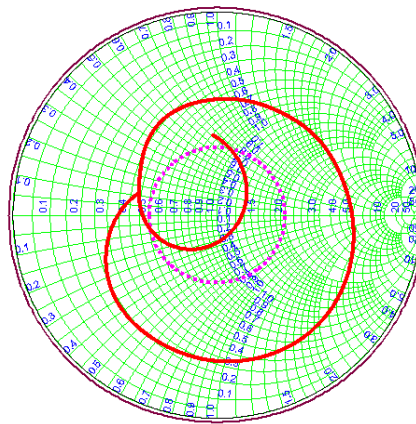
(b)

Fig.4.3 Measured and simulated returnloss characteristics of FGCPW fed SMA. (L_g = 15mm, W_g = 10mm, g = 0.35mm, W_c = 3mm, L_m = 20mm, h=1.6mm and ε_r=4.4)

It is evident from the plot that the simulation result predicts the resonant frequency and bandwidth of the antenna with a reasonable accuracy. It is seen experimentally that the FGCPW fed strip monopole is resonating at 2.58GHz with a 2:1 VSWR bandwidth of 15 % covering 2.41 GHz to 2.80 GHz while the simulated result gives a resonant frequency of 2.56 GHz covering the impedance band from 2.38GHz to 2.77GHz.

4.4 Polarization:

The polarization of the antenna can be observed from the current density plot in vector form at the resonance and is illustrated in fig.4.4
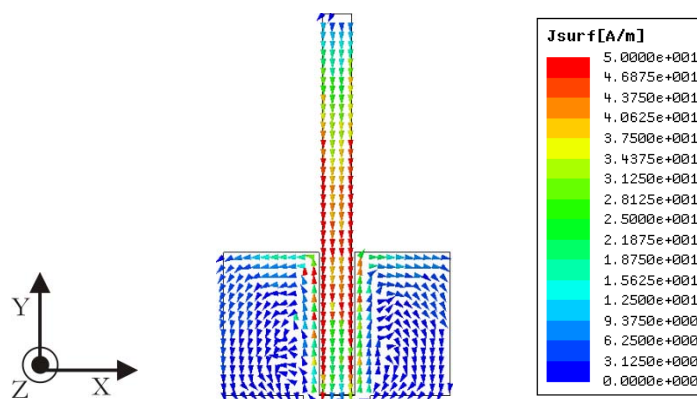
Fig.4.4 computed surface current density of the FGCPW fed strip monopole antenna at 2.53 GHz in vector format. (L_g = 15mm, W_g = 10mm, g = 0.35mm, W_c = 3mm, L_m = 20mm, h=1.6mm and ε_r=4.4)

It is found from the computed surface current plot of the FGCPW fed strip monopole antenna that the strip monopole has a strong radiation at the resonance while the ground has feeble effect. The direction of the current at both sides of the gap which separate the centre conductor and ground plane are almost equal in magnitude and opposite in direction. It is also worth to note that the current at the top edges of the ground plane are equal and opposite of phase.

Therefore they cancel each other in the far field and do not contribute for any radiation.

By analyzing the strip-monopole, it is found that the current direction throughout the strip is along the Y-direction which results Y polarized radiation.

In order to experimentally verify the polarization of the strip monopole, the far field transmission characteristic is measured by utilizing highly linearly polarized standard horn antenna as the receiver and the test antenna as the transmitter. Both the antennas are aligned in bore sight direction so as to receive maximum power. The measured transmission characteristics are plotted in fig.4.5
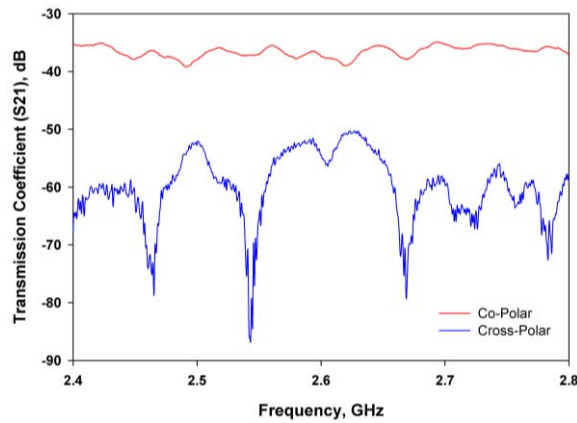
Fig.4.5 Measured transmission characteristics of the FGCPW fed strip monopole (L_g = 15mm, W_g = 10mm, g = 0.35mm, W_c = 3mm, L_m = 20mm, h=1.6mm and ε_r=4.4)

It is clear from the measurement results that the cross polarization level throughout the resonant band is better than 10 dB. The measurement results are in good agreement with the predicted polarization of the antenna from the simulated current density plots.

4.5 Radiation Pattern.

The simulated 3D radiation pattern at 2.56GHz extracted from the simulation results, using Ansoft HFSS is shown in the fig.4.6. It can be seen from the plot that the FGCPW fed strip monopole is a good radiator with almost omni-directional radiation coverage and can be used for applications in mobile terminals.
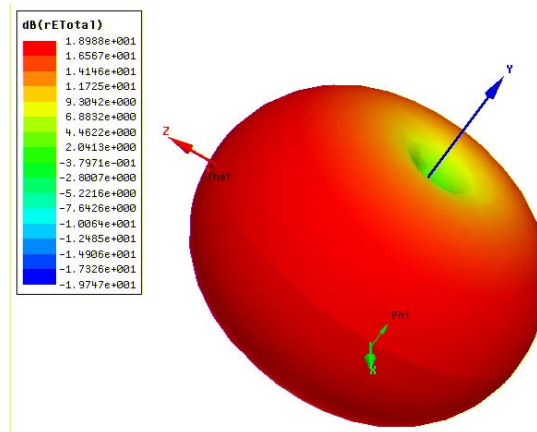
Fig.4.6 Simulated 3D radiation pattern of the strip monopole. (L_g = 15mm, W_g = 10mm, g = 0.35mm, W_c = 3mm, L_m = 20mm, h=1.6mm and ε_r=4.4)

In order to validate the computed 3D radiation pattern, the radiation pattern measurements are carried out in the two principal planes of the antenna at the resonant frequency and are plotted in fig. 4.7

XZ-Plane   YZ-Plane
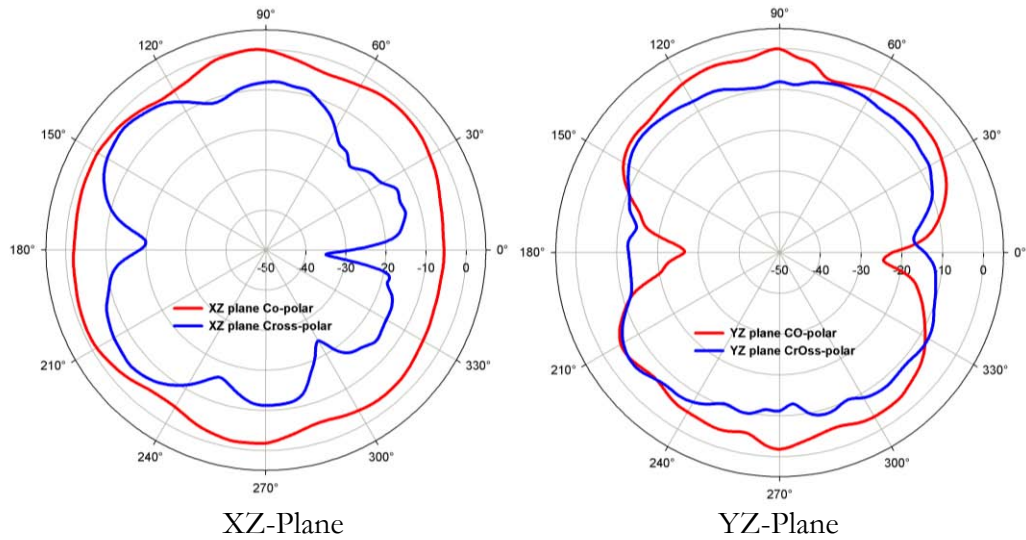
Fig.4.7. Measured radiation patterns at 2.58 GHz in the two orthogonal planes. (L_g = 15mm, W_g = 10mm, g = 0.35mm, W_c = 3mm, L_m = 20mm, h=1.6mm and ε_r=4.4)

The experimental results confirms the radiation behavior obtained through simulation and it can be seen that the strip monopole has almost omni-directional radiation behavior in the xz-plane and highly directional pattern in the yz plane.

4.6 Gain and Efficiency.

The gain and efficiency are two important figure of merit of the antenna. The gain of the antenna is measured using gain comparison method while the efficiency of the proposed antenna is measured using wheeler cap method. The measured gain of the antenna is depicted in fig.4.8. A peak gain of 4dBi is observed at 2.6GHz and it is also worth to note that the antenna provides almost uniform gain throughout the band.
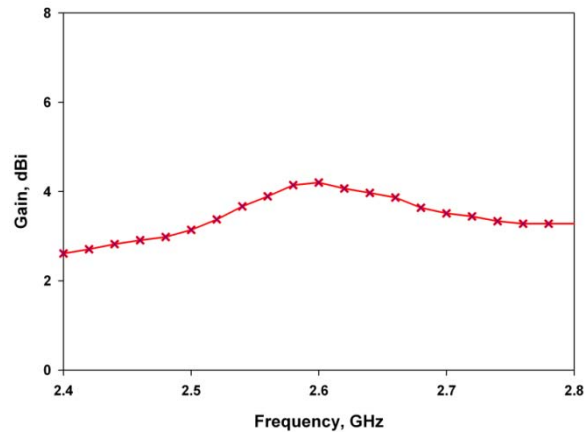
Fig.4.8: Measured peak gain of the FGCPW fed strip monopole. (L_g = 15mm, W_g = 10mm, g = 0.35mm, W_c = 3mm, L_m = 20mm, h=1.6mm and ε_r=4.4)

The average radiation efficiency of the strip monopole is found to be 75% in the resonant band.

4.7 Parametric Analysis:

A parametric analysis is performed for the FGCPW fed strip monopole antenna in order to investigate the effect of various antenna parameters over the antenna characteristics. The study conducted is the effect of dielectric properties (relative permittivity of the material and thickness of the substrate) and effect of structural parameters (various geometrical parameters)on the various radiation characteristics. The following sessions provide discussions on the effect of each parametric analysis and conclusions derived from the analysis.

4.7.1 Effect of Monopole Length(L_m)

The length of the strip monopole is varied from 16mm to 24mm and analyzed its effect over the resonant frequency. The variation of return loss characteristics with Lm is plotted in fig.4.9a.
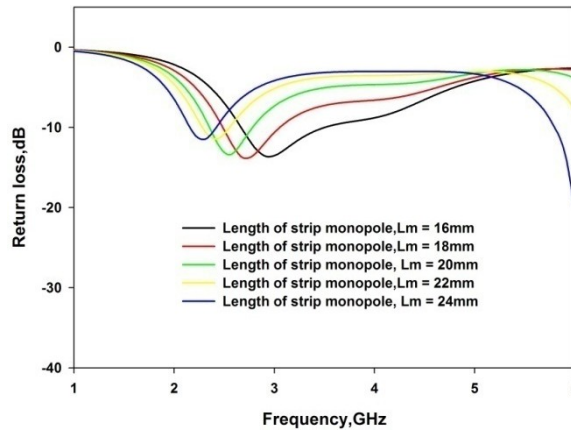
(a)
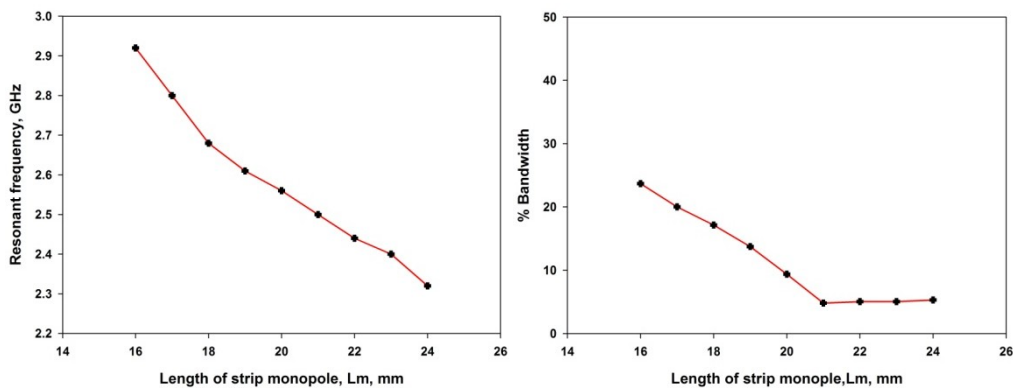
(b)   (c)

Fig.4.9 Effect of monopole length over (a) returnloss (b) resonant frequency (c) fractional bandwidth (L_g = 15mm, W_g = 10mm, g = 0.35mm, W_c = 3mm, h=1.6mm and ε_r=4.4)

It is clear from the results that the length of the strip monopole is inversely proportional to the resonant frequency. It is also observed from the resonant frequency variations that the shift in resonant frequency for lower values of Lm is

higher than that of large values of Lm. That is as the length of the center strip becomes higher, the effect of it over the resonant frequency becomes less.

The percentage bandwidth of the antenna is also extracted from the returnloss characteristics and plotted in fig.4.9c. It is observed from the analysis that a drastic variation in the bandwidth is observed for small values of Lm while the bandwidth variations are almost stable for higher values of Lm.

4.7.2 Effect of Finite ground dimensions:

The ground dimensions of any radiator, especially the monopole devices, play an important role in the antenna characteristics. The following session provides the effect of finite ground dimensions of the strip monopole (L_g and W_g) over the antenna characteristics.

4.7.2.1 Effect of Finite Ground Width(Wg)

A slight variation in resonant frequency is also observed when the width W_g is increased. But this change is found to be negligible. It is found from the return loss characteristics that W_g has an effect on impedance matching while the resonant frequency remains almost unaltered. The variations of antenna characteristics with W_g is plotted in fig.4.10

Fig.4.10 (a)

(b)   (c)
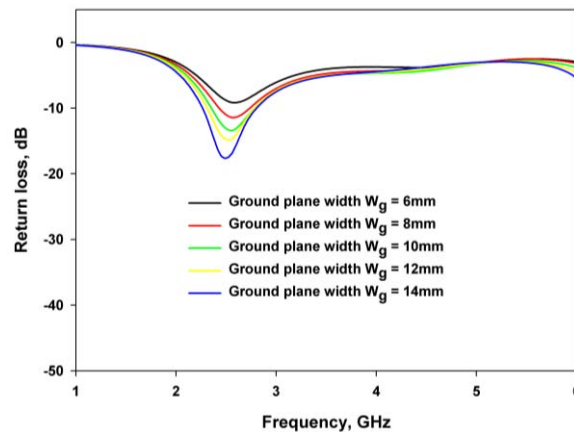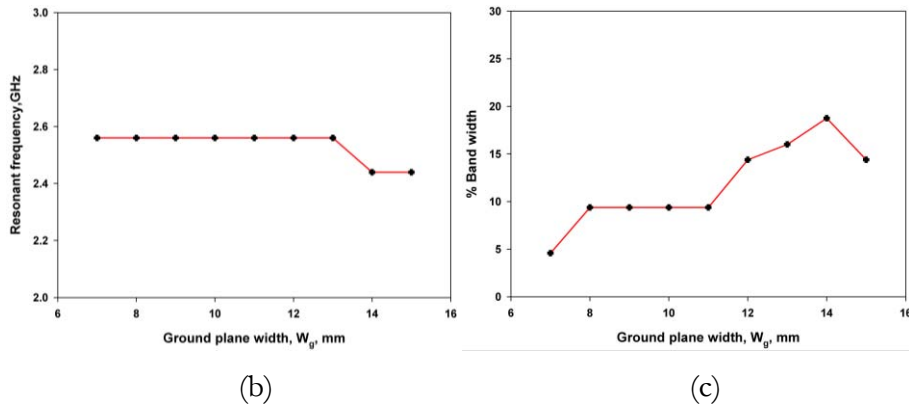
Fig.4.10(*contd*) Effect of ground plane width (a) returnloss (b) resonant frequency (c) fractional bandwidth (L_g = 15mm, W_g = 10mm, g = 0.35mm, W_c = 3mm, L_m = 20mm, h=1.6mm and ε_r=4.4)

It is seen from the analysis that the resonant frequency of the strip monopole remains almost unaltered with the ground plane width variation. It is also worthwhile to notice from the fig.4.10(c) that the bandwidth has a drastic change as groundplane width varies from 11mm to 14mm.

4.7.2.2 Effect of finite ground length (Lg)

Fig.4.11 illustrates the variations in return loss characteristics for different ground plane length Lg. It is found from the plots that the center frequency remains unaltered when the length of the ground plane changes from 10mm to 20mm. A close examination of return loss curve reveal that there is only a slight change is observed in the return loss characteristics with Lg. It is also observed from the bandwidth plot that the percentage bandwidth remains unaltered up to Lg=17mm but it varies as the Lg goes up.
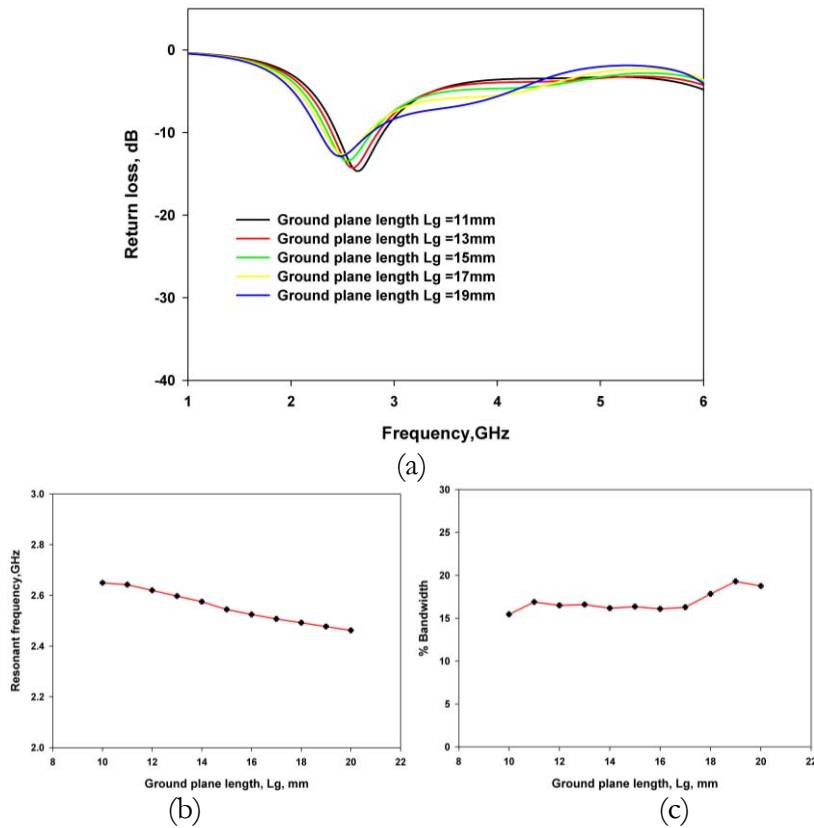
Fig.4.11 Effect of ground plane length (a) returnloss (b) resonant frequency (c) fractional bandwidth. (W_g = 10mm, g = 0.35mm, W_c = 3mm, L_m = 20mm, h=1.6mm and ε_r=4.4)

4.7.3 Effect of substrate parameters

The influence of substrate parameters – dielectric constant and thickness of the substrate are investigated in this session.

4.7.3.1 Effect of dielectric material

The effect of substrate dielectric constant is illustrated in fig. 4.12. It is found from the variations in the returnloss characteristics that the increase of dielectric constant of the material results high Q for the resonant device and hence decrease in bandwidth.
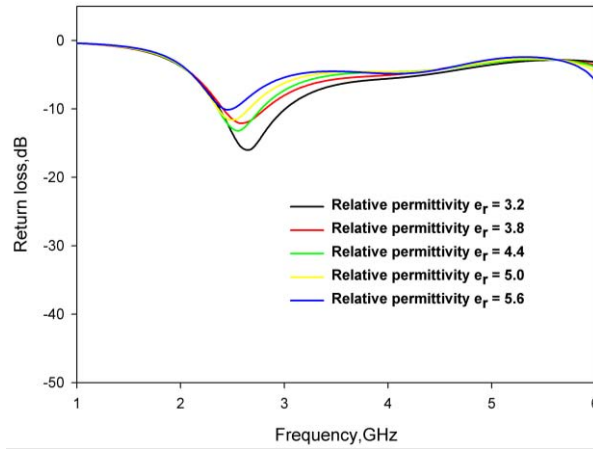
(a)
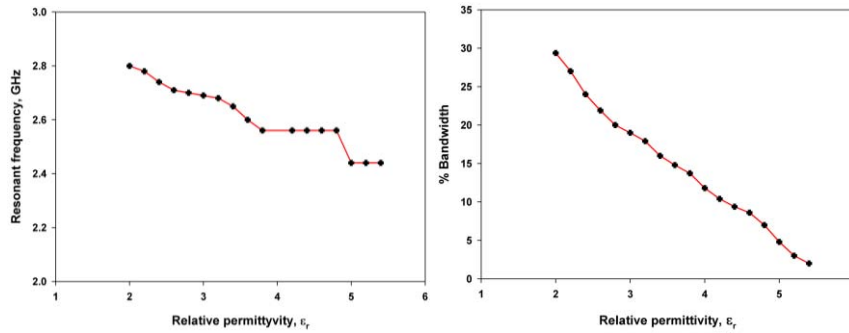
(b)   (c)

Fig.4.12 Effect of dielectric constant (a) returnloss characteristics (b) resonant frequency (c) fractional bandwidth. (L_g = 15mm, W_g = 10mm, g = 0.35mm, W_c = 3mm, L_m = 20mm, h=1.6mm)

It is also found from the plot in fig.4.12(b) that the shift in resonant frequency from 2.8 GHz to 2.5 GHz is observed for a variation of εr from 2 to 5.5 The percentage bandwidth of the strip monopole is found to be decreasing as the dielectric constant of the material is varied from 2 to 5.5. Therefore it can be concluded that the dielectric constant of the substrate has greater effect over the resonant frequency and percentage bandwidth.

4.7.3.2 Effect of dielectric thickness (h)

The thickness of the dielectric material is also varied and the effect over the antenna characteristics is studied. fig.4.13 depicts the influence on return loss

99

characteristics, resonant frequency and bandwidth. As the dielectric thickness increases most of the electric fields under the structure traps inside the dielectric substrate, thus the effective dielectric constant value increases slightly and produces decrease in resonant frequency.

(a)

(b)   (c)
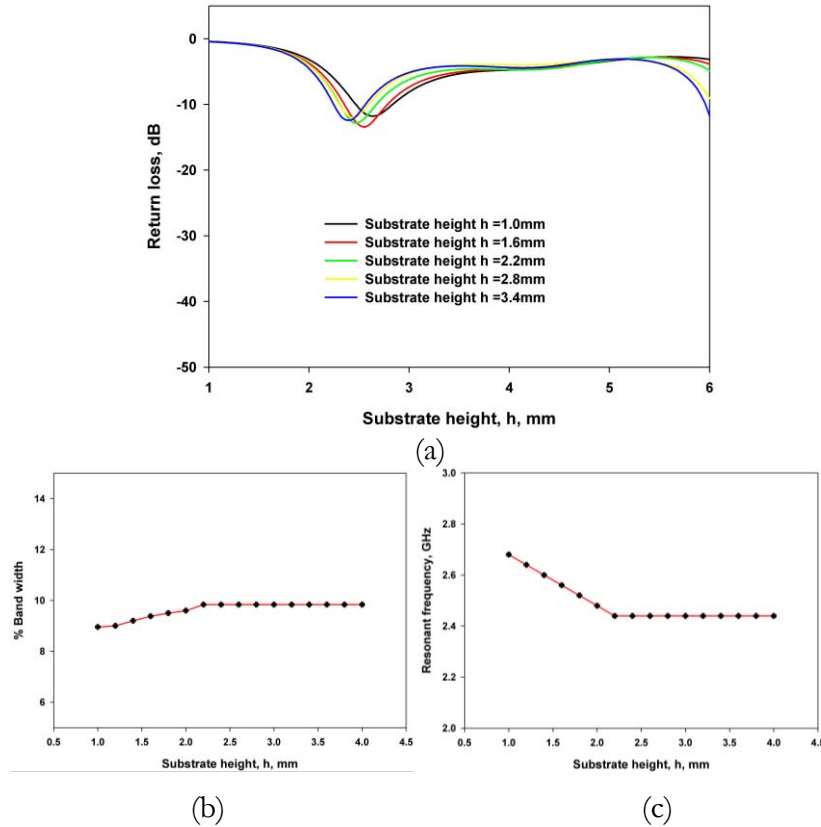
Fig.4.13 Influence of dielectric constant on antenna characteristics. (a) returnloss characteristics(b) Resonant frequency (c) Fractional bandwidth (L_g = 15mm, W_g = 10mm, g = 0.35mm, W_c = 3mm, L_m = 20mm, h=1.6mm and ε_r=4.4)

4.8 Conclusions:

The finite ground coplanar waveguide can be converted to an efficient radiator by extending the center strip length. From the analysis it is found that the length of the extended center strip determines the resonance and is approximatly $\lambda g/4$. The effect of ground plane dimensions over the resonant frequency is found to be almost negligible. The antenna exhibits linear polarization and nearly omnidirectional radiation characteristics with moderate gain and efficieny.

4-II. Development of a FGCPW fed Flared Monopole Antenna

The analysis of a FGCPW fed strip monopole is carried out in the previous section. The parametric analysis along with the experimental results predicted the finite ground coplanar waveguide fed strip monopole antenna as an efficient radiator and can be utilized for modern wireless communication gadgets. The major disadvantage of the strip-monopole antenna is that it becomes more bulky for the low frequency applications. The investigations are done to develop an antenna which maintains the radiation characteristics of a strip monopole while keeping its compactness. The method implemented in this section is the development of a flared monopole antenna in which a flaring is incorporated in the strip-monopole. Simulation results along with experimental verifications reveal that the flared monopole antenna can be used as a compact radiator compared to the FGCPW fed strip monopole for various communication gadgets.

This section of the thesis provides a detailed discussion about the development of a flared monopole antenna. The simulation results are experimentally verified and an exhaustive parametric analysis is performed to study the effect of various antenna parameters including the material properties of the device.

4.9 Geometry of the flared monopole antenna

Fig.4.14 illustrates the geometry of the flared monopole antenna. The antenna structure consists of a FGCPW fed flared strip monopole fabricated on a substrate with effective dielectric constant ε_r=4.4 and thickness h=1.6mm. The FGCPW is designed for an input impedance of 50Ω with design parameters gap, g = 0.35mm and the centre conductor width, Wc=3mm with finite ground plane with dimension L_gxW_g . A flaring with dimension L_f and W_f is introduced in this geometry. The optimum parameters of the antenna geometry are L_g = 15mm, W_g = 10mm, L_m = 25mm, W_f = 23mm, L_f = 10mm.
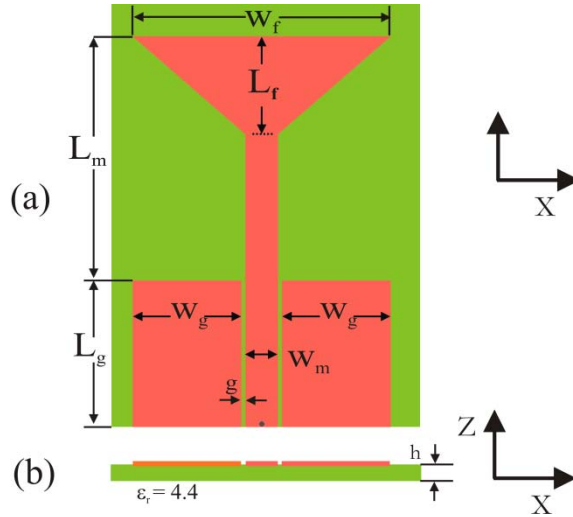
Fig.4.14 Geometry of the FGCPW fed flared monopole.(L_g = 15mm, W_g = 10mm, g = 0.35mm, W_c = 3mm, L_m = 25mm,W_f = 23mm, L_f = 10mm, h=1.6mm and εr=4.4)

4.10 Surface current:

The simulated surface current density plot of the flared FGCPW fed strip monopole antenna is shown in fig. 4.15
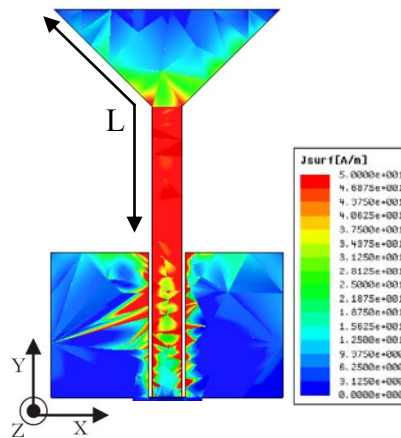
Fig.4.15 Surface current density plot of the flared monopole at 2.1GHz. (L_g = 15mm, W_g = 10mm, g = 0.35mm, W_c = 3mm, L_m = 25mm,W_f = 23mm, L_f = 10mm, h=1.6mm and εr=4.4)

It is clear from the current density plot that the flared strip monopole contributes strongly for the radiation as in the previous case of the strip monopole. The implementation of the flaring results in increasing the effective resonant length of the strip monopole and in turn results a shift in the resonant frequency to the lower frequency region. A quarter wavelength variation is observed along the length, L of the flared monopole antenna, which corresponds to the resonant frequency.

It is also observed that the magnitude of current variation along the ground plane is much small compared to that of the flared monopole. But it is quite bit high compared to the current variation in the FGCPW fed strip monopole antenna discussed in the previous session. Therefore we can conclude that this slight variation of current in the ground plane can result slight variation of antenna parameters with ground plane dimensions.

The vector plot of the current of the antenna is depicted in fig.4.16.
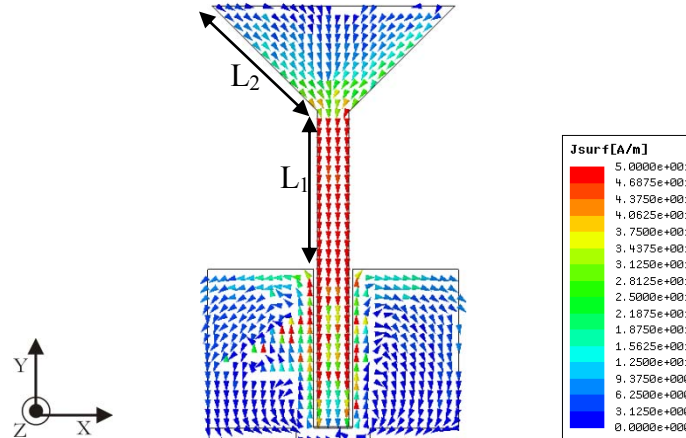
Fig.4.16 computed current density plot in vector notation at the resonance. (L_g = 15mm, W_g = 10mm, g = 0.35mm, W_c = 3mm, L_m = 25mm, W_f = 23mm, L_f = 10mm, h=1.6mm and εr=4.4)

The analysis of current direction and magnitude of the flared monopole antenna provides better understanding about the resonance and radiation behavior.

It is seen that the direction of current along the segment L_1 is Y while that of L_2 is slightly slanted. Moreover the magnitude of current along L_1 is very much higher than that of L_2. Therefore the effective polarization produced by the flared monopole segments L_1 and L_2 will be in Y direction.

4.11 Returnloss characteristics

The FGCPW fed flared monopole antenna is analyzed through software simulation and verified experimentally as shown in fig. 4.17. By simulation the antenna is found to resonate at 2.14GHz with 300 MHz bandwidth (14%). It is observed that only 2.3% error is measured between the simulated and experimental resonant frequency. This is due to the finite computational domain used during simulation.
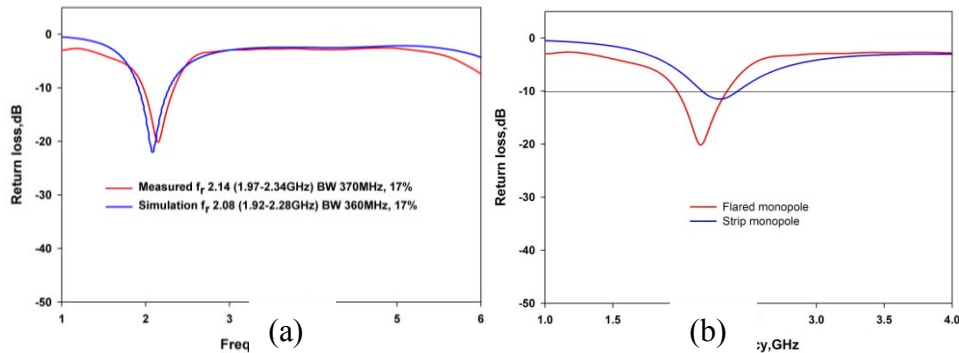
Fig.4.17(a) Measured and simulated returnloss characteristics of the FGCPW fed Flared strip monopole antenna(b) Comparison between the FGCPW fed strip monopole and Flared monopole antenna. (L_g = 15mm, W_g = 10mm, g = 0.35mm, W_c = 3mm, L_m = 25mm, W_f = 23mm, L_f = 10mm, h=1.6mm and εr=4.4)

A comparison of S_{11} for the FGCPW fed strip monopole and flared Monopole is depicted in fig. 4.17(b). It is seen from the plot that the introduction of flaring results shifts in frequency to a lower frequency region.

4.12 Polarization

The received power at boresight throughout the resonat band is depicted in fig.4.18 .
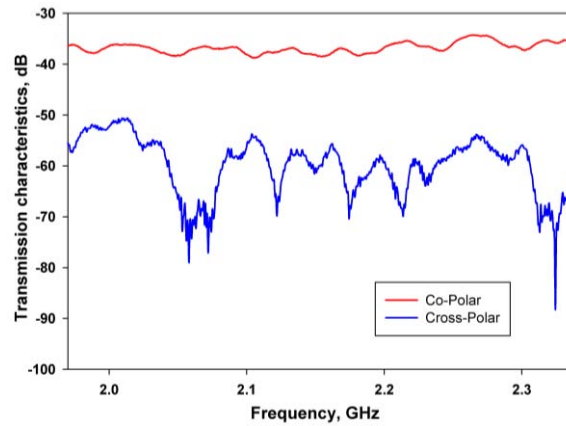
Fig.4.18 Transmission characteristics(S_{21}) of the flared strip monopole in the resonant band. (L_g = 15mm, W_g = 10mm, g = 0.35mm, W_c = 3mm, L_m = 25mm,W_f = 23mm, L_f = 10mm, h=1.6mm and εr=4.4)

It is clear from the transmission characteristics plotted in fig. 4.18 that the antenna exhibits linear polarization throughout the band with cross polar level better than 10dB. The measurement results confirm the predictions from the current density plot in the previous section.

4.13 Radiation Pattern.

The simulated, 3D radiation pattern of the flared monopole antenna is depicted in figure 4.19. It is observed from the radiation pattern that the antenna provides almost omni-directional radiation coverage which is suitable for the communication devices. It is worthwhile to note that the flaring introduced in the FGCPW fed strip monopole does not disturb the radiation pattern. Experimental radiation pattern plotted in the two principle planes are also illustrated in the fig 4.20. The experimental results also agree that the radiation pattern remains unaltered by embedding flaring to the strip monopole.

106
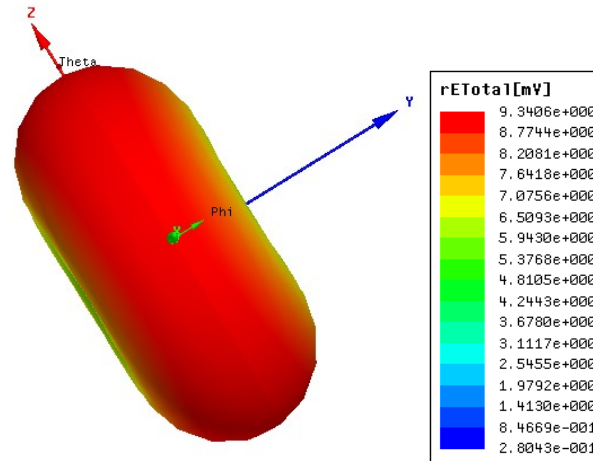
Fig.4.19 Simulated 3D radiation pattern at the resonant frequency at 2.08 GHz(L_g = 15mm, W_g = 10mm, g = 0.35mm, W_c = 3mm, L_m = 25mm,W_f = 23mm, L_f = 10mm, h=1.6mm and ɛr=4.4)
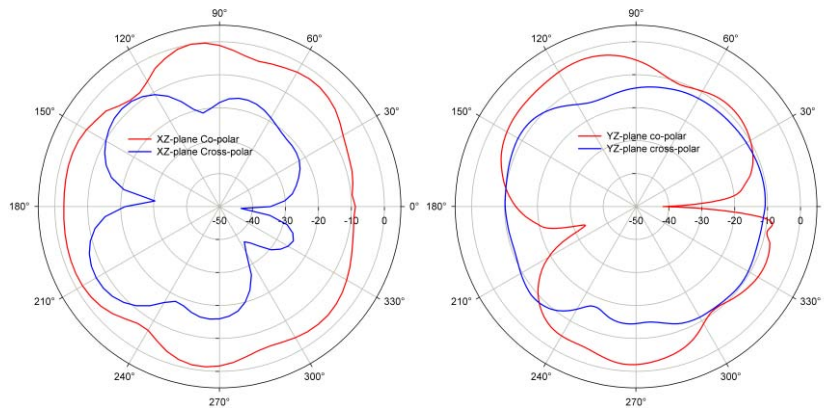
Fig.4.20 Measured radiation patterns in two orthogonal planes of the FGCPW fed flared monopole antenna at 2.11GHz. (L_g = 15mm, W_g = 10mm, g = 0.35mm, W_c = 3mm, L_m = 25mm,W_f = 23mm, L_f = 10mm, h=1.6mm and ɛr=4.4)

4.14 Gain and efficiency:

The gain of the FGCPW fed flared monopole antenna is depicted in fig. 4.21.
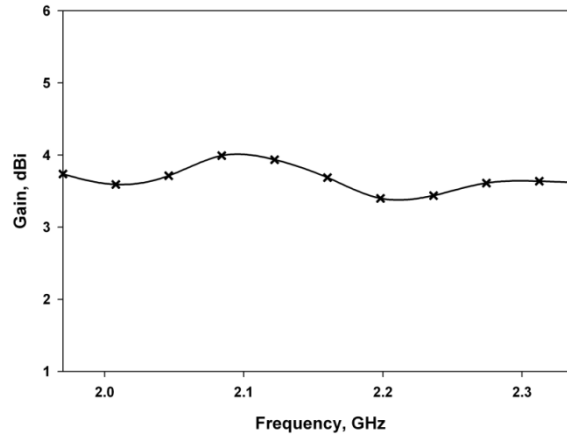
Fig.4.21: Gain of the flared monpole antenna (L_g = 15mm, W_g = 10mm, g = 0.35mm, W_c = 3mm, L_m = 25mm,W_f = 23mm, L_f = 10mm, h=1.6mm and εr=4.4)

It is observed from the plot that the gain of the antenna remains almost constant throughout the resonant band. It is also worth to note that the gain remains almost unaltered by the introduction of flaring.

4.15 Parametric Analysis

4.15.1 Effect of flaring over the antenna characteristics:

In this section we investigate the effect of flaring over the antenna characteristics. The width of flaring (W_f) and Length of flaring (L_f) are studied and various antenna parameters are computed.

4.15.1.1 Effect of Flaring width (W_f):

The flaring width is varied from 10 to 25 mm and its influence is studied over the antenna characteristics. Fig.4.22 illustrates the effect of W_f over the return loss characteristics. It is seen from the analysis that the variation in W_f results in tuning the resonant frequency to a lower value. The variation of W_f from 10 mm to 25 mm results a shift of resonant frequency by 270 MHz. The increase of W_f

results increase in resonant length, as explained in the previous section, that in turn tunes the resonant frequency to a lower value.

The bandwidth variation with W_f is illustrated in Fig4.22(c). It is seen that the percentage bandwidth remains almost unaltered as the W_f varies from 10mm to 24mm. Therefore we can conclude that by flaring the monopole, without increasing its length, we can tune the resonance frequency without much change in the bandwidth.
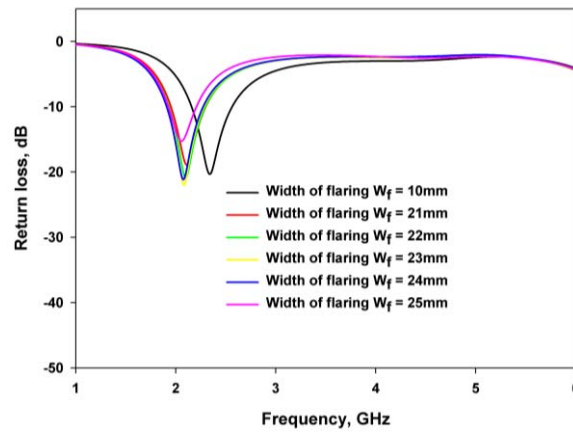
(a)
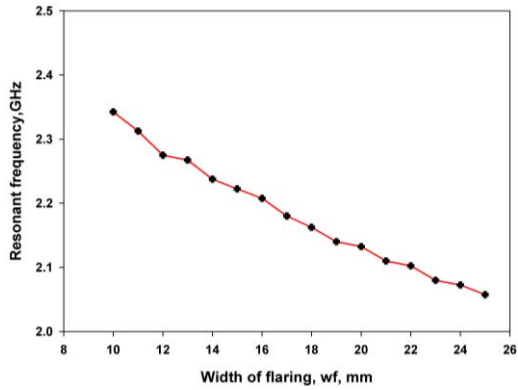
(b)
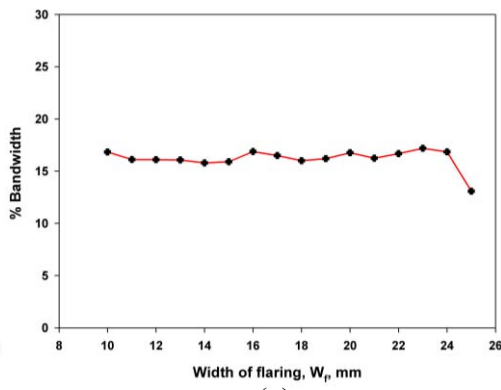
(c)

Fig.4.22: Effect of width of flaring (a) Return loss characteristics (b) Resonant frequency (c) Percentage bandwidth. (L_g = 15mm, W_g = 10mm, g = 0.35mm, W_c = 3mm, L_m = 25mm, L_f = 10mm, h=1.6mm and εr=4.4)

4.15.1.2 Effect of Flaring length(L_f):

The length of the flaring L_f is varied from 5mm to 15mm and studied its effect over the return loss characteristics. It is found that the resonant frequency moves to a lower band as the length of flaring increases because resonant length is more dependent on L_f than W_f. The shift in resonance for the L_f variation from 5 to 15mm is 400MHz.

The variation in percentage bandwidth with L_f is shown in fig.4.23(c). It is found that for lower values of L_f the bandwidth is low and more dependent, whereas, as L_f goes beyond 8mm, the bandwidth remains almost constant.

(a)

(b)   (c)
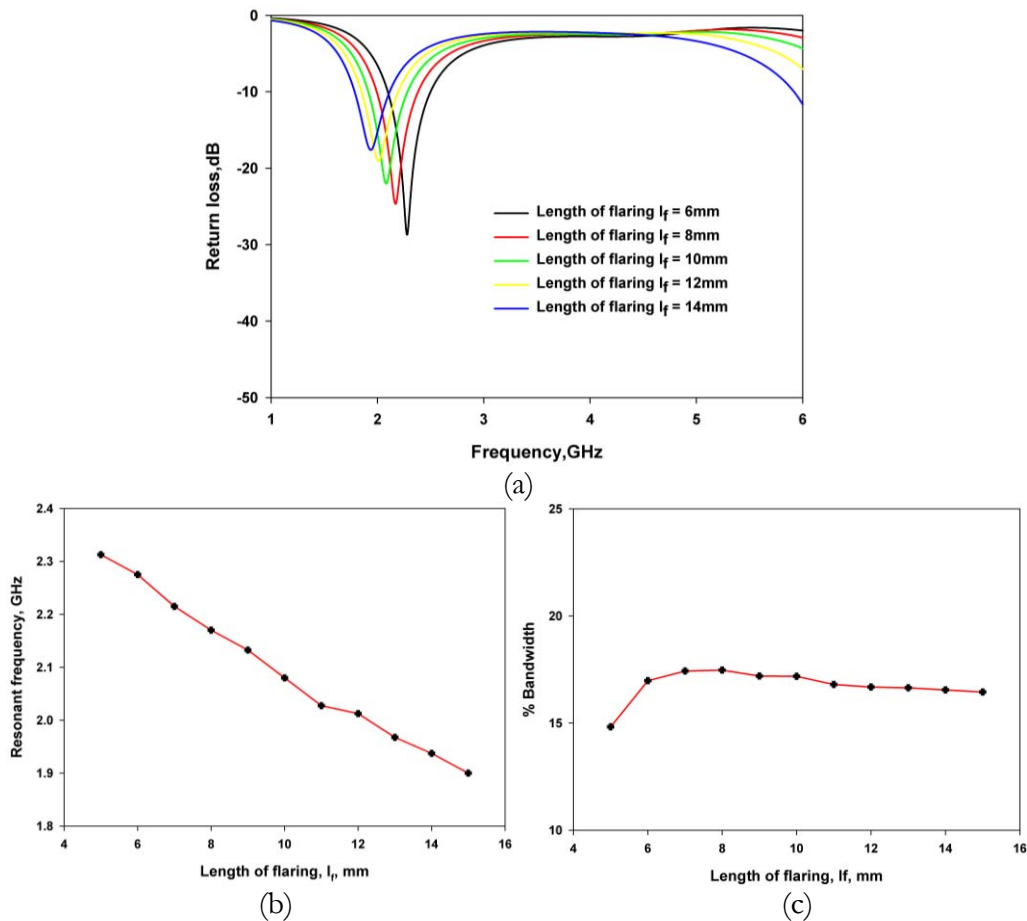
Fig 4.23. Effect of flaring length over (a) Return loss Characteristics (b) Resonant frequency (c) Percentage Bandwidth(L_g = 15mm, W_g = 10mm, g = 0.35mm, W_c = 3mm, L_m = 25mm, W_f = 23mm, h=1.6mm and ɛr=4.4)

4.15.2 Effect of Ground plane parameters over the antenna characteristics:

It is already observed from the current density plots that the ground plane has influence over the antenna characteristics. The parametric analysis performed in the flared monopole antenna also reveals the same and are as follows

4.15.2.1 Effect of ground plane width(Wg)

The effect of ground plane width, Wg, over the returnloss characteristics is illustrated in fig. 4.24. It is observed from the results that the resonant frequency has feeble effect over the ground plane width as predicted form the current density plots.

Fig. 4.24(a)

(b)   (c)
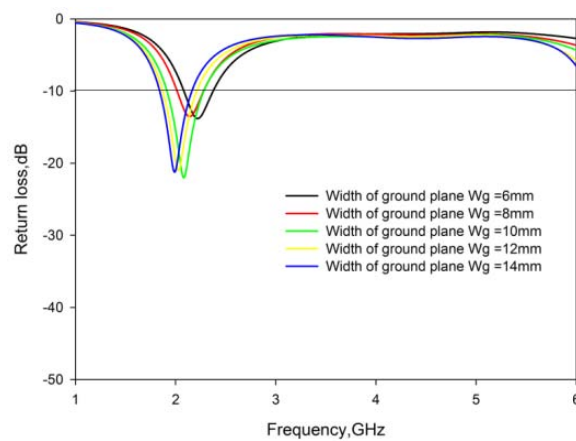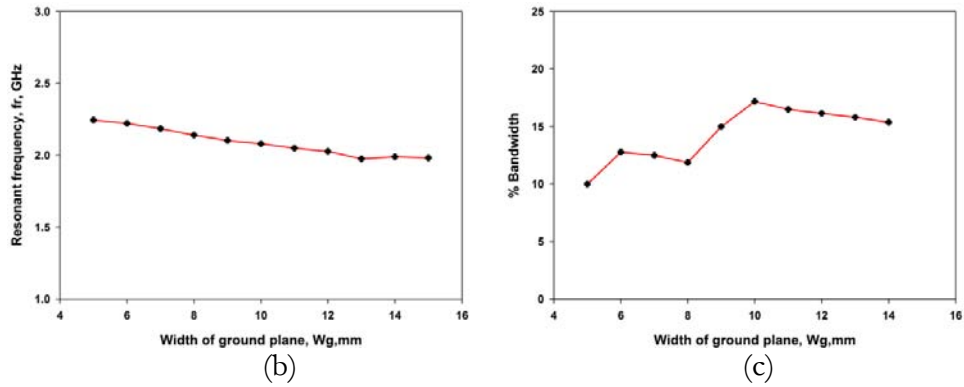
Fig 4.24(*contd*). Effect of ground plane width over Return loss Characteristics (b) resonant frequency (c) Percentage Bandwidth(L_g = 15mm, g = 0.35mm, W_c = 3mm, L_m = 25mm, W_f = 23mm, L_f = 10mm, h=1.6mm and εr=4.4)

4.15.2.2 Effect of ground plane length(Lg).

The effect of ground plane length is studied and depicted in fig.4.25. It is observed that there is a slight shift in the resonant frequency towards the low frequency region as Lg increases. It is also observed that the bandwidth variations are almost negligible compared to the variations with Wg.

Fig. 4.25(a)

(b) (c)
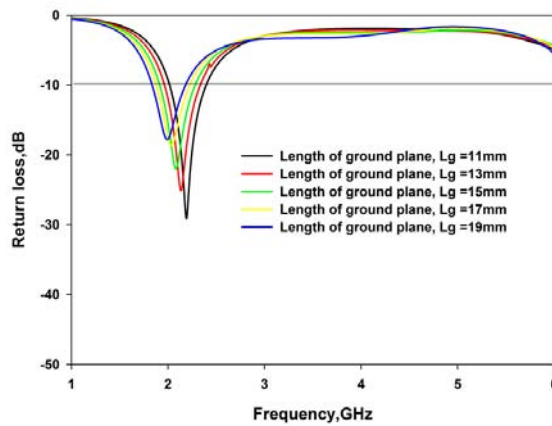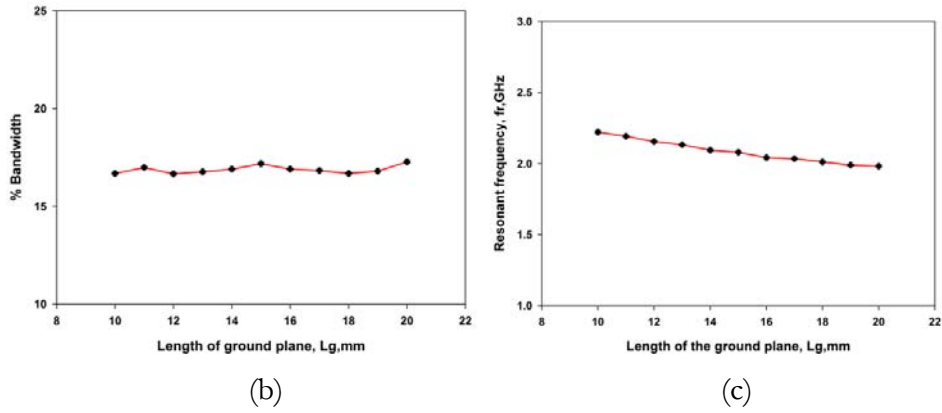
Fig 4.25 (*contd*). Effect of Ground plane length (a) Return loss Characteristics (b) Resonant frequency (c) Percentage Bandwidth(W_g = 10mm, g = 0.35mm, W_c = 3mm, L_m = 25mm, W_f = 23mm, L_f = 10mm, h=1.6mm and εr=4.4)

4.15.3 Effect of Substrate parameters:

The influence of substrate parameters – relative permittivity (ε_r) and thickness (h) against the antenna characteristics are studied and depicted in the flowing session.

4.15.3.1 Influence of Substrate dielectric constant(ε_r):

The variation of returnloss characteristics are depicted in fig.4.26. It is found that the resonant frequency of the device is found to be almost constant for the ε_r variation from 2 to 7. The bandwidth is found to be reduced by 10% when the dielectric constant is varied from 2 to 7.

Fig 4. 26 (a)

113

<div align="center">(b)   (c)</div>
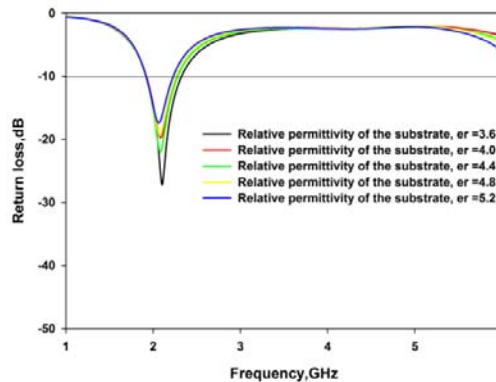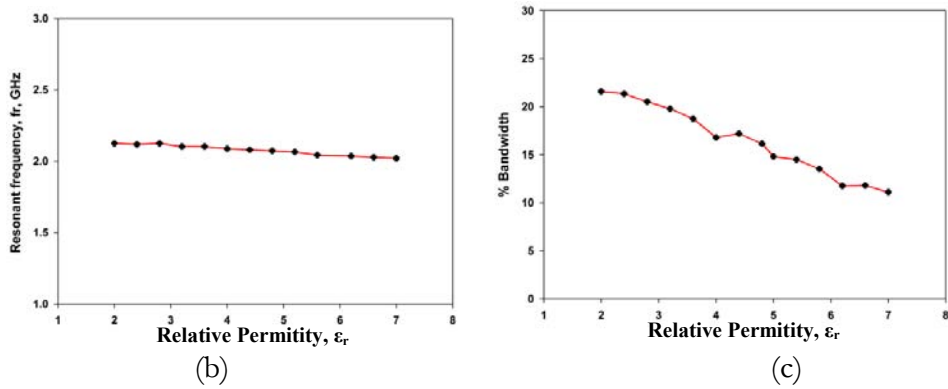
Fig 4. 26(*contd*): Effect of Relative permittivity (a) Return loss Characteristics (b) Resonant frequency (c) Percentage Bandwidth (L_g = 15mm, W_g = 10mm, g = 0.35mm, W_c = 3mm, L_m = 25mm, W_f = 23mm, L_f = 10mm, h=1.6mm)

4.15.3.2 Influence of substrate thickness(h)

The resonant frequency remains almost stable with the variation of substrate thickness. This may be because of the uni-planar design of the radiator in which the chance of strong filed across the dielectric substrate is minimum. The bandwidth of the device is found to be slightly influenced by thickness. Figure 4.27 illustrates the influence of substrate thickness.

<div align="center">Fig 4.27(a)</div>

(b)   (c)
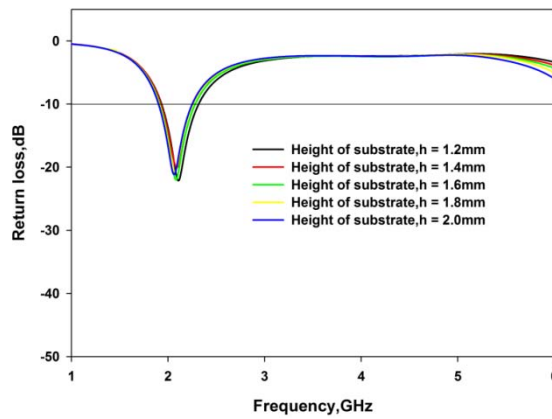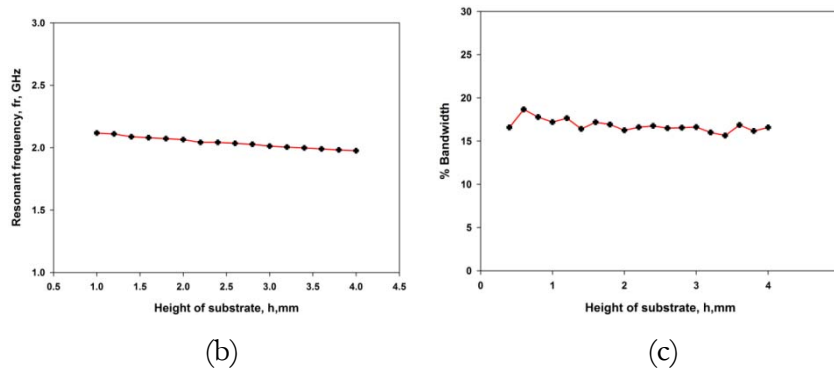
Fig 4. 27 (*contd*). Effect of Height of substrate, h (a) Return loss Characteristics (b) Resonant frequency (c) Percentage Bandwidth (L_g = 10mm, W_g = 15mm, g = 0.35mm, W_c = 3mm, L_m = 25mm, W_f = 23mm, L_f = 10mm, and εr=4.4)

4.16 Conclusions.

The introduction of flaring in the FGCPW fed strip monopole antenna results in increase in the effective resonant length which in turn results a shift in the resonant frequency to a lower frequency region. The polarization and radiation pattern of the strip monopole remains unaltered by the flaring. The flaring parameter L_f and W_f along with L_m determines the resonant frequency of the antenna. A feeble effect of the ground plane dimensions on the antenna characteristics is observed. The peak gain of the antenna is found to be more than 3dBi throughout the resonant band.

Development of a Flared Monopole Antenna with V-Shaped Element for Dual Band Applications

The Flared Strip Monopole Antenna discussed in the previous chapter is extended to develop as a dual band monopole antenna without much disturbing its radiation pattern and gain. An additional V-shaped element is integrated to the flared monopole at the optimum position in order to excite a second resonance at a higher frequency band without much disturbing the first resonant band. The bandwidth of the second resonance is improved by loading the add-on element with a slot.

5-I Dual band Coplanar Waveguide Flared Monopole with V-Element

5.1 Antenna geometry:

The geometry of the dual band monopole antenna fabricated on FR4 substrate with dielectric constant 4.4 and thickness 1.6mm is shown in fig.5.1
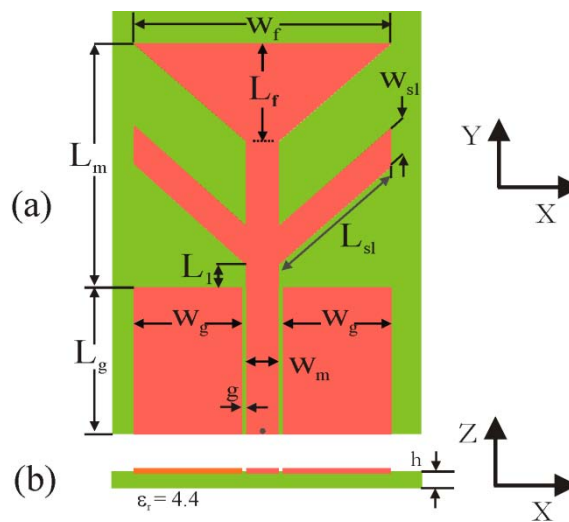
Fig.5.1. Geometry of the dual band flared monopole antenna.(L_g = 15mm, W_g = 10mm, g = 0.35mm, W_m = 3mm, L_m = 25mm,W_f = 23mm, L_f = 10mm, L_1 = 2.5mm, L_{sl} =15 mm, W_{sl} =2.5mm, h=1.6mm and ε_r=4.4)

The flared strip monopole with L_m = 25 mm is employed to produce the first resonant frequency while the 'V' shaped element with dimension L_{sl} = 15mm and W_{sl} = 2.5mm results second resonance. The feed line is a coplanar waveguide with truncated ground plane dimensions L_g= 15mm and W_g = 10mm that couples the energy to the antenna through 50Ω SMA connector.

5.2 Return loss characteristics

The returnloss characteristics of the flared monopole antenna integrated with a 'V'-shaped element is depicted in fig.5.2. It is observed that the antenna provides dual band characteristics by operating in two resonant bands. The measured results show a resonance from (2.03- 2.29) GHz in the first resonant band with a bandwidth of 12% and (3.20 – 4.84) GHz in the second band with 41% bandwidth.
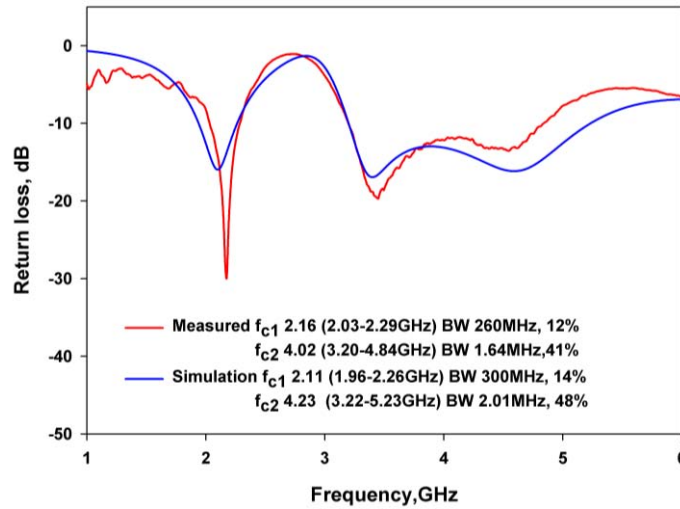
Fig.5.2: Measured and simulated return loss characteristics of the flared monopole antenna for dual band applications. (L_g = 15mm, W_g = 10mm, g = 0.35mm, W_m = 3mm, L_m = 25mm, W_f = 23mm, L_f = 10mm, L_1 = 2.5mm, L_{sl} =15 mm, W_{sl} =2.5mm, h=1.6mm and ε_r=4.4)

The simulation results are in good agreement with the measured results. The small discrepancy between the simulated and measured result is due to the limited computational domain in the simulation.

The dual band characteristics of the V-shaped element (sleeve) loaded flared monopole antenna, as compared to the single band flared monopole antenna, discussed in the previous section is illustrated in fig. 5.3
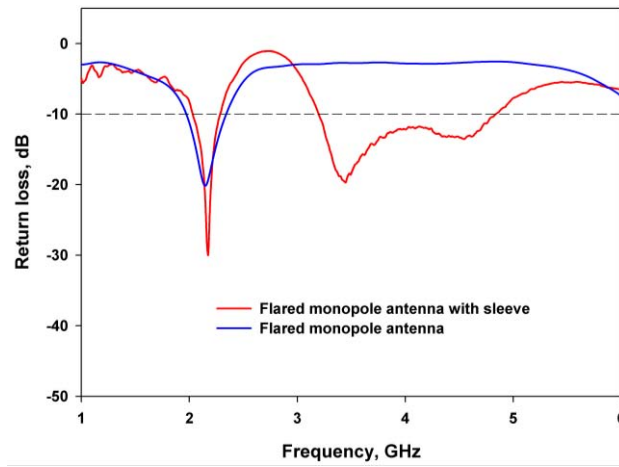
(a)
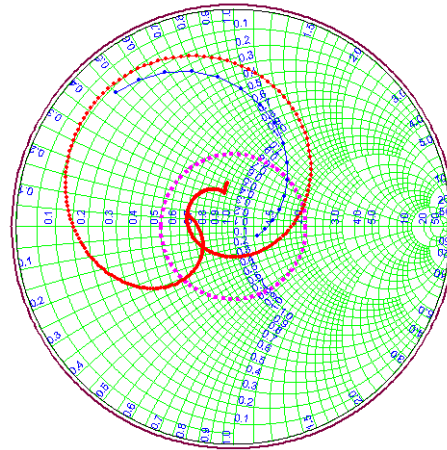
(b)

Fig.5.3: Measured antenna characteristics of flared monopole antenna and flared monopole antenna with add on element (a) Return loss (b) Smith chart(L_g = 15mm, W_g = 10mm, g = 0.35mm, W_m = 3mm, L_m = 25mm, W_f = 23mm, L_f = 10mm, L_1 = 2.5mm, L_{sl} =15 mm, W_{sl} =2.5mm, h=1.6mm and ε_r=4.4)

It is worth to note that by embedding a 'V' shaped element in the flared monopole provides an additional wideband resonance at a higher frequency region without much change in the first resonance. The impedance plot of the flared monopole and dual band antenna is also illustrated in fig. 5.3b

5.3 Surface current plot.

The simulated surface current density plot of the dual band flared monopole antenna is illustrated in fig.5.4 at 2.11GHz.
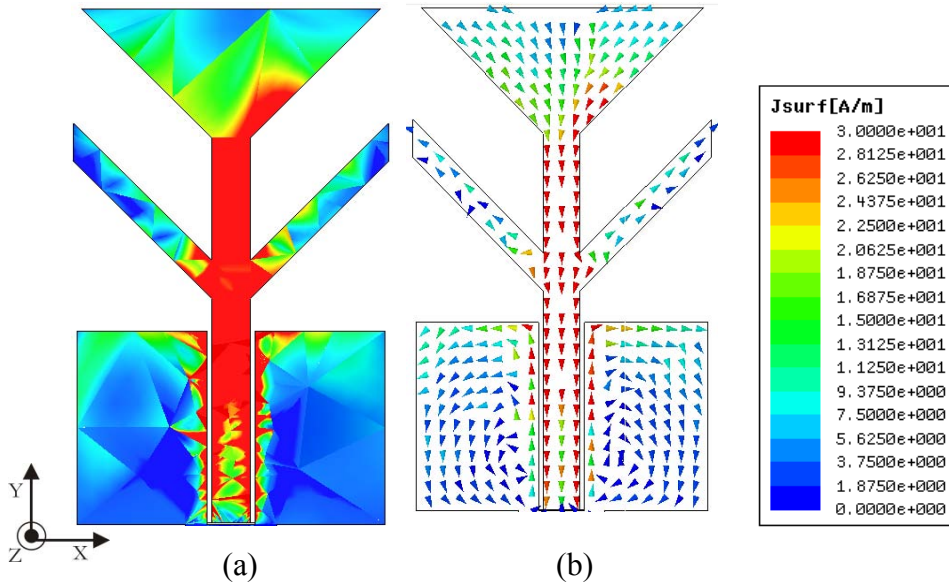
Fig.5.4: Surface current plots at 2.11 GHz (a) Magnitude (b) vector (L_g = 15mm, W_g = 10mm, g = 0.35mm, W_m = 3mm, L_m = 25mm,W_f = 23mm, L_f = 10mm, L_1 = 2.5mm, L_{sl} =15 mm, W_{sl} =2.5mm, h=1.6mm and ε_r=4.4)

It is evident from the magnitude plot of current density in fig.5.4 (a) that the flared monopole contributes for the first resonance. It is found that the intensity variation along the flared monopole is approximately quarter wave. That is, a maxima at the FGCPW end and minima at the top of the flared monopole. The intensity of current density at the V-shaped element is negligible and therefore it contributes much less for the radiation compared to the flared monopole. The vector notation of the plot is also provided in fig. 5.4(b), which illustrates that the direction of current in the flared monopole is almost similar throughout the structure and in turn, results linear polarization along Y-direction.

It is also observed that the current density in the ground plane along Y-direction is almost constant, while the current along X-direction is slightly varying. Thus the influence of ground-plane width will be higher than that of the ground plane length.

(a)   (b)
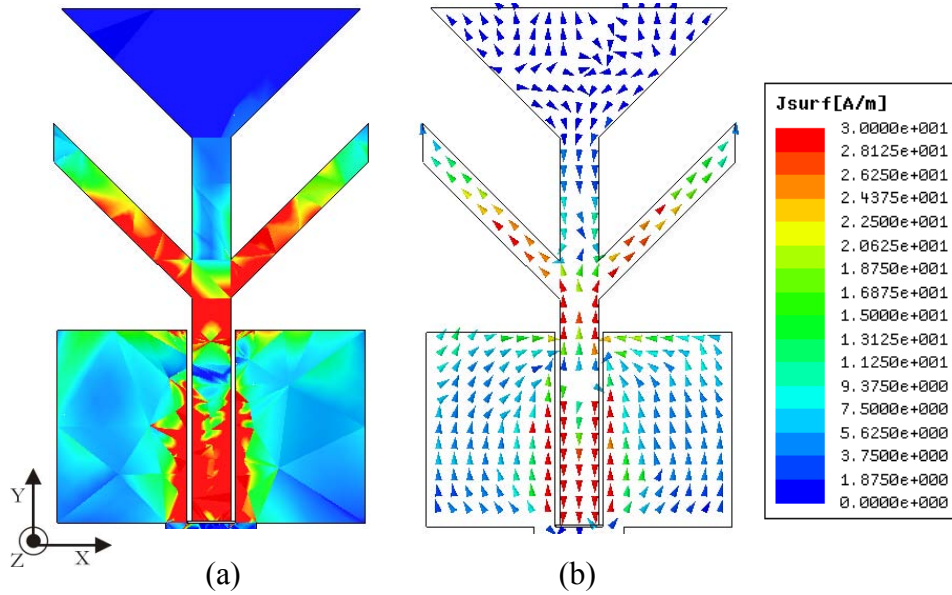
Fig.5.5: Surface current plots at 4.23 GHz (a) Magnitude (b) vector. (L_g = 15mm, W_g = 10mm, g = 0.35mm, W_m = 3mm, L_m = 25mm, W_f = 23mm, L_f = 10mm, L_1 = 2.5mm, L_{sl} =15 mm, W_{sl} =2.5mm, h=1.6mm and ε_r=4.4)

It is observed from the magnitude of current density as illustrated in fig.5.5(a) drawn at 4.23GHz, that the add-on 'V' element contributes for radiation at the second resonance while the current plot of the flared monopole indicate that the contribution of flared monopole is negligible compared to the V-element at second resonant frequency.

The vector notation provides more clear idea about the resonant length and radiation behavior of the flared monopole antenna. It is observed that the direction of current in the finite ground plane is almost equal in magnitude and opposite in direction compared to the centre strip of the FGCPW. It is also observed that the magnitude of current in both the slanted edges of the 'V'-shaped

element is almost equal magnitude and the direction is upward. Therefore the resultant vector is in Y-direction, which results Y-polarized radiation.

5.4 Polarization:

The transmission characteristics (S_{21}) of the antenna is measured and plotted in fig.5.6. The analysis of the received power in the two orthogonal planes reveals that the two resonant modes are linearly polarized along the 'Y'-directon.
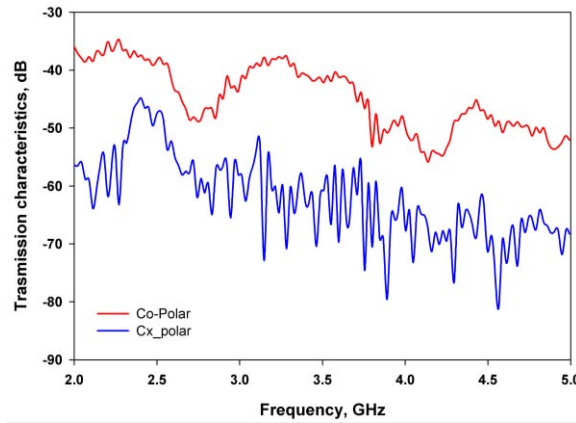
Fig.5.6: Measured transmission characteristics(S_{21}) of the dual band flared monopole antenna. (L_g = 15mm, W_g = 10mm, g = 0.35mm, W_m = 3mm, L_m = 25mm,W_f = 23mm, L_f = 10mm, L_1 = 2.5mm, L_{sl} =15 mm, W_{sl} =2.5mm, h=1.6mm and ε_r=4.4)

It is seen from the transmission characteristics that the antenna has almost linear polarization throughout the resonant band and cross polarization levels is better than 10dB.

5.5 Radiation behavior:

The simulated 3D radiation pattern at both the resonant bands are illustrated in fig. 5.7. It is seen that both the radiation patterns are almost omni-directional in nature and suitable for mobile communication devices. It is also important to note

that the integration of 'V'-element with the flared monopole provides omni-directional radiation pattern without disturbing the radiation behavior of the first resonant band.
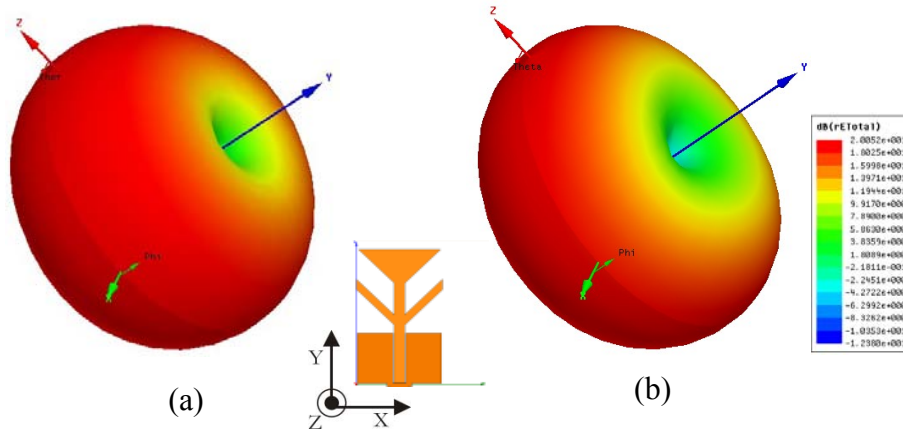
Fig.5.7 : Simulated 3D radiation pattern of the dual band antenna plotted at   (a) 2.11 GHz (b) 4.23GHz. (L_g = 15mm, W_g = 10mm, g = 0.35mm, W_m = 3mm, L_m = 25mm,W_f = 23mm, L_f = 10mm, L_1 = 2.5mm, L_{sl} =15 mm, W_{sl} =2.5mm, h=1.6mm and ε_r=4.4)

The measurement is also conducted in order to ensure the radiation behavior, as predicted by simulation method. The measured radiation characteristics of the proposed antenna in two orthogonal planes are depicted in fig. 5.8.

<div align="center">(a)   (b)</div>

<div align="center">(c)   (d)</div>
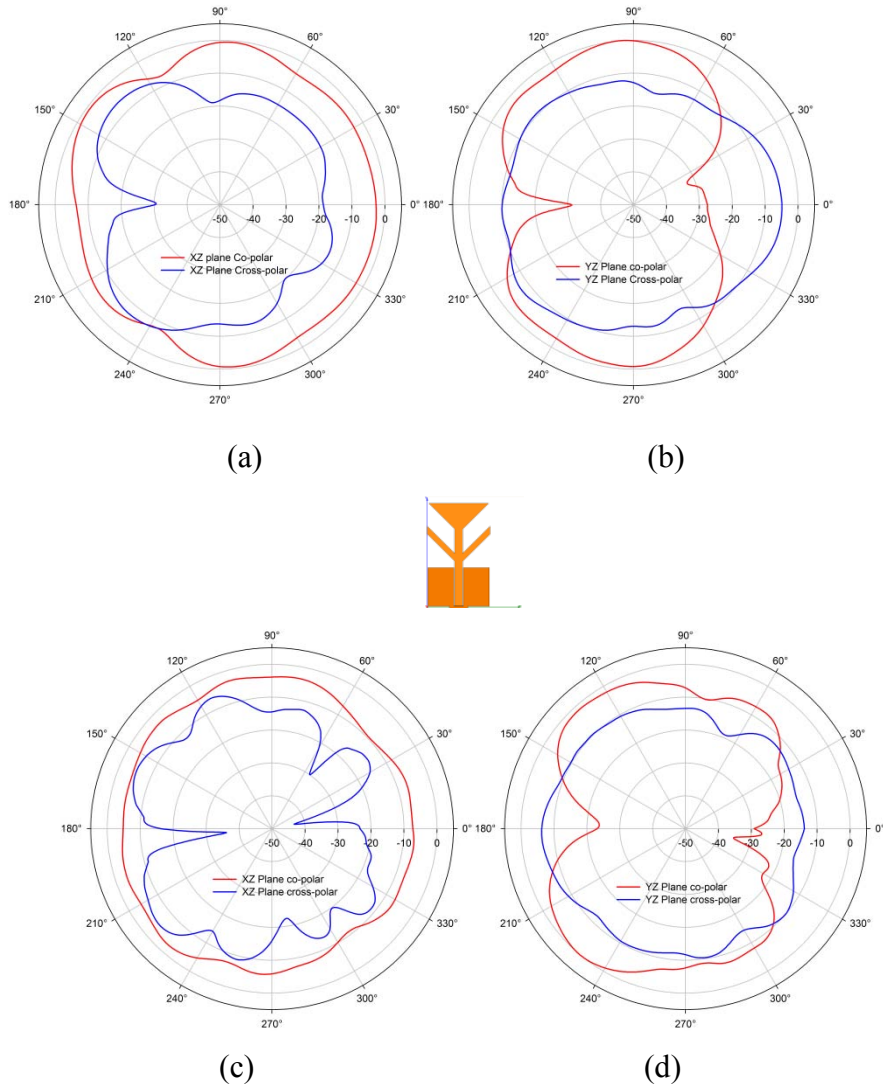
Fig.5.8: Measured radiation patterns in the two orthogonal planes at 2.16GHz [fig (a)-(b)] and at 4.0 GHz [fig(c)-(d)]. (L_g = 15mm, W_g = 10mm, g = 0.35mm, W_m = 3mm, L_m = 25mm, W_f = 23mm, L_f = 10mm, L_1 = 2.5mm, L_{sl} =15 mm, W_{sl} =2.5mm, h=1.6mm and ε_r=4.4)

It is observed that the antenna has wide radiation coverage in the XZ-plane while it has directional pattern in the YZ plane.

5.6 Gain and efficiency:

The peak gain of the antenna measured at each frequency points by gain comparison method is illustrated in fig.5.9
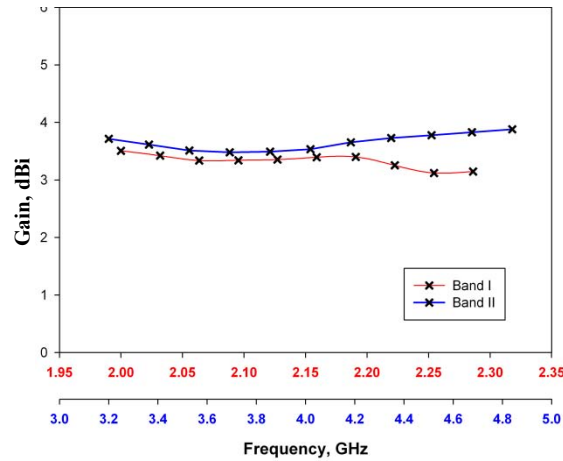
Fig.5.9: Measured peak gain of the FGCPW fed Flared monopole antenna with embedded element (L_g = 15mm, W_g = 10mm, g = 0.35mm, W_m = 3mm, L_m = 25mm, W_f = 23mm, L_f = 10mm, L_1 = 2.5mm, L_{sl} =15 mm, W_{sl} =2.5mm, h=1.6mm and ε_r=4.4)

The antenna offers moderate gain in the desired frequency bands. It shows a peak gain of 3.5 dBi in the first resonant band and 3.9dBi in the second resonant band. It is also worth to note that the gain variation of the antenna in the first and second bands is almost 0.5dBi and 0.6dBi respectively.

The radiation efficiency of the dual band antenna is measured using wheeler cap method. The measured average efficiency of the antenna in the first and second resonant bands, are approximately 65% and 73% respectively.

5.7 Parametric Analysis:

A parametric analysis is performed to study the effect of 'V'-shaped element over the antenna characteristics. Various antenna parameters of the add-on

element including its length, width and position are studied and the results are discussed in the following sections.

5.7.1 Effect of V-element length(L_{sl})

The effect of L_{sl} over the resonant frequencies is illustrated in the fig.5.10. The length of the V-element is varied from 10mm to 20mm and found that the first resonant frequency remains unaltered while the second resonant band is shifted from 4.5GHz to 4.0GHz. It is also seen from the analysis that the impedance matching around the center frequency of the second band becomes poor as Lsl increases. Therefore it can be concluded that the length of the sleeve can act as a tuning element for the second resonant band.

Fig.5.10 (a)

(b)   (c)
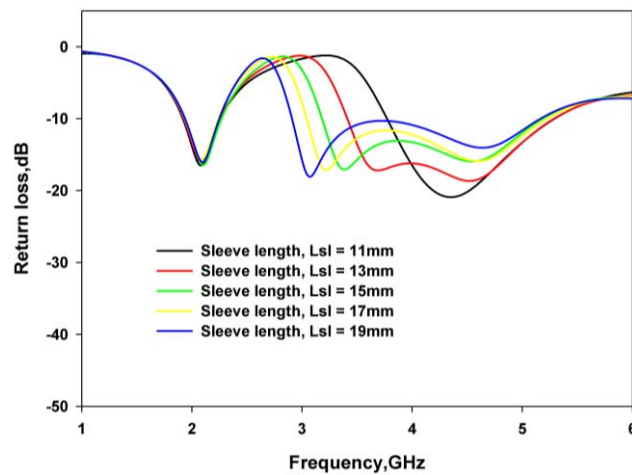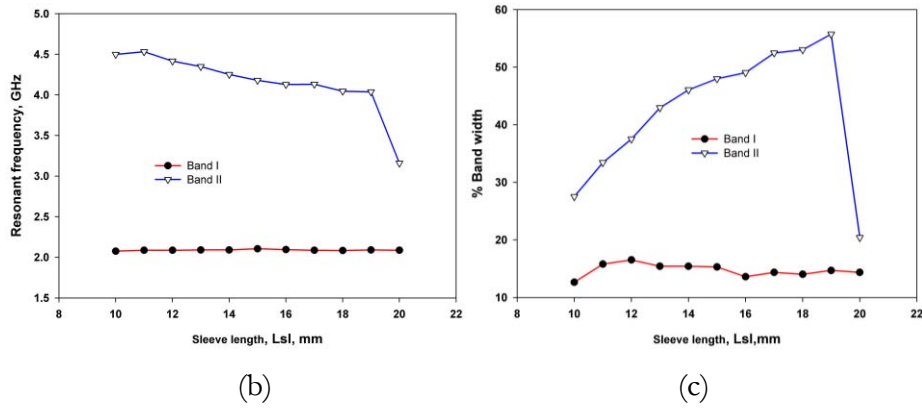
Fig.5.10(*Contd*). Effect of v-element length over (a) Returnloss (b) center frequency (c) percentage bandwidth. (L_g = 15mm, W_g = 10mm, g = 0.35mm, W_m = 3mm, L_m = 25mm, W_f = 23mm, L_f = 10mm, L_1 = 2.5mm, W_{sl} =2.5mm, h=1.6mm and ε_r=4.4)

The band widths of two resonant bands are also investigated to study the effect of sleeve. It is found that the bandwidth of the first resonant band remains almost unaltered while that of the second has a variation of about 30% as L_{sl} varies from 10 to 20mm. It is found that the bandwidth decreases drastically when the L_{sl} goes beyond the width of the ground plane because of poor interaction with ground plane.

5.7.2 Effect of W_{sl}

The width of the add-on element is also varied from 0.5mm to 6mm and the effect over the return loss characteristics is depicted in fig. 5.11. It is seen that both the resonant band remains almost unaltered with the W_{sl} variation. As explained with the surface current plot, the width of the sleeve does not depend on the resonant length. Thus it has feeble effect over the resonance.

It is observed from Fig.5.11(c) that the width of sleeve has only a feeble effect over the bandwidth.
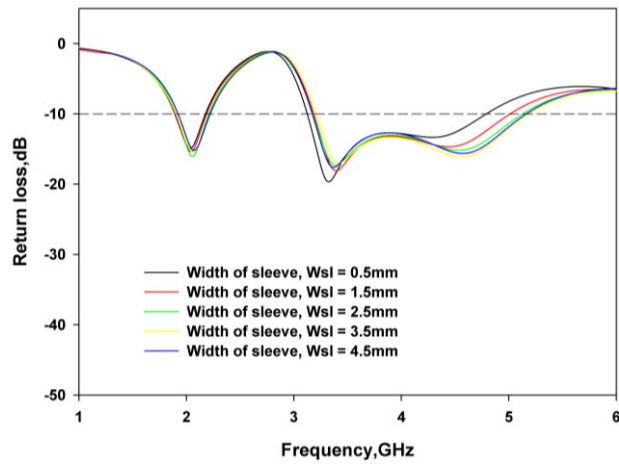
(a)
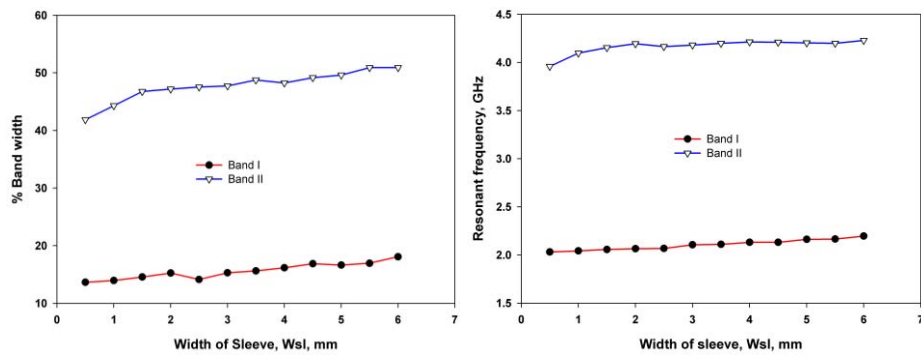

(b)   (c)

Fig.5.11: Effect of sleeve width over the antenna resonance (a) returnloss (b) resonant frequency (c) percentage bandwidth (L_g = 15mm, W_g = 10mm, g = 0.35mm, W_m = 3mm, L_m = 25mm, W_f = 23mm, L_f = 10mm, L_1 = 2.5mm, L_{sl} =15 mm, h=1.6mm and ε_r=4.4)

5.7.3 Effect of position, L_1

The position of the sleeve in the flared monopole is varied and its influence over the return loss characteristics is studied. The variation of returnlosss with sleeve position is depicted in fig.5.12. It is found that for small values of L_1, the coupling to the ground plane is high which in turn results a better impedance matching.
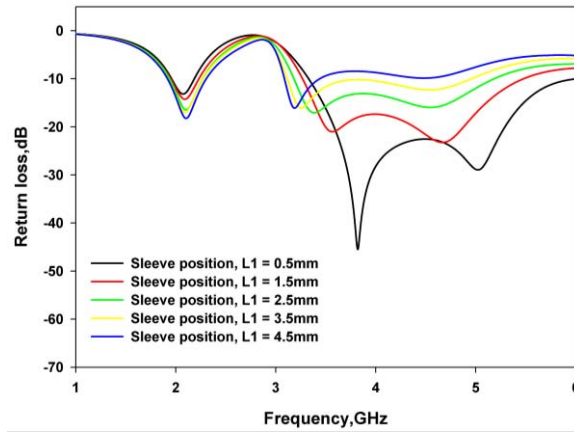
(a)
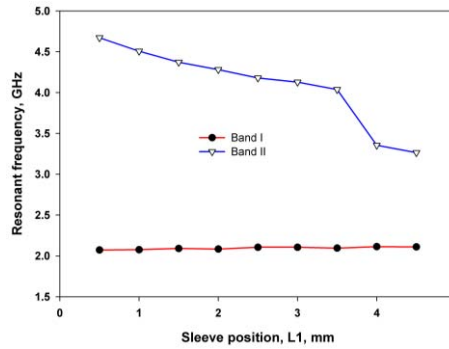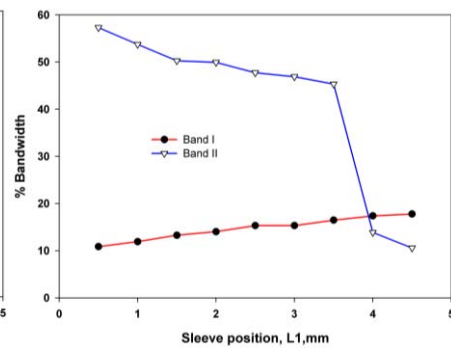
(b)   (c)

Fig.5.12: The variation of antenna characteristics with sleeve position (a) returnloss(b) Center frquency (c) Bandwidth. (L_g = 15mm, W_g = 10mm, g = 0.35mm, W_m = 3mm, L_m = 25mm, W_f = 23mm, L_f = 10mm, L_{sl} =15 mm, W_{sl} =2.5mm, h=1.6mm and ε_r=4.4)

It is observed that the first resonant remains almost unaltered while the second resonance moves to a lower frequency region. The resonant length for the second band includes L_1 and thus the shift is as expected from the current density plot. The bandwidth is found to be slightly increasing for the first band while it is decreasing throughtout the second resonant band due the poor impedance matching.

5.8 Conclusions:

The following conclusions can be made from the analysis,

- A dual band antenna is developed from the finite ground coplanar waveguide fed flared strip monopole antenna by integrating a 'V' shaped element(Sleeve)

- The measurement results reveal that, the integration of the add on element has only a feeble influence over the resonance and radiation behavior of the first resonance.

- The position and length of V-element can act as tuning parameters for the antenna.

- It is found from the measured antenna characteristics that the antenna provides almost omni-directional radiation patterns with moderate gain and efficiency.

5-II Dual band Coplanar Waveguide Flared Monopole
with Slotted V-Element

Development of antenna designs to achieve broadband operation at two separate frequencies by maintaining omni-directional radiation pattern has received much attention in recent years. This module of the chapter describes the bandwidth broading technique by integrating a slot in the V-shaped element. Both theoretical and experimental results are discussed along with the parametric analysis of the antenna.

5.9 Antenna Geometry

The dual band FGCPW fed flared monopole antenna geometry is illustrated in fig.5.13. A suitable microwave material with dielectric constant ε_r=4.4 and thickness 1.6 mm is used to fabricate the device. The present design parameters for the proposed antenna include L_g=15mm, W_g=10mm, g=0.35mm, W_m=3mm, L_1=2.5mm, W_f=23mm, L_f=10mm, L_{sl}=15mm, W_{sl}=3mm, L_s=14mm and W_s=1mm.
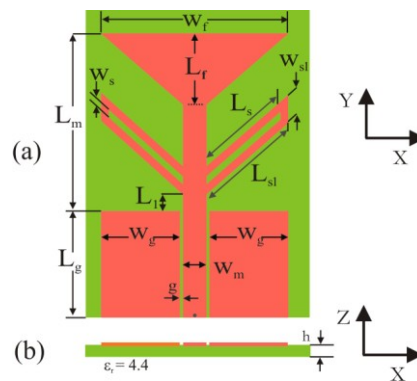

Fig.5.13: The Geometry of the flared monopole antenna for dual band applications.(L_g=15mm, W_g=10mm, g=0.35mm, W_m=3mm, L_m=25mm, L_1=2.5mm, W_f=23mm, L_f=10mm, L_{sl}=15mm, W_{sl}=2.5mm, L_s=14mm and W_s=1mm)

- **FDTD Computational domain:**

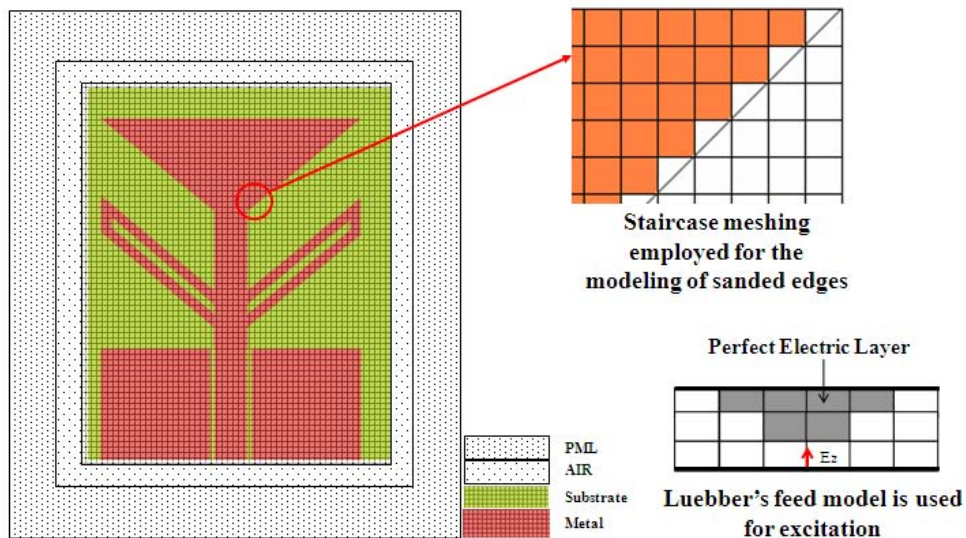 The computational domain for 3D-FDTD analysis is illustrated in Fig.5.14.

Fig.5.14 The computational domain for the dual frequency antenna (L_g=15mm, W_g=10mm, g=0.35mm, W_m=3mm, L_m=25mm, L_1=2.5mm, W_f=23mm, L_f=10mm, L_{sl}=15mm, W_{sl}=2.5mm, L_s=14mm and W_s=1mm)

The geometry in the computational domain is modeled using the classical FDTD technique. The grid layout and other parameters of the antenna is optimized to Nx x Ny x Nz = 109 x 170 x 57 cells in which the antenna is modeled with in 61 x 122 x 4 Cells and the remaining cells are treated as air boundary around the antenna geometry. The Absolute boundary condition employed on walls of the air boundary is Perfectly Matched Layer. The slanting edge of the antenna geometry is modeled with staircase approximation scheme.

The antenna is excited with time domain Gaussian pulse at the feed point and the results were extracted. The optimum code parameters for the analysis is depicted in Table. 5.2

Time domain parameters		Geometrical Parameters	
Gaussian pulse half width, T	20ps	Δx	0.35mm
Time delay, τd	3T	Δy	0.35mm
Time step, Δt	0.66ps	Δz	0.4mm
Number of time steps	4000		

Table 5.2 : Optimum code parameters for the FDTD analysis

5.10 Return loss Characteristics:

The measured , simulated(HFSS) and computed(FDTD) return loss characteristics is illustrated in fig.5.15 along with the impedance plot in smith chart.

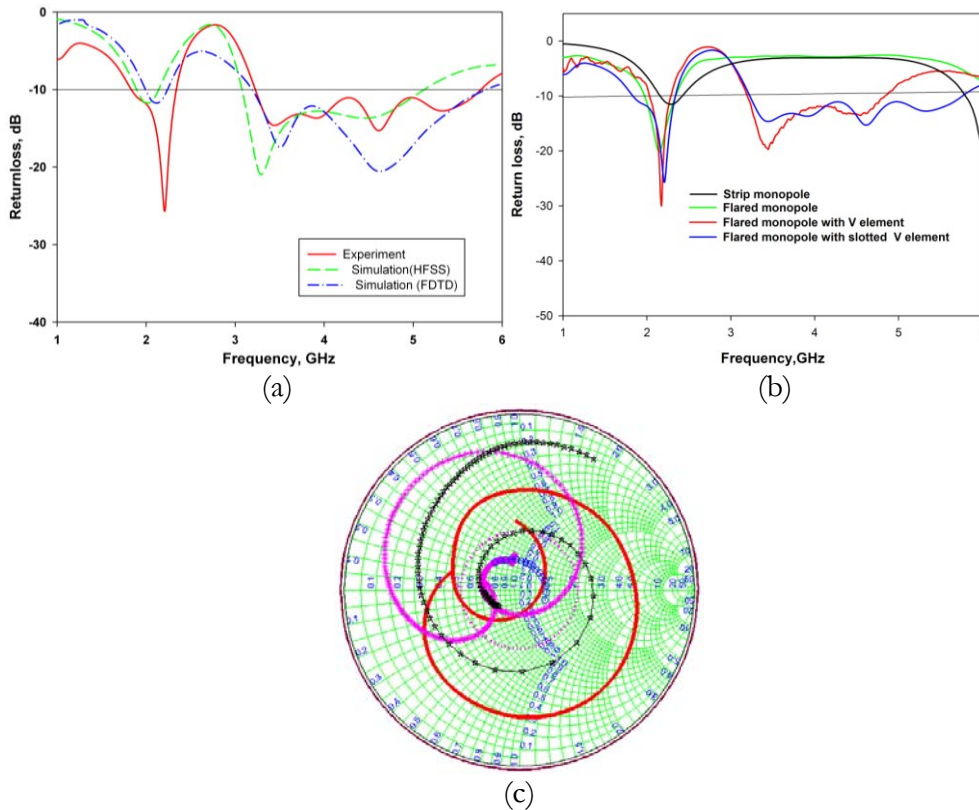
(a)   (b)

(c)

Fig.5.15: Measured antenna characteristics of the dual band monopole antenna (a) Return loss (b) Development of the antenna from the strip monopole (c) Impedance plot. (L_g=15mm, W_g=10mm, g=0.35mm, W_m=3mm, L_m=25mm, L_1=2.5mm, W_f=23mm, L_f=10mm, L_{sl}=15mm, W_{sl}=2.5mm, L_s=14mm and W_s=1mm)

It is evident from the plot in fig.5.15b that the conventional FGCPW fed strip monopole antenna has only a single resonance in the 1-6GHz band. The introduction of flaring to the strip results a shift in the resonant frequency to a lower frequency band. The antenna become dual band, without disturbing the first resonance by embedding a 'V' shaped element. The shape of the add-on element helps to maintain the polarization of the second band same as that of first. A slot loading in the 'V'-element results improvement in the bandwidth without disturbing other antenna parameters. The impedance plot of the proposed dual band monopole antenna is also provided along with the impedance of other antennas for comparison.

It is seen that the monopole antenna can operate over two frequency bands 1.83-2.34 GHz and 3.23-5.76GHz, with a 10-dB returnloss bandwidth of 24.5% at the center frequency 2.09GHz and 56.3% at the center frequency 4.50 GHz. Good agreement between simulated and measured results is observed.

5.11 Current density plots

The surface current density plots of the proposed dual band flared monopole antenna integrated with a 'V'-shaped element at first resonance is illustrated in fig.5.16. The magnitude of current density plot shown in fig.5.16b reveals that there is approximately a quarter wave magnitude variation along the length of the flared monopole while the 'V'-element embedded with slot has feeble current variation at the first resonance. Therefore it can be concluded that the flared monopole contributes for the first resonance. Only a slight current variation is observed along the finite ground plane. The analysis of the vector plot of current pattern in fig. 5.16b reveals that the polarization of the antenna in the first resonant band is along Y-direction as discussed in chapter 4. It is worth to note that the polarization of the radiation is not disturbed by the slotted 'V' element.
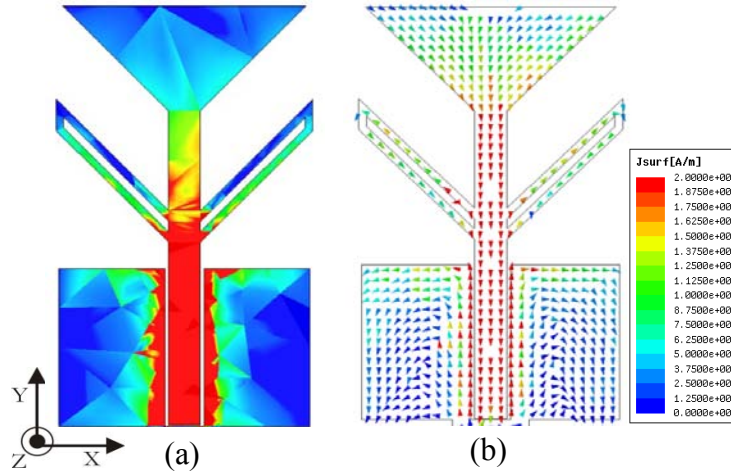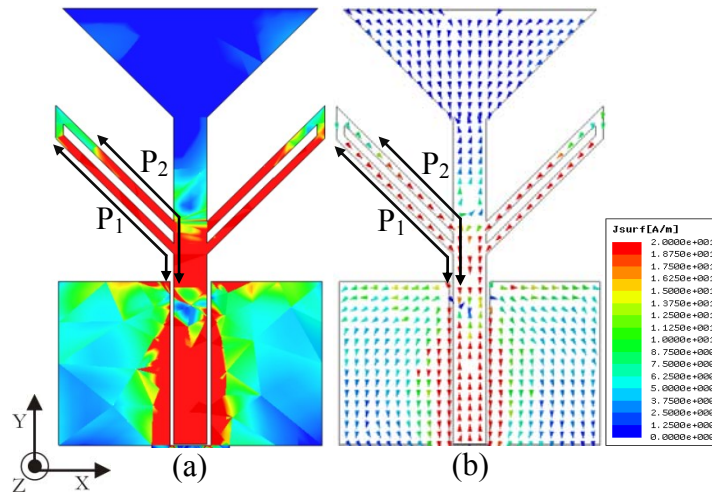
Fig.5.16: The current density plots of the dual band flared monopole antenna at 2.11 GHz (a) Magnitude (b) Vector(L_g=15mm, W_g=10mm, g=0.35mm, W_m=3mm, L_m=25mm, L_1=2.5mm, W_f=23mm, L_f=10mm, L_{sl}=15mm, W_{sl}=2.5mm, L_s=14mm and W_s=1mm)

The current density plots drawn in second resonance at 4.5 GHz is depicted in fig. 5.17

Fig.5.17: The current density plots of the dual band flared monopole antenna at 4.5 GHz (a) Magnitude (b) Vector.(L_g=15mm, W_g=10mm, g=0.35mm, W_m=3mm, L_m=25mm, L_1=2.5mm, W_f=23mm, L_f=10mm, L_{sl}=15mm, W_{sl}=2.5mm, L_s=14mm and W_s=1mm)

It is clearly understood from the magnitude of the current density plot shown in fig.5.17(a) that the slotted V-element is excited strongly for the second resonance while the flared monopole has almost no current density variation. It is also worth to note that the slot loading resulted the excitation of two resonant paths P1 and P2 in the V-element, as illustrated in the figure, which made the merging of two resonant frequencies close to each other. Thus resulted the broad bandwidth in the antenna.

It is also observed from the vector plot depicted in fig.5.17(b) that the direction of the resultant current vector in the sleeve is in Y-direction and therefore the polarization remains same as that of flared monopole antenna discussed in the previous chapter.

5.12 Polarization:

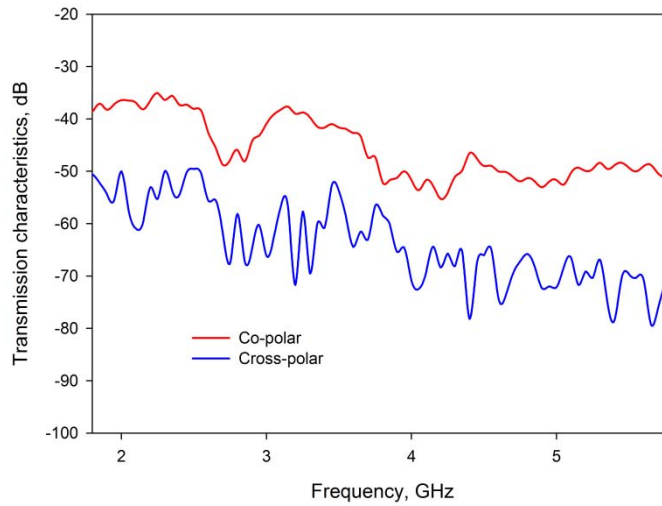The polarization of the antenna in the bore sight direction is measured and plotted in fig. 5.18.

Fig.5.18: Measured transmission characteristics(S_{21}) of the dual band flared monopole antenna with sleeve with slot.(L_g=15mm, W_g=10mm, g=0.35mm, W_m=3mm, L_m=25mm, L_1=2.5mm, W_f=23mm, L_f=10mm, L_{sl}=15mm, W_{sl}=2.5mm, L_s=14mm and W_s=1mm)

It is observed that the cross polarization levels in the two resonant bands are better than 10dB. It is also seen from the plot that the polarization in both the bands is in y-direction as expected from the current analysis through simulation.

5.13 Radiation Pattern:

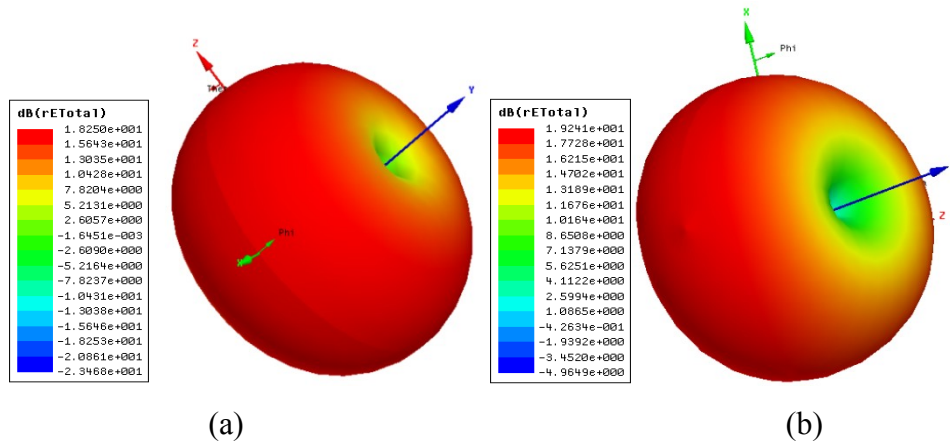The 3D radiation pattern obtained from simulation in both the resonant band is depicted in fig.5.19.

<div align="center">(a)   (b)</div>

Fig.5.19: Simulated 3D radiation patterns of the dual band antenna.(a) 2.1GHz, (b) 4.5GHz (L_g=15mm, W_g=10mm, g=0.35mm, W_m=3mm, L_m=25mm, L_1=2.5mm, W_f=23mm, L_f=10mm, L_{sl}=15mm, W_{sl}=2.5mm, L_s=14mm and W_s=1mm)

It is found that the dual band flared monopole antenna provides almost Omni-directional radiation coverage in both the resonant bands. It is worth to note that the slot loading over the add-on element does not disturbed the radiation patterns.

Measured radiation patterns at the centre frequencies of each application bands are plotted in fig.5.20. It is seen that the radiation patterns are almost omni-directional with reasonable cross polarization level in the proposed application band.
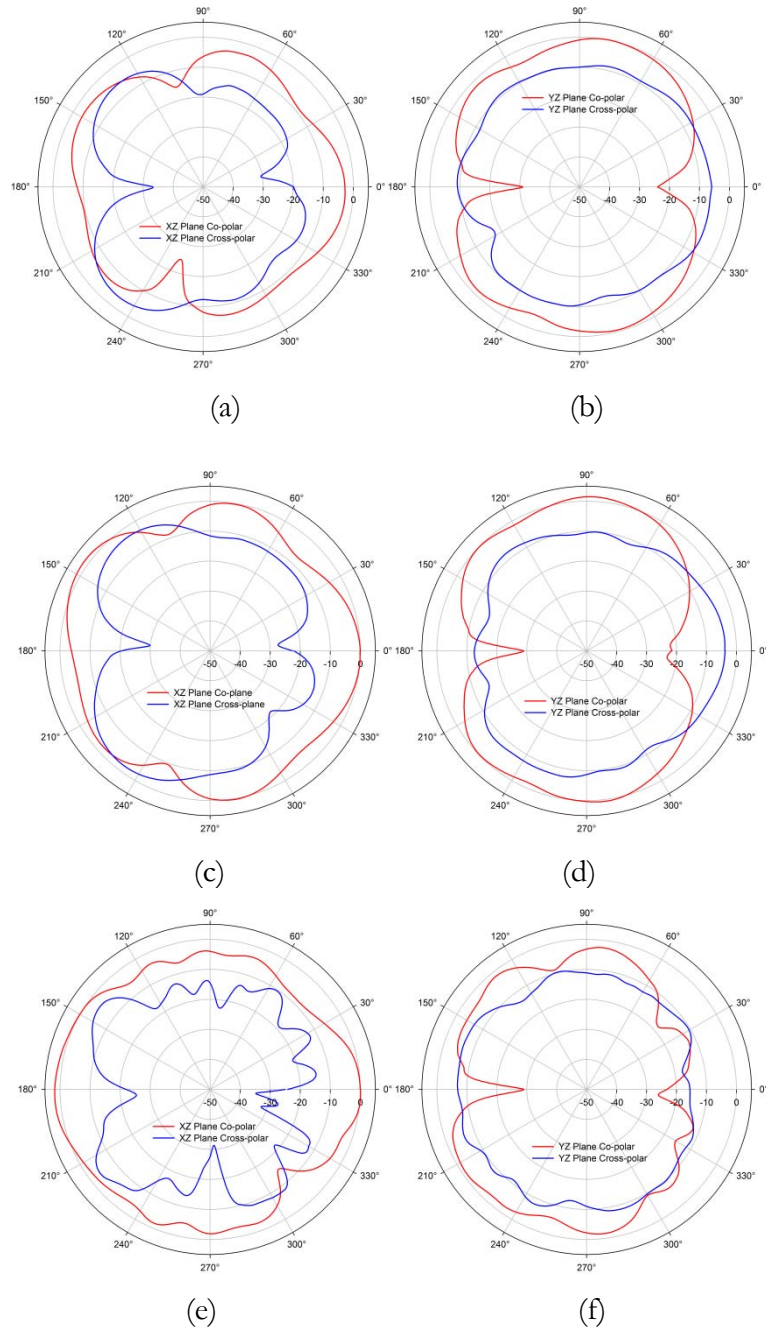
Fig.5.20: Measured radiation patterns in the two orthogonal planes.(a)-(b): 1.92GHz, (c)-(d): 2.05GHz, (e)-(f):5.25 GHz(L_g=15mm, W_g=10mm, g=0.35mm, W_m=3mm, L_m=25mm, L_1=2.5mm, W_f=23mm, L_f=10mm, L_{sl}=15mm, W_{sl}=2.5mm, L_s=14mm and W_s=1mm)

5.14 Gain and efficiency:

Measured peak gain of the antenna in the 1.83-2.34 GHz and 3.23 -5.76 GHz bands are depicted in fig.5.21. It is seen from the plot that the gain in the first band has a maximum variation of 3dBi while the gain in the second band has a variation of 2dBi.
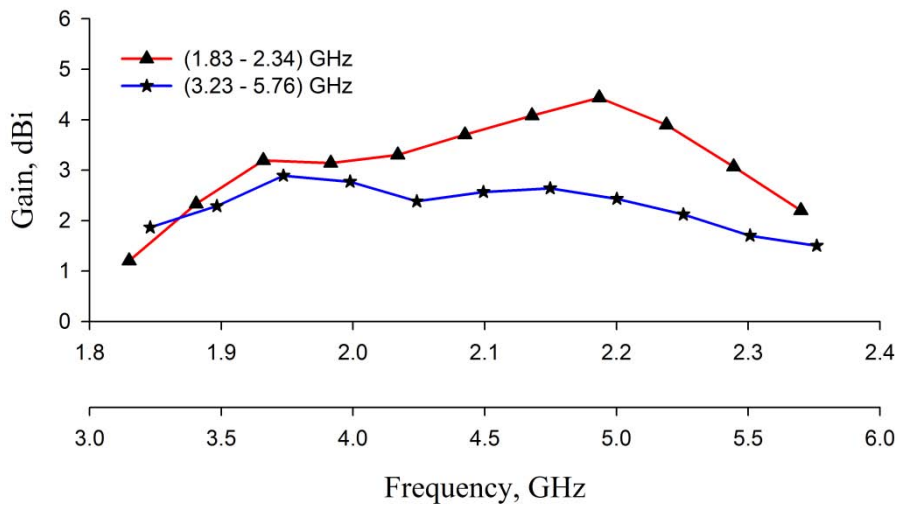

Fig.5.21: Measured peak gains of the dual band antenna(L_g=15mm, W_g=10mm, g=0.35mm, W_m=3mm, L_m=25mm, L_1=2.5mm, W_f=23mm, L_f=10mm, L_{sl}=15mm, W_{sl}=2.5mm, L_s=14mm and W_s=1mm)

The radiation efficiency of the proposed monopole antenna is measured using wheeler cap method. The measured, average efficiency of the antenna in the first and second resonant bands, are 79.8% and 68.9% respectively.

5.15 Parametric Analysis.

A parametric analysis is conducted through software simulation in order to investigate the effect of different antenna parameters over the antenna characteristics.

5.15.1 Effect of Finite ground dimensions

The finite ground dimensions, L_g and W_g are varied and studied its influence over the slot loaded antenna characteristics.

5.15.1.1 Effect of finite ground width, W_g

Fig.5.22. shows the variation in return loss characteristics, centre frequency and percentage bandwidth with finite ground width, W_g

(a)

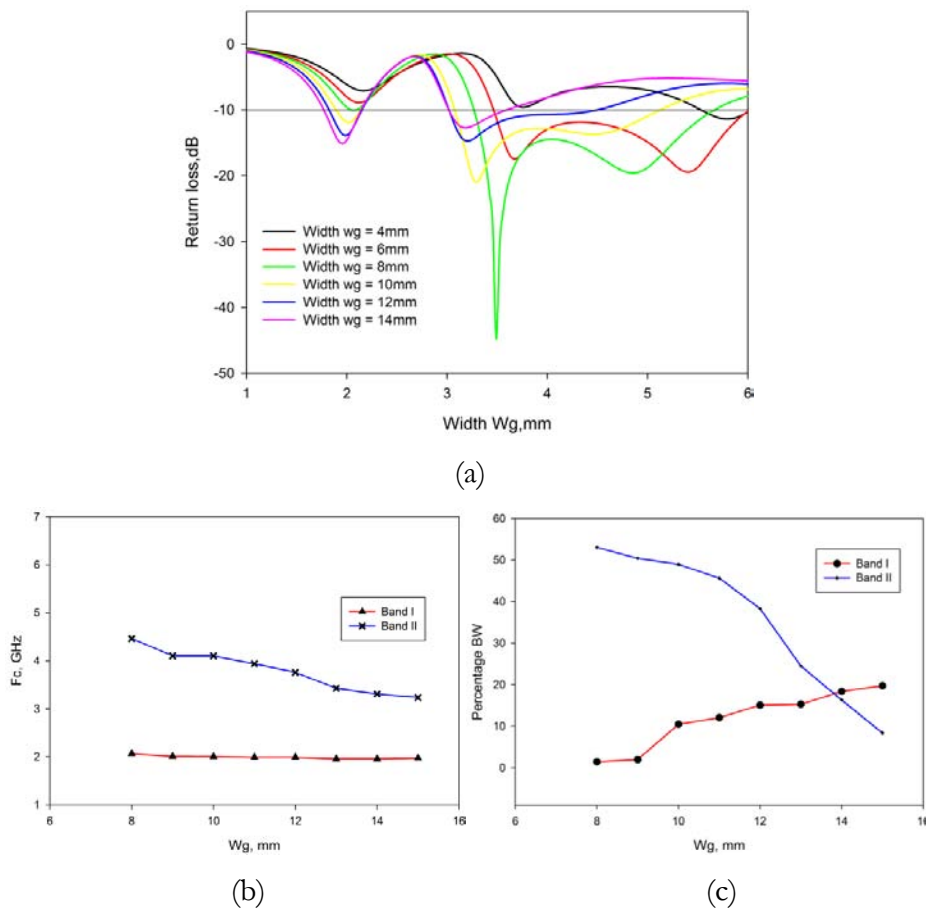(b)   (c)

Fig.5.22: Influence of ground plane width over both the resonant bands (L_g=15mm, g=0.35mm, W_m=3mm, L_m=25mm, L_1=2.5mm, W_f=23mm, L_f=10mm, L_{sl}=15mm, W_{sl}=2.5mm, L_s=14mm and W_s=1mm)

It is seen from the parametric analysis over the return loss characteristics of the proposed antenna that, the first resonant band remains unaltered with w_g while the matching at the higher portion of the second resonant band decreases drastically. This in turn results in reduction of bandwidth of the second resonance.

5.15.1.2 Effect of finite ground length, Lg.

The ground plane length, L_g of the slot loaded antenna is varied from 13mm to 20mm and it is observed that the both the resonances remains almost unaltered but the percentage bandwidth of the second resonant band decreases as Lg increases. The variations are depicted in fig.5.23
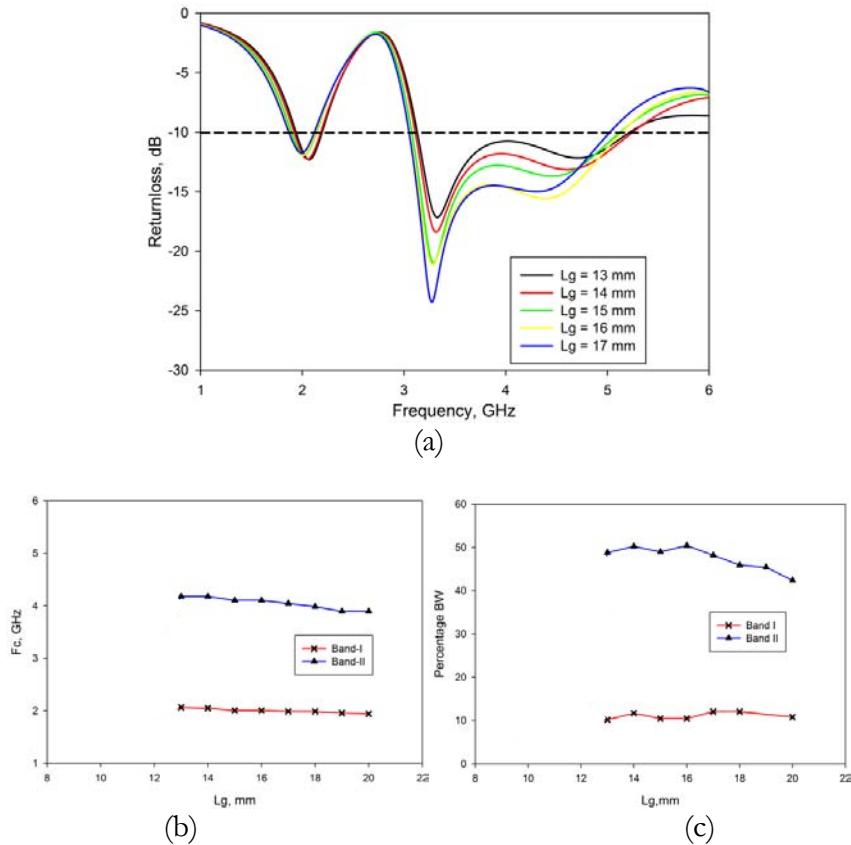

(a)

(b)   (c)

Fig 5.23 Effect of finite ground plane width over the (a)returnloss characteristics (b) Resonant frequency (c) Percentage bandwidth(W_g=10mm, g=0.35mm, W_m=3mm, L_m=25mm, L_1=2.5mm, W_f=23mm, L_f=10mm, L_{sl}=15mm, W_{sl}=2.5mm, L_s=14mm and W_s=1mm)

5.15.2 Effect of flaring width, W_f

To investigate the effect of flaring employed in the finite ground coplanar waveguide antenna integrated with slot loaded V-element, the width of flaring is varied from 15mm to 25mm and is illustrated in fig.5.24

(a)

(b)   (c)
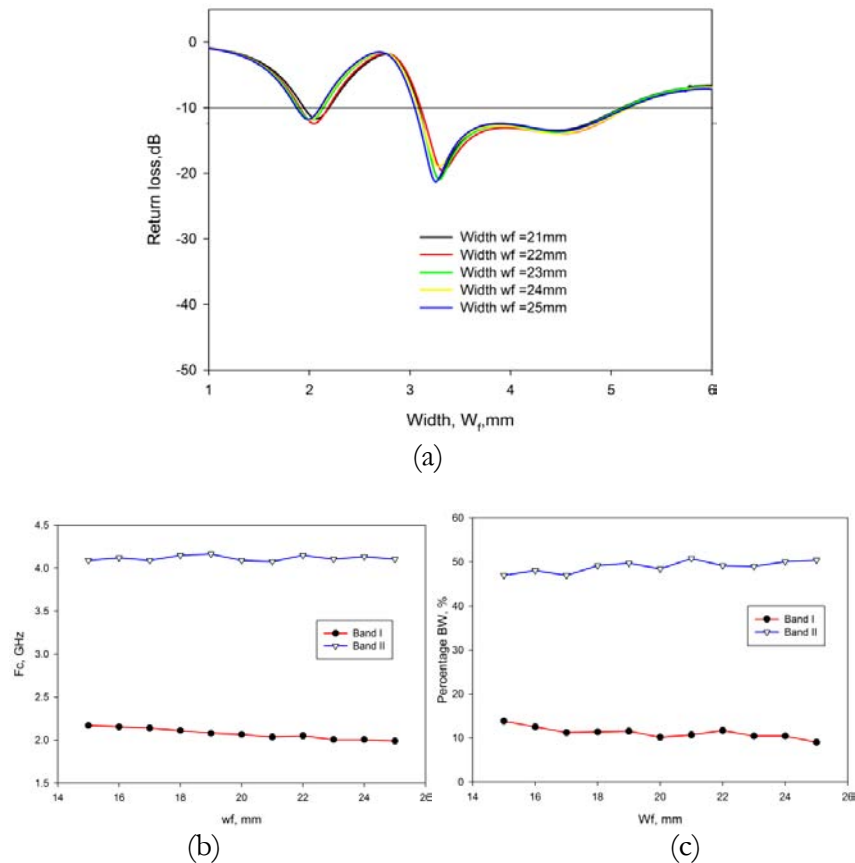
Fig.5.24: Influence of W_f over both the resonant band (a) Returnloss (b) percentage bandwidth (c) Center frequency(L_g=15mm, W_g=10mm, g=0.35mm, W_m=3mm, L_m=25mm, L_1=2.5mm, L_f=10mm, L_{sl}=15mm, W_{sl}=2.5mm, L_s=14mm and W_s=1mm)

It is observed from the plot that the both the resonances has feeble effect over the antenna characteristics. Both the resonant frequencies and corresponding bandwidth remains almost stable with the W_f variation.

144

5.15.3 Effect of 'V' element length(L_{sl})

The effect of 'V'-element length over the resonant frequencies are studied and plotted in fig.5.25
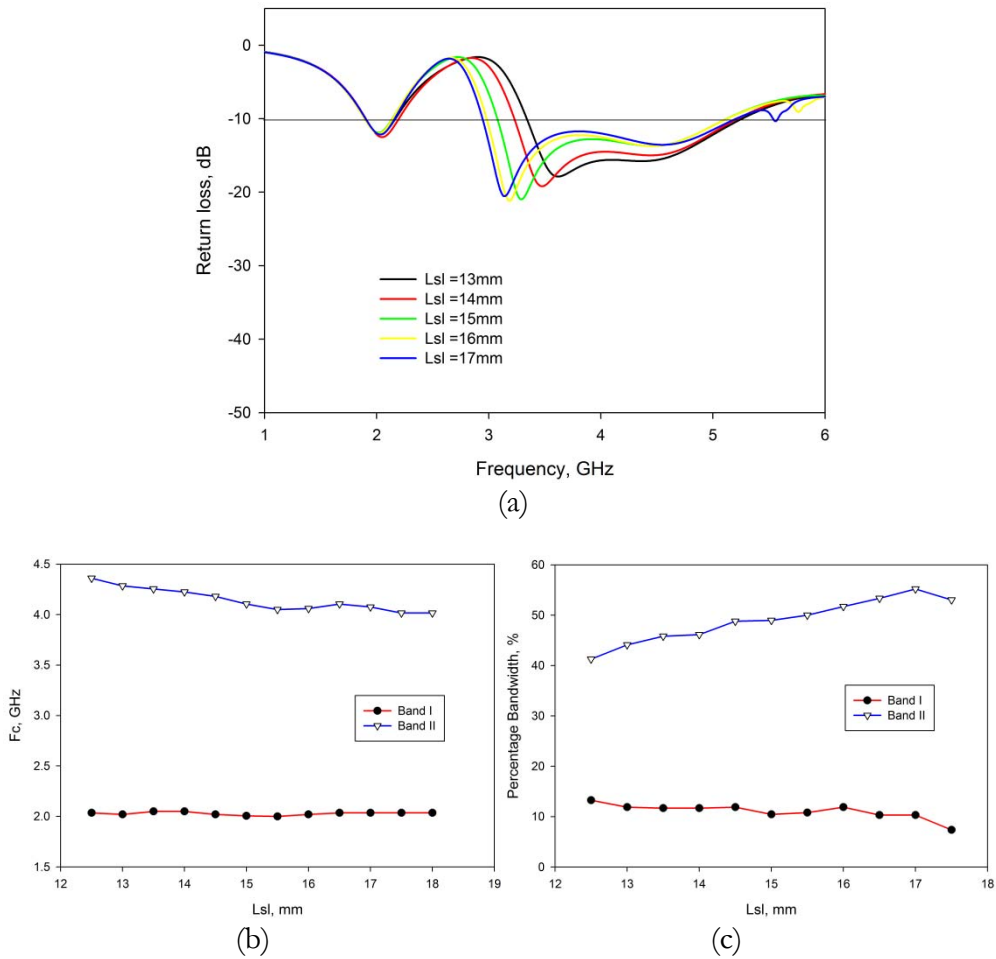

(a)

(b)

(c)

Fig.5.25: Influence of L_{sl} over the antenna characteristics. (a) returnloss (b) center frequency (b) percentage bandwidth(L_g=15mm, W_g=10mm, g=0.35mm, W_m=3mm, L_m=25mm, L_1=2.5mm, W_f=23mm, L_f=10mm, W_{sl}=2.5mm, L_s=14mm and W_s=1mm)

It is observed from the analysis that the second resonance is get tuned by the variation in the length of the add-on element. This conforms the prediction of the resonant length in the surface current analysis in section 5.11. From the bandwidth variations it can be concluded that the length of the V-element will slightly affect the bandwidth of the second resonant frequency while the bandwidth of the first resonant frequency remains unaltered.

5.15.4 Effect of slot length, Ls

The effect of slot over the bandwidth and both the resonances are studied through parametric analysis. The results are plotted in fig.5.26.

(a)
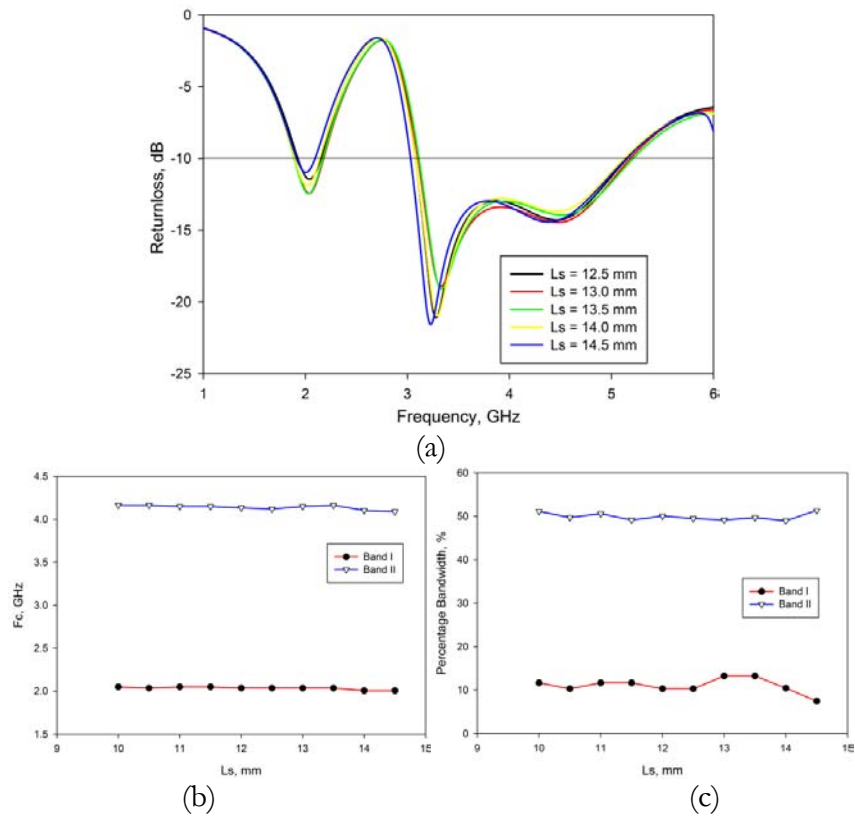

(b)   (c)

Fig.5.26: Influence of slot on the 'v' element over the antenna characteristics. (a) Returnloss characteristics(b) Resonant frequency(c)Bandwidth(L_g=15mm, W_g=10mm, g=0.35mm, W_m=3mm, L_m=25mm, L_1=2.5mm, W_f=23mm, L_f=10mm, L_{sl}=15mm, W_{sl}=2.5mm and W_s=1mm)

It is found from the analysis that, even though the implementation of the slot results improvement in the bandwidth due to the merging of two resonant frequencies, the variation in the slot length has only a feeble effect over the bandwidth variations.

5.15.5 Effect of sleeve position(L_1)

The variation of sleeve over the return loss characteristics, on the slot loaded antenna, is studied and the effect of sleeve position is plotted in fig.5.27
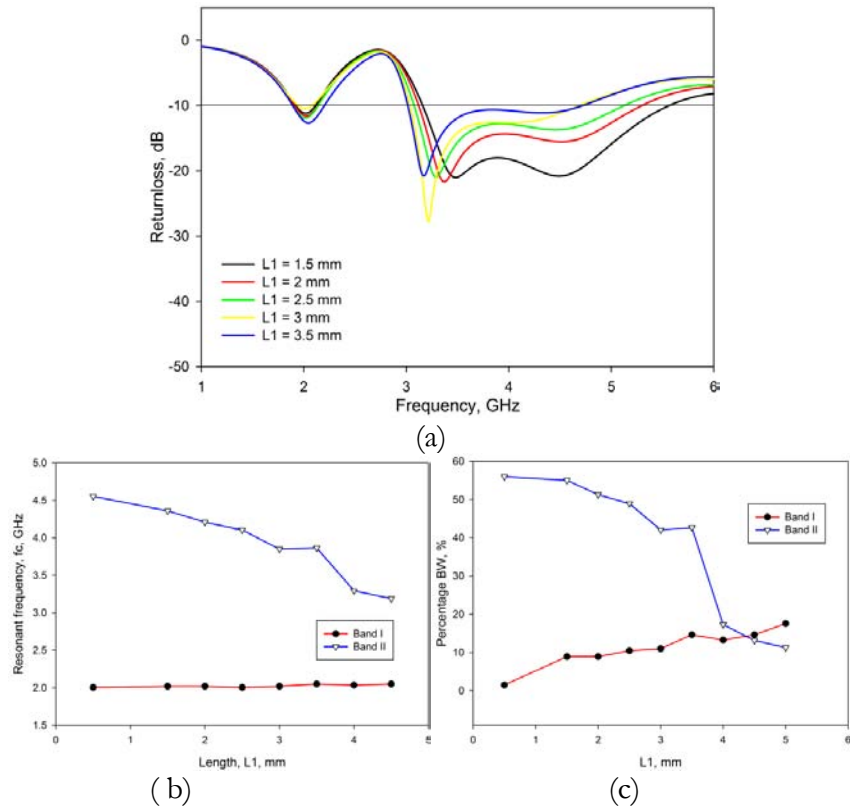
Fig.5.27. Variation of the sleeve position over the return loss characteristics. (a) returnloss (b) resonant frequency (c) percentage bandwidth(L_g=15mm, W_g=10mm, g=0.35mm, W_m=3mm, L_m=25mm, W_f=23mm, L_f=10mm, L_{sl}=15mm, W_{sl}=2.5mm, L_s=14mm and W_s=1mm)

It is observed that as L_1 varies from 0.5mm to 5mm the first resonant band remains almost stable. This is because the resonant length corresponds to the first band, as depicted in the previous section by analyzing current plots, does not depend on L_1. Alternatively the second resonance is highly shifting to a lower frequency region as L_1 increases. It is also clear from the plot in fig.5.27(b) that the position of the sleeve in the flared monopole is a crucial factor in determining bandwidth.

5.16 Conclusions.

The following conclusions can be made from the analysis,

- The bandwidth enhancement for the proposed antenna can be achieved by loading a slot in the add-on element without much disturbing the radiation characteristics of the antenna.
- The resonant band can be tuned by modifying appropriate antenna elements.
- The antenna exhibits linearly polarized, nearly omni-directional radiation patterns which are highly suitable for mobile communication applications.

CONCLUSION AND FUTURE PERSPECTIVE

*T*his chapter highlights the conclusions drawn from numerical and experimental investigations conducted on the flared monopole antenna for dual band applications. The important features of the geometry are examined. Suggestions for future work in the field are also included in this chapter.

6.1 Thesis highlights and Key contributions

This chapter brings the thesis to the closing stages by summarizing the important concepts drawn from the numerical and experimental analysis of printed strip flared monopole antenna. Aim of the work is to investigate the effect of antenna parameters on antenna characteristics and development of dual band flared monopole antenna suitable for the use in wireless gadgets like PDAs, PCs, WLANs and mobile phones.

Chapter 1 provides the general information about the antenna engineering with a brief history in the field. It describes the different types of antennas with a special emphasis to the printed antenna technology. Motivation of the present work in the context of today's technology advancement is also provided in this chapter

The literature review of the developments in the antenna design around the world is depicted in chapter 2. It includes recent developments reported in the literature with a special attention to the developments in the field of coplanar wave guide antennas. The literature review also includes the developments in the field of numerical modeling using FDTD.

The theoretical and experimental methodology for the antenna characterization has been explained in the chapter 3. It clearly illustrates sophisticated instruments used for the antenna measurements and simulations tools utilized for the simulation. A brief description about the FDTD technique is also outlined in this chapter.

Chapter 4 provides the development of a flared strip monopole antenna from the coplanar fed strip monopole. It illustrates the experimental and theoretical results of the proposed antenna .

Chapter 5 provides the development of a dual band antenna from flared monopole with slotted V-element. The effect of various antenna elements is studied in detail. The chapter discusses the dual band mechanism of the antenna.

Chapter 6 is the concluding section of this thesis. It describes important inferences based on results and salient features of the proposed dual band antenna and its applications. The scope of future work is also discussed in this chapter.

Appendix 'A' provides a strip monopole fed triangular patch antenna for wireless access point. A microstrip leaky-wave antenna for low cost beam steering applications is provided in Appendix B. Appendix C presents an electronically scannable log-periodic leaky wave antenna.

6.2 Inferences from flared monopole antenna

- The implementation of flaring in the finite ground coplanar wave guide fed strip monopole antenna results in increase in the effective resonant length which in turn results a shift in the resonant frequency to a lower frequency region.

- The polarization and radiation pattern of the strip monopole remains unaltered by the flaring.

- The flaring parameter L_f and W_f along with Lm determines the resonant frequency of the antenna.

- A feeble effect of the ground plane dimensions on the antenna characteristics is observed.

- Experimental results shows that the antenna exhibits almost omnidirectional radiation characteristics with a peak gain of 3dBi throughout the resonant band.

- By providing a symmetric flaring in the strip monopole, a resonance can be generated just before the fundamental resonant frequency of the monopole.

6.3 Inferences from the Dual band flared monopole antenna with a 'V' shaped element.

An additional resonant band at a higher frequency region is formed by integrating a 'V' shaped add on element in the flared monopole antenna without disturbing the first resonance.

- The first resonance is controlled by the dimensions of the flared monopole antenna while the second resonance is defined by the dimensions of the additional 'V' shaped element.

- The FDTD method is employed for the numerical computation in Matlab. The returnloss characteristics using FDTD code, Ansoft HFSS and measurements are in good agreement.

- Bandwidth enhancement for the antenna is obtained by slot loading along the add-on 'V' element.

- The antenna provides linearly polarized, nearly omni-directional radiation patterns with moderate gain better than 3.5 dBi.

6.4 Suggestions for future work

Printed monopole array can be realized to modify the radiation pattern suitable for special applications. The modifications in the design to achieve electronic tuning of the resonant frequencies by the integrateion of varactor diodes is another area for future work. Redome for the antenna can be developed for the protection form environmental variations

A Compact Dual Band Antenna for Wireless Access Point

A compact dual band printed antenna covering the 2.4 GHz (2400 – 2485 MHz) and 5.2GHz (5150 – 5350 MHz) WLAN band is presented. The experimental analysis shows a 2:1 VSWR bandwidth of upto 32% and 8% for 2.4 GHz and 5.2GHz respectively. The measured radiation patterns are nearly omni directional with moderate gain in both the WLAN bands

A.1 Introduction

Wireless Local Area Networks (WLAN) have recorded tremendous growth in recent years. A Wireless access point facilitates wireless connection between PCs, laptops, wireless routers and other wireless modules. To meet the miniaturization and bandwidth requirements of modern wireless communication equipments, the design of a compact, broad band antenna is of prime interest. As per IEEE recommendation, the 2.4 GHz WLAN occupies a spectrum from 2400 MHz – 2485 MHz whereas the 5.2 GHz Hyperlan occupies the 5150 MHz – 5350 MHz. The present scenario in the wireless communication systems indicates a shift of operating frequency from the 2.4 GHz band to the 5.2 GHz band for various reasons. Hence a single, compact antenna supporting both these WLAN bands is of great significance.

In this session, we propose a novel dual band planar antenna suitable for the wireless communication systems. Various antenna parameters are optimized using Ansoft HFSS™ v10, to meet the design goals at both frequency bands of interest. The measured performance of the proposed geometry are presented and discussed.

A.2 Antenna Design

The proposed geometry comprises of a triangular slot loaded patch antenna, on layer 1, excited by the planar strip monopole as shown in fig.A1. The dimensions of the patch are optimized for 2.4/5.2 GHz WLAN application, on a substrate of thickness 1.6mm and the dielectric constant ε_r 4.2 A 50Ω microstrip line with truncated ground plane etched on layer 2 serves as the feed and radiating monopole. The overall size of the antenna, including the feed structure, is (20 x 50) mm^2. The dual band performance of the proposed antenna is obtained from the dual resonant structures of different dimensions. In the geometry, the resonant
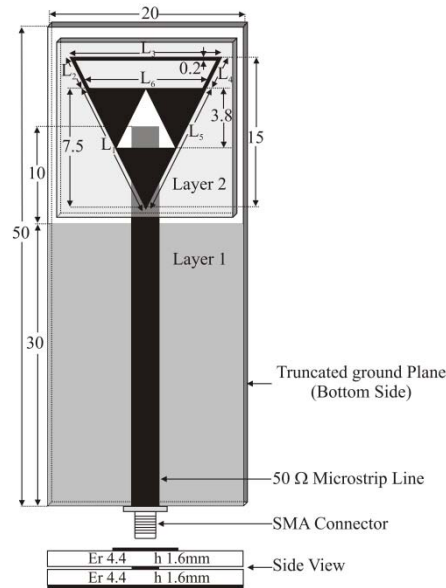
Fig. A1 Geometry and dimensions of the proposed antenna. [L_1 = 13.5mm, L_2 = 3.5 mm, L_3 = 20mm, L_4 = 3.5mm, L_5 = 13.5 mm, L_6 = 12 mm.]

path length L1 + L_2 + L_3 + L_4 + L_5 is set close to λ_g at 2.4 GHz and the slot dimension L_2 + L_3 + L_4+ L_6 corresponds to λ_g at 5.2 GHz. The relative position of the patch on the feed monopole is optimized using the optimization tool of HFSS™ v10 to obtain good impedance matching.

A3 Results and discussions:

The simulated results obtained using HFSS™ v10 is validated experimentally from measurements using HP8510C vector network analyzer. The measured and simulated return loss characteristics of the proposed antenna are shown in figure A2.
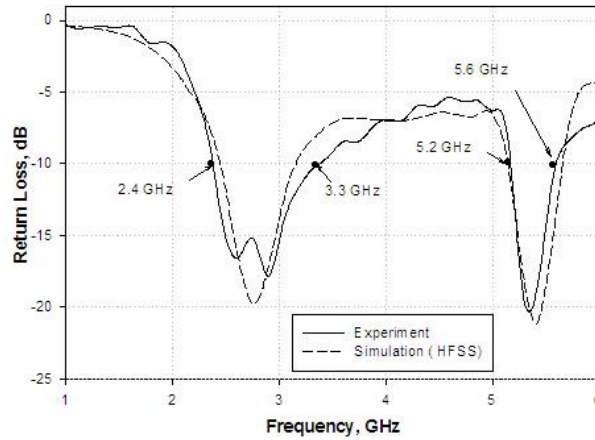
Fig. A2 Measured and simulated return loss of the proposed antenna [L_1 = 13.5mm, L_2 = 3.5 mm, L_3 = 20mm, L_4 = 3.5mm, L_5 = 13.5 mm, L_6 = 12 mm]

It is seen that the lower resonant mode covers the 2.45 GHz WLAN band and the upper resonance covers the 5.2 GHz band. In the lower resonant band, the 2:1 VSWR bandwidth is about 936.625 MHz (2.386 – 3.323 GHz) which corresponds to 32.8% at the centre frequency of 2.85 GHz. This meets the bandwidth requirement for IEEE 802.11 b/g WLAN applications. In the 5.2 GHz band, the -10 dB return loss bandwidth is about 435.125 MHz (5.17 – 5.60 GHz) with 8.1 % bandwidth at the centre frequency of 5.384 GHz. Measured return loss behavior shows reasonably good agreement with the simulated results.

The simulated surface current distributions, for the proposed antenna at 2.4 GHz and 5.2 GHz are presented in Fig A3.
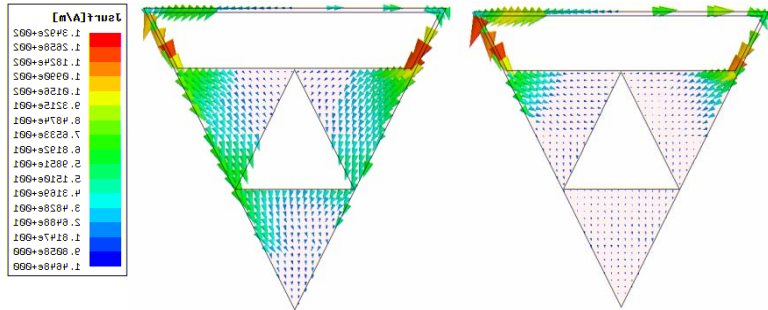
Fig. A3 Simulated surface current distributions on the antenna.
a) 2442 MHz ; b) 5250 MHz[L$_1$ = 13.5mm, L$_2$ = 3.5 mm, L$_3$ = 20mm, L$_4$ = 3.5mm, L$_5$ = 13.5 mm, L$_6$ = 12 mm]

It can be seen that the upper part of the triangle contribute to the 2.45 GHz resonance and the slot contributes to 5.2 GHz. Measured radiation patterns in the orthogonal x-z, y-z planes are plotted in Fig A4. Fig A5 shows the measured gain in the two operating bands. For the lower band the antenna gain varies from 3.7dBi to 4.7dBi. As for the upper band, the antenna gain lies between 2.8 dBi and 5.3 dBi.]
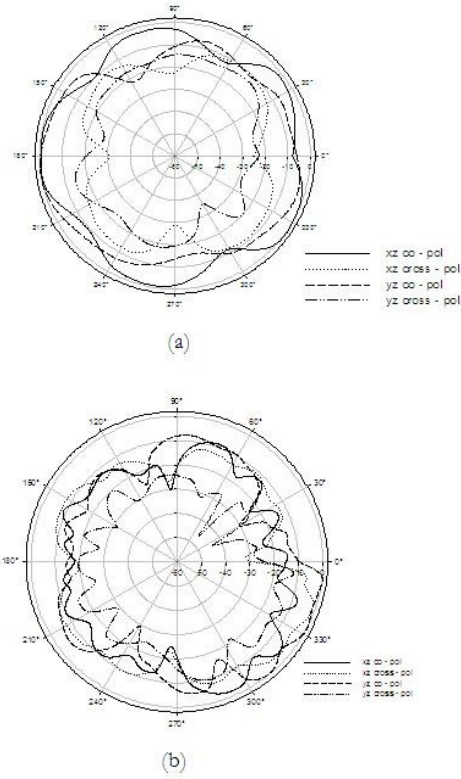
Fig. A4 Measured radiation patterns of the proposed antenna a) 2442 MHz ; b) 5250 MHz [$L_1 = 13.5$mm, $L_2 = 3.5$ mm, $L_3 = 20$mm, $L_4 = 3.5$mm, $L_5 = 13.5$ mm, $L_6 = 12$ mm]
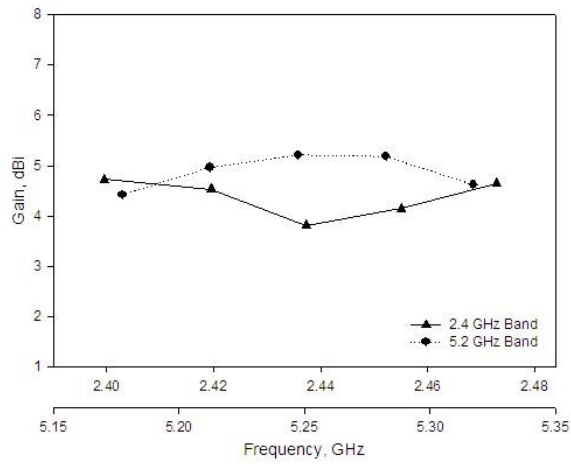
Fig. A5 Measured gain of the proposed antenna [$L_1 = 13.5$mm, $L_2 = 3.5$ mm, $L_3 = 20$mm, $L_4 = 3.5$mm, $L_5 = 13.5$ mm, $L_6 = 12$ mm]

161

A4 Conclusion: A compact dual band monopole excited patch antenna for wireless access point is designed, fabricated, tested and simulated. The proposed antenna of dimension (20 x 50)mm^2 is suitable for integration with the wireless access point. It exhibits two broad 2:1 VSWR bands covering the 2.45 GHz (2386 – 3323 MHz) and 5.2 GHz (5167 - 5602 MHz) WLAN bands with good radiation characteristics in the bands.

References

1. H.R.CHUANG, and C.C. LIN. : 'A Printed UWB Triangular Monopole Antenna', *Microwave Journal*, 2006, 49,(1),pp. 108-120.
2. W.-C. LIU and C.-F. HSU: ' Dual-band CPW-fed Y-Shaped monopole antenna for PCS/WLAN application', *Electron. Lett.*, 2005, 41(18), pp. 390-391.
3. HORNG-DEAN CHEN, HONG-TWU CHEN: 'A CPW Fed Dual Frequency Monopole Antenna', *IEEE Trans. on Antennas and Propagation*, 2004, 52, (4) , pp 972 – 982.
4. CHEN, T.L : 'Multi-band printed sleeve dipole antenna', *Electron. Lett.*, 2003, 39, (1), pp. 14-15.

An Electronically Beam Steering Log-Periodic slot loaded Leaky Wave Antenna

An innovative phaseshifterless, wideband, leaky wave antenna with electronically steerable dual pencil beam pattern in the H-plane is presented. The log periodic geometry of the leaky slots of the antenna results a wide band width of 21.84 %. The fan beam can be steered upto 14 degree over the wide resonating band of the antenna. The beam is also steerable at a fixed frequency, by reactively loading the slot and a maximum steering angle of 13 degree is observed for different capacitor values with an improved bandwidth of 33.3%. The concept is studied using passive components but it can be extended to varactors and reactive switching pin diodes.

B.1 Introduction:

Simple beam scanning techniques found applications in low coast radar systems, wireless communication, imaging and side looking sensors in automotives. Frequency scanning is the cost effective alternative to phase scanning in the above applications because phase shifters and associated elements are not required to steer the antenna beam. Microstrip leaky wave antenna has the excellent advantage of wider bandwidth, pencil beam and frequency scanning capability. The leaky wave antenna has a narrow fan beam in the H plane, with single excitation, which make it suitable for integrated antenna array applications. Here we demonstrate a log periodic slotline microstrip antenna with a wide scanning angle of 14 degree and 10 dB bandwidth of 33.4 %. Log periodic construction of the leaky slots gives wide band width and hence more frequency scannability. The H- plane pencil beam of the proposed antenna is scannable at a fixed frequency by varying the capacitance , loaded at the leaky slots. The wide bandwidth of the proposed antenna provides a large steering angle when frequency scanning in the band is required. Moreover, the reactive loading enables beam steering at a fixed frequency by changing the capacitance values loaded at the leaky slotslines. The design has been successfully implemented and proved with passive components, but can be modified with varactors for beam steering by dc bias.

B.2 Antenna Design:

The geometry of the proposed log periodic leaky wave antenna is shown in the Fig. B1. The log periodic slotline structure is etched on a substrate of dielectric constant $\varepsilon r = 4.17$ and thickness, $d = 1.6mm$. The width of the log periodic slotline is optimized for 1mm using Zeland IE3D 7.15 . The logperiodic vertical slots are studied for different values of τ and studied the effect of τ over bandwidth. The log periodic dimension of the leaky wave antenna is so selected

164

that it will suppress the dominant mode and radiate the first higher order mode. The antenna is fed by a 50 ohm microstrip feed line. The leaky slots of the antenna is loaded with SMD capacitors which results beam steering at fixed frequency.
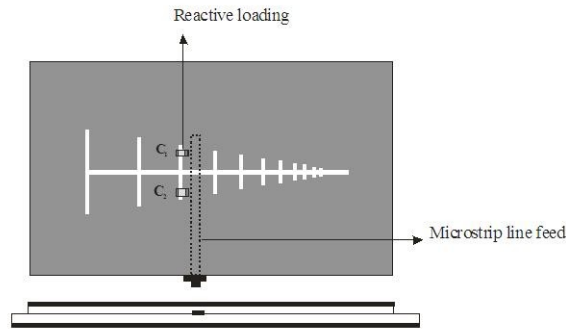
Fig. B1 Geometry of the proposed Log periodic Leaky wave antenna. The slots are arranged in log periodically with toea = 0.8 and the slot width is 1mm.

B.3 Results and discussions:

The log periodic leaky wave antenna has been designed and studied experimentally. The measured return loss and transmission characteristics of the log periodic leaky wave antenna with $\tau = 0.8$ is shown in fig.B2 Good matching performance is obtained in the frequency region from 4.8 GHz to 5.88 GHz resulting a bandwidth of 21.84 %. An improvement of bandwidth is observed by loading capacitors over the third arm as shown in fig.B3. The -10dB band is 4.53GHz to 6.34GHz which results a percentage band width of 33.3%.
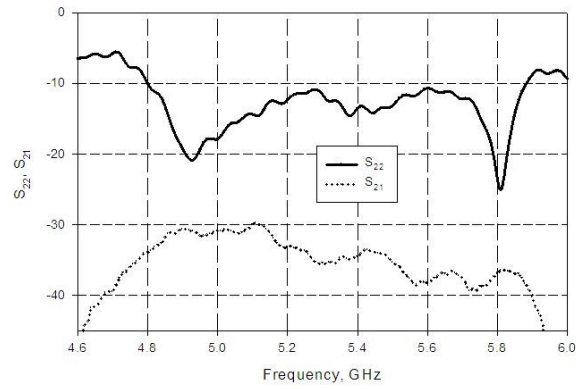
Fig.B2 Measured return loss and transmission characteristics of the antenna for optimized log periodic structure, observed a 10dB band width of 21.84 %.
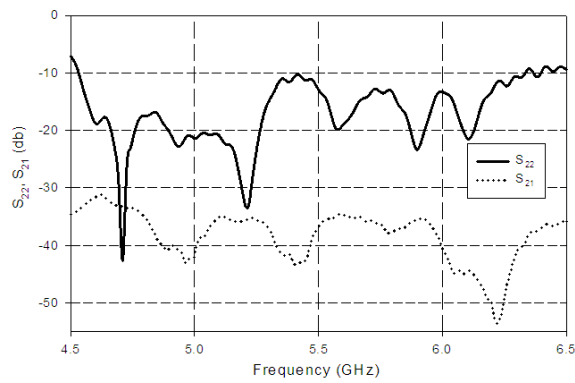
Fig. B3 Measured return loss and transmission characteristics of the reactive loaded, Log periodic leaky-wave antenna, observed an improved band width of 33.3 %.

The radiation pattern was measured under the far-field condition. The measured H-Plane radiation patterns are shown in fig.B4
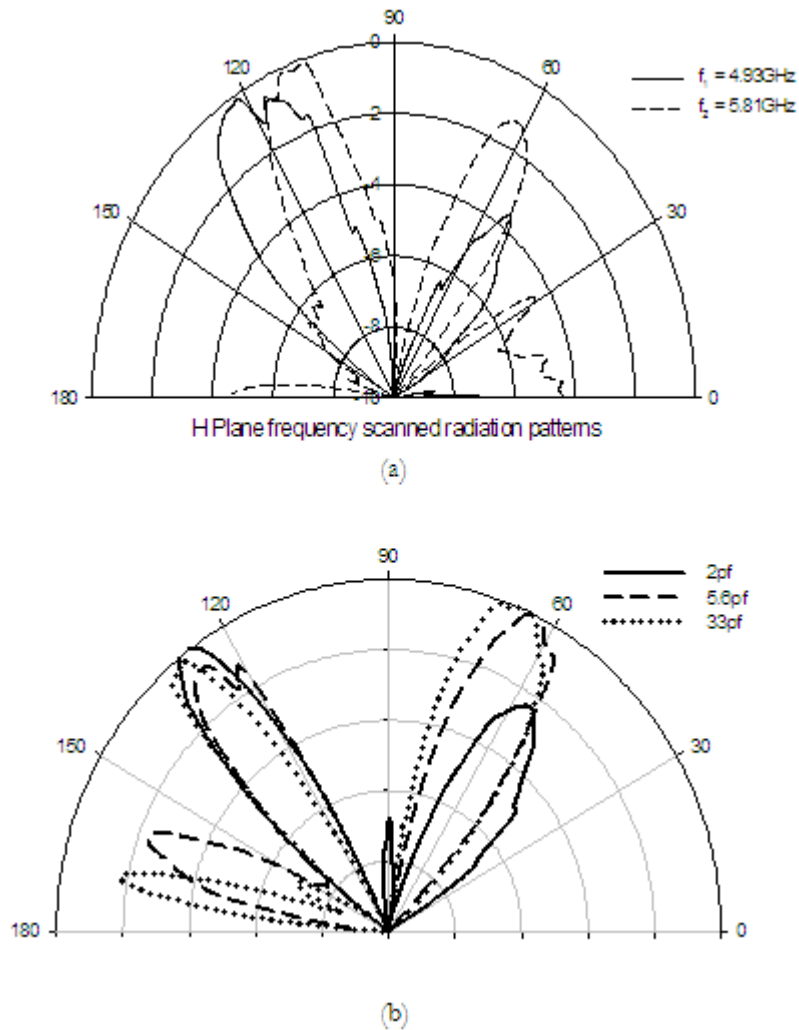
Fig. B4 Measured H Plane patterns. (a)The Frequency scanned patterns (b) Fixed frequency beam steering.

Two maxima are observed which indicate the dual-beam and frequency-scanning characteristics of the log-periodic leaky wave antenna. The observed beam steering is about 14° and the half-power beam widths of the H-plane are less than 20°. Fig.B4 (b) presents the measured H plane radiation patterns at 5 GHz for different values of loaded capacitors; the measured beam steering is about 13° when capacitor value changed from 2pf to 33pf.

B.4 Conclusion:

The work reported in this letter presents a wideband, beam steering leaky wave antenna without a phase shifter. The main beam can be made to point at different points. The reactive loading over the leaky slots of the antenna results beam steering at fixed frequency. Extension of the work using varactors or switching diodes has applications in side looking radars for automotive sensors or such low cost tracking radars.

B.5 References:

1. C. Luxey, J.M. Laheurte, Simple design of dual-beam leaky-wave antennas in microstrips, IEE Proc.Micrw. Antennas Propag., Vol 144, No.6 , December 1997.
2. C. Luxey, J.M. Laheurte, Effect of reactive loading in microstrip leaky wave antennas., Electronics Letters, Vol. 36, No.15, July 2000.
3. Chih-Chiang Chen and Ching-Kuang C. Tzuang, Phase-shifterless beam-steering micro-slotline antenna, Electronic Letters, Vol.38, No.8, April 2002.

Reactive loaded microstrip leaky-wave antenna for low cost beam steering applications

A slotline leaky wave antenna for beam steering applications in low cost tracking and side looking sensors in collision avoidance systems for automobiles is presented. The antenna exhibits both frequency scannability of 80° as well as fixed frequency beam steering of 68° over the -10 dB resonating band of 4.56 to 5.06 GHz.

C.1 Introduction:

Collision avoidance systems in vehicles and side looking sensors need a compact, low profile easy to integrate antenna with wide scanning angle. Frequency scanning of microstrip leaky wave antennas is best suited for this purpose. However, this frequency dependence of the scanning angle, limits the use of these types of antennas if narrow frequency bandwidth is available and wide angle coverage is required. Fixed frequency beam scanning is the right alternative, but new feeding configurations and phase shifter circuits integrated to the antenna are required. As the phase velocity along the microstrip and the cut off frequency of its first higher order mode are functions of the reactance across the slots, capacitive loading along the leaky slot line provides a simple method for fixed frequency beam steering. In this letter we propose a microstrip slot line leaky-wave antenna, loaded with MIM capacitors, capable of both frequency scannability and fixed frequency beam steering. The proposed antenna design and experimental results are presented.

C.2 Design :

The design consists of a rectangular microstrip patch of L = 44mm, W = 26mm, fabricated on a substrate of dielectric constant, ε_r = 4.7 and h = 1.6mm and depicted in fig. C1. A central slot of length 22mm with five horizontal slots of linearly decreasing length are loaded on either side, in the patch. Ansoft High Frequency Structure Simulator (HFSS) is used to optimize the dimensions and positions of the horizontal slots. The optimization is done to suppress the dominant resonant mode of the original patch and to excite the first higher mode with a single 50Ω microstrip feed line.
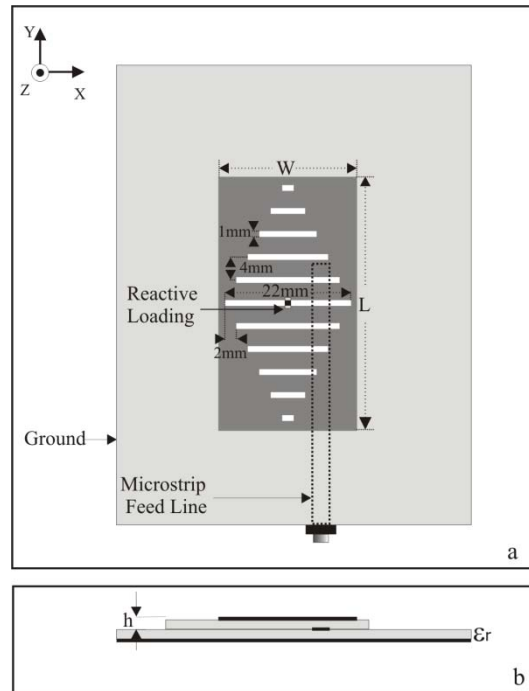
Fig. C1. Geometry of proposed low profile Leaky Wave Antenna . L = 44mm, W = 24 mm, h = .6mm (a) Top view (b) Side view

C.3 Results and discussions.

The experimental return loss characteristics, using Agilent 8263B PNA Series Network Analyzer, of the proposed design is shown in fig.C2(a). The leaky region of the antenna is characterized by its normalized phase constant (β / k0 < 1), the value of which determines the direction of the radiated beam. To understand the radiation characteristics of the LWA, we obtained its complex propagation constant (α + jβ) as a function of frequency. In fig.C2(b) it is seen that the space leaky region is fixed as 4.56 5.06 GHz corresponds to an antenna configuration of L = 44mm, W = 26mm, h = 1.6mm and ε_r = 4.7 Since β is a function of the surface reactance of the radiating patch, fixed frequency beam steering is accomplished by reactively loading the slot line embedded in the patch. This is achieved by integrating MIM capacitors(Q-Max, Capax Technologies) of different

172

values across the center horizontal slot. A good matching below -10dB over the predicted leaky band of 4.56 to 5.06 GHz is observed
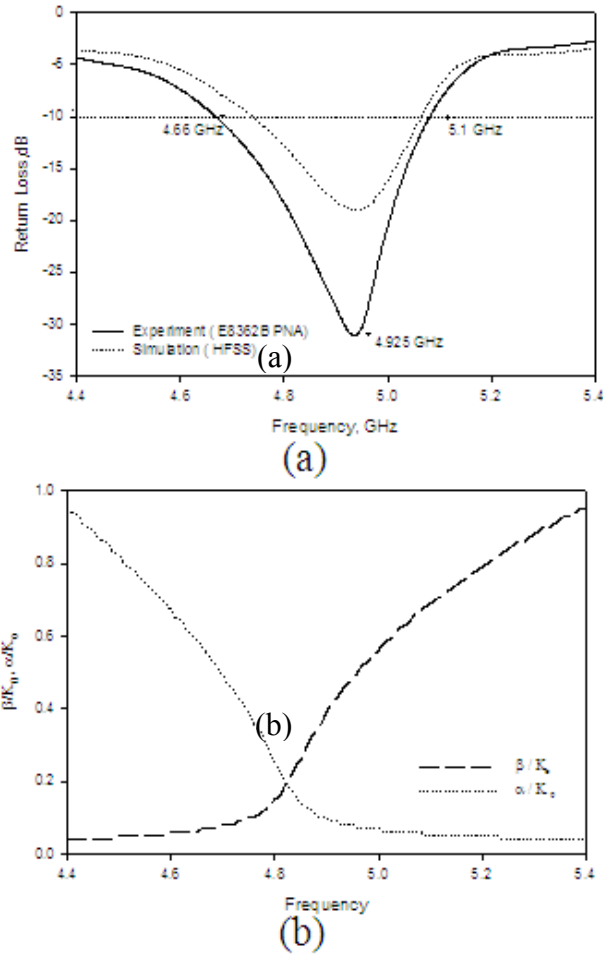

Fig C2 (a) Return loss characteristics of the Leaky Wave Antenna (b). Behavior of normalized phase constant β/k_0 and attenuation constant α/k_0 of first higher order leaky mode of Leaky wave antenna over the leaky band.

The frequency scanning feature of the antenna is shown in fig C3. When the frequency is varied from 4.56 GHz to 5.06 GHz, the direction of the main radiated

beam in the elevation plane is tilted from 31 ^{o} to 112 ^{o} resulting a frequency scanability of 81 ^{o}
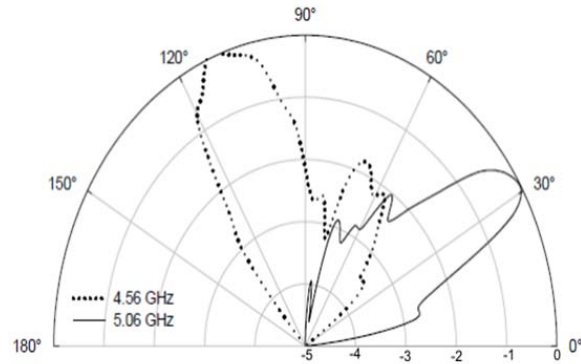
Fig. C3. Measured H- Plane radiation patterns of the Leaky-wave antenna at different frequencies.

Effect of reactive loading over the slot line is studied from the radiation pattern measured at 4.9 GHz for different values of loaded reactance. The unloaded leaky wave antenna has a radiation beam directed towards 113 ^{o} . Loaded tilt angle is 45 ^{o} and 41 ^{o} for capacitance values 1 pF and 2.2 pF respectively. We observe that a variation of capacitance from 1 pF to 2.2 pF gives a tilt of the radiated beam by 4 ^{o}. The fixed frequency beam-steering is depicted in fig.C3.

Fig. C3. Measured H- Plane radiation patterns of Capacitively Loaded Leaky-wave antenna (C = 2.2 pF, 5.6 pF) and Unloaded Leaky Wave Antenna at 4.9GHz.

Fig. C4 illustrates the computed surface current plot of the proposed antenna. It is observed that two current peak-points are visible in the horizontal direction which demonstrates the excitation of the higher order mode.
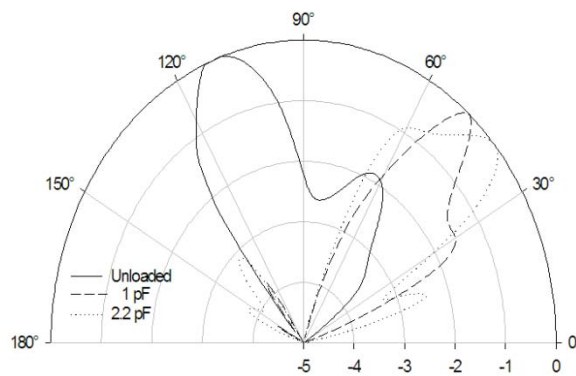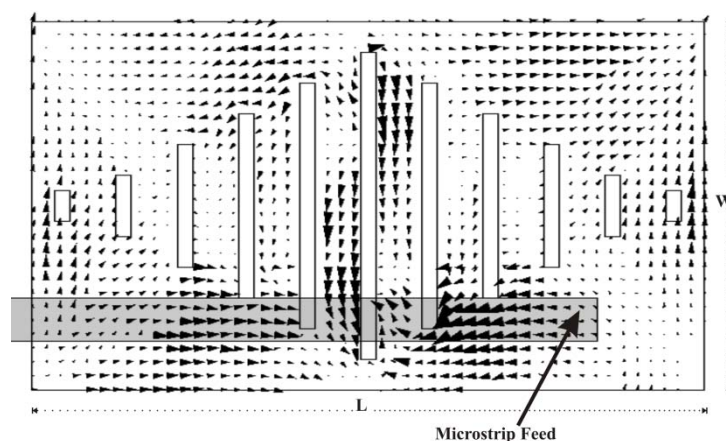

Fig. C4: Surface- current distribution of the Leaky wave antenna at 4.9 GHz.

C.4 Conclusion:

A novel reactively loaded slot line leaky wave antenna which finds application in side looking radars or any type of low cost tracking systems is presented. The antenna is capable of both frequency scanning of 80 ^{o} (160 ^{o} /GHz) and fixed frequency beam steering of 68 ^{o}

C.5 Reference

1. Yu-De Lin, Jyh- Wen Sheen and Ching _Kuang C Tzuang , " Analysis and Design of Feeding Structures for Microstrip Leaky-Wave Antenna" *IEEE Trans. Microwave Theory Tech.*, Vol44, No.9,1996, pp 1540 – 1547
2. Chin-Chiang Chen, Ching – Kuang C., "Phase Shifter less Beam Steering micro-slot line antenna" *Electronic Letters*, vol. 8, pp. 354-355.
3. Noujeim, K.M., " Wave propagation characteristics of a reactively loaded microstrip", *Microwave Symposium Digest*, 2003, pp. 821-824.
4. Jan Zehentner, Jan Machac and Petr Lorenz, " Space Leakage of Power from the Slot line", *MTT-S Digest 2001* , pp 1217 – 1220.
5. C. Luxey, J.-M Laheurte, "Simple design of dual beam leaky-wave antennas in microstrip", *Proc- Microwave antennas Propagag.*, 1997, vol. 6, pp 397

LIST OF PUBLICATIONS

International Journal

1. **Gijo Augustin**, Bybi P.C., Sarin V.P., C.K. Aananda, P.Mohanan and K.Vasudevan, "*A Compact dual band Antenna for DCS-1900/PCS/PHS, WCDMA/IMT-2000 and WLAN Applications*", IEEE Antennas and Wireless Propagation Letters, Vol.7, pp.108-111,2008.

2. P.C. Bybi, **Gijo Augustin**, B. Jitha, C.K. Aanandan, K.Vasudevan and P.Mohanan, "*A Quasi-omnidirectional antenna for modern wireless communication gadgests*", IEEE Antennas and Wireless Propagation Letters, Vol.7, pp.504-507, 2008

3. M.S. Nisha, V.P. Sarin, **Augustin Gijo**, V.Deepu, C.K. Aanandan, P. Mohanan and K.Vasudevan, " *Compact dual frequency dual polarized cross patch antenna with X-Slot*", Microwave and optical technology letters,Vol.50, No.12, pp.3198-3201, 2008.

4. V.P. Sarin, M.S. Nisha, **Gijo Augustin**, P.Mohanan, C.K. Aanandan, K.Vasudevan, "*An electromagnetically coupled dual-band dual polarized microstrip antenna for WLAN applications*",Microwave and optical Technology letters, Vol.50, No.7, pp.1867-1870, 2008

5. P.C. Bybi, **Gijo Augustin**, B. Jitha, Binu Paul, C.K.Aanandan , K. Vasudevan and P.Mohanan, "*Compact Monopole Excited Drum Shaped Antenna for AWS/ DCS/ PCS/ DECT/ 3G/ UMTS/ BLUETOOTH Application*," International Journal on Wireless and optical communications, Vol. 4, No.2,pp. 195-206, 2007.

6. **Gijo Augustin**, Shynu S.V., Mohanan P., C.K.Aanandan and K.Vasudevan, "*Compact dual band antenna for wireless access point*",IET Electronics Letters,Vol.42, No.9, pp.502-503, 2006.

7. Shynu S.V., **Gijo Augustin**, C.K. Aanandan, P.Mohanan and K.Vasudevan, "*C-Shaped slot loaded reconfigurable microstrip antenna*", IET Electronics Letters, Vol.42, No.6, pp.316-318, 2006.

8. **Gijo Augustin**, Shynu S.V., P.Mohanan, C.K. Aanandan and K.Vasudevan, "*Reactive loaded microstrip leaky wave antenna for low cost beam steering applications*", Microwave and Optical Technology Letters, Vol.48, No.11, pp.2299-2301, 2006.

9. Shynu S.V., **Gijo Augustin**, C.K.Aanandan P.Mohanan and K.Vasudevan, "*Design of a compact reconfigurable dual frequency microstrip antenna using varactor diodes*", Progress in electromagnetics research(PIER), Vol. 60,pp.197-205, 2006.

10. Shynu S.V., **Gijo Augustin**, C.K.Aanandan, P.Mohanan and K.Vasudevan, "*Development of a varactor controlled dual frequency reconfigurable microstrip antenna*", Microwave and Optical Technology Letters, Vol.46, No.4, pp.375-377, 2005.

11. **Gijo Augustin**, S.V. Shynu, C.K. Aanandan, P.Mohanan and K.Vasudevan, "*A Novel electronically scannable log periodic leaky wave antenna*", Microwave and Optical Technology Letters, Vol.45, No.2, pp. 163-165, 2005.

12. Shynu S.V., **Gijo Augustin**, C.K.Aanandan, P.Mohanan and K.Vasudevan, "*A reconfigurable dual frequency slot loaded microstrip antenna controlled by pin diodes*", Microwave and Optical Technology Letters, Vol. 44, No.4, pp.374-376, 2005.

13. Shynu S.V., **Gijo Augustin**, C.K. Aanandan, P.Mohanan and K.Vasudevan, "*A compact electronically reconfigurable dual frequency microstrip antenna for L Band applications*", International Journal on wireless and optical communications, Vol.2, No.2, pp.181-187, 2005

International Conference

1. **Gijo Augustin**,C.K. Aanandan, P.Mohanan, and K.Vasudevan "*A Compact wideband Antenna for modern wireless communication systems,*" Proceedings of URSI General Assembly 20008, Chicago, USA.

2. **Gijo Augustin**, P.C. Bybi, V.P. Sarin, M.S. Nisha, P.Mohanan, C.K. Aananda, K.Vasudevan, " *Compact dual band antenna for handheld wireless communication gadgets,*" Proceedings of IEEE Antennas and Propagation Society International Symposium 2008, Sandiago, USA.

3. **Gijo Augustin**, Sarin V.P., Nishamol M.S., Mohanan P. Aanandan C.K., Vasudevan K., "*A compact dual band planar antenna for IMT 2000 and WLAN applications",* Proceedings of IEEE Applied Electromagnetics Conference 2007, Kolkatta, India.

4. **Gijo Augustin**, Shynu S.V., Mohanan P., Aanandan C.K. and Vasudevan K., "*A Novel leaky wave Antenna capable of Electronics Beam steering",*Proceedings of IEEE Antennas and Propagation Symposium, pp. 4255-4258, 2006, New Mexico, USA.

5. Shynu S.V., **Gijo Augustin**, Mohanan P., Aanandan C.K. and Vasudevan K., *"Meandered slot arm loaded electronically tunable microstrip antenna using varactors"*, Proceedings of IEEE Antennas and Propagation Symposium, pp. 221-224, 2006, New Mexico, USA.

6. **Gijo Augustin**, Shynu S.V., Mohanan P., Aanandan C.K. and Vasudevan K., *"Wideband electronically scannable leaky wave antenna for low cost beam steering applications"*, Proceedings of Asia-Pacific Microwave Conference(APMC), December 2005, Suzhou, China.

7. Shynu S.V., **Gijo Augustin**, Mohanan P., Aanandan C.K. and Vasudevan K., *"Triple slot arm loaded reconfigurable dual frequency microstrip antenna using varactors"*, Proceedings of IEEE Antennas and propagation symposium, Vol. 2B, pp. 609-612, Washington, USA.

8. **Gijo Augustin**, Bybi P.C., Sarin V.P., Nishamol M.S., P.Mohanan, C.K. Aanandan and K.Vasudevan, *"Compact dual-band planar antenna for IMT-2000 application"*, Proceedings of International conference on Microwaves Antennas Propagation and Remote Sensing(ICMARS-2008), Jodpur, India

9. **Gijo Augustin**, Shynu S.V., C.K. Aananadan, P.Mohanan and K Vasudevan, *"An omni-directional multiband antenna for wireless networks"*, Proceedings of International Symposium on Antennas and Propagation (ISAP-2007), Niigata, Japan.

10. **Gijo Augustin**, Shynu S.V., C.K. Aananadan, P.Mohanan and K Vasudevan, *"A novel multiband antenna for modern short range wireless communication devices"*, Proceedings of International Symposium on Signals, Systems, and Electronics(ISSE 2007), Montreal, Quebec, Canada.

11. **Gijo Augustin**, Shynu S.V., C.K. Aananadan, P.Mohanan and K Vasudevan, *"Triangular Patch Loaded Monopole Antenna for Multiband Operation"*, Proceedings of IEEE Symposium on Antennas and Propagation, June2007, Honolulu,USA.

12. **Gijo Augustin**, Shynu S.V., C.K. Aananadan, P.Mohanan and K Vasudevan, *"Triple band antenna for wireless network systems"*, Proceedings of progress in Electromagnetics Symposium (PIERS 2007), March 2007, Beijing, China.

13. **Gijo Augustin**, Shynu S.V, C.K Aanandan, P. Mohanan and K. Vasudevan *"A novel omnidirectional antenna for WLAN modules"*, Proceedings of International conference on Microwaves,Antenna, Propagation and Remote Sensing(ICMARS-2006), December 2006, Jodpur, India.

14. **Gijo Augustin**, Shynu S.V, C.K Aanandan, P. Mohanan and K. Vasudevan, "*Triangular patch loaded monopole antenna for triple band operation*", Proceedings of Computers and devices for communication (CODEC-06), December 2006, Kolkata, India

15. Shynu S. V, **Gijo Augustin**, C.K Aanandan, P. Mohanan and K. Vasudevan. "*A Novel Reconfigurable Hexagonal Slot Loaded Microstrip Antenna*", Proceedings of URSI General Assembly- 2005 International Symposium, July-2005, New Delhi, India.

16. **Gijo Augustin**, Shynu S. V, C.K Aanandan, P. Mohanan and K. Vasudevan. "*An Electronically Scannable Wide Band Leaky – Wave Antenna Using Varactor Diodes*" Proceedings of URSI General Assembly, 23-29 October 2005, New Delhi, India.

National Conference

1. P.C.Bybi, **G. Augustin**, B.Jitha, Binu Paul, C.K. Aanandan, K Vasudevan and P.Mohanan "*Compact Drum Shaped Monopole Antenna for New Generation Mobile Applications*", Proc. Of National Symposium on Antennas and Propagation (APSYM2006), pp.249-252, Dec. 2006.

2. Shynu S.V, **Gijo Augustin**, C.K Aanandan, P. Mohanan and K. Vasudevan, "*A Varactor Controlled Electronically Reconfigurable Dual Frequency Microstrip Antenna*", Proceedings of Emerging and Futuristic Communication Systems-EFCoS-2005 Symposium, IETE, Bangalore, India.

3. **Gijo Augustin**, Shynu S.V., P Mohanan, C.K. Aanandan and K Vasudevan, "*Compact Multiband Antenna for Wireless Access Point*", Proc. of the National Symposium on antennas and propagation(APSYM-2006), 14-16 Dec. 2006, pp.207-212, Cochin University of Science and Technology, Kochi, India.

4. Deepthi K.V., Shameena V.A., **Gijo Augustin**, Binu Paul, C.K. Aanandan, K Vasudevan and P Mohanan, "*CREMA SOFT – Microwave Measurement Automation Software*", Proc. Of the National Symposium on Antennas and Propagation (APSYM- 2006), 14-16 Dec. 2006, pp.207-212, Cochin University of Science and Technology, Kochi, India.

5. Bybi P.C., **Gijo Augustin**, Jitha B, Binu Paul, C.K. Aanandan, K Vasudevan and P Mohanan, "*Compact Drum Shaped monopole antenna for new generation mobile applications*", Proc. of the National Symposium on antennas and propagation(APSYM-2006), 14-16 Dec. 2006, pp.207-212, Cochin University of Science and Technology, Kochi, India.

6. Shynu S.V, **Gijo Augustin**, C.K Aanandan, P. Mohanan and K. Vasudevan *"Electronically reconfigurable Dual Frequency Microstrip Antenna Using Varactor Diode"* Proc.of the National Symposium on Antennas and Propagation (APSYM-2004), 21-23 Dec. 2004, 127-130, Cochin University of Science and Technology, Kochi, India.

7. Shynu S.V, **Gijo Augustin**, C.K Aanandan, P. Mohanan and K. Vasudevan *"Electronically Reconfigurable Dual Frequency Microstrip Antenna Using Varactor Diode"* Proc. of the National Symposium on Antennas and Propagation (APSYM-2004), 21-23 Dec. 2004, 131-134, Cochin University of Science and Technology, Kochi, India.

Citations

1. Reference to the paper- **Gijo Augustin**, Shynu S.V., Mohanan P., C.K.Aanandan and K.Vasudevan, *"Compact dual band antenna for wireless access point"*,IET Electronics Letters,Vol.42, No.9, pp.502-503, 2006 in the paper- Ravi Kumar Joshi and Ayyangar Ranganath Harish, *"A modified Bow-Tie Antenna for Dual Band Applications"*, **IEEE Antennas and Wireless Propagation Letters**, Vol. 6, 2007.

2. Reference to the paper- **Gijo Augustin**, S.V. Shynu, C.K. Aanandan, P.Mohanan and K.Vasudevan, *"A Novel electronically scannable log periodic leaky wave antenna"*, Microwave and Optical Technology Letters, Vol.45, No.2, pp. 163-165, 2005..in the paper entitled *"A new bi faced log periodic printed antenna"* E. Avila Navarro, J.M. Blanes, J.A. Carrasco, C.Reig and E.A. Navarro, ***Microwave and Optical Technology Letters***, VOL. 48, No.2, 2006.

3. Reference to the paper-Shynu S.V., **Gijo Augustin**, C.K. Aanandan, P.Mohanan and K.Vasudevan, *"C-Shaped slot loaded reconfigurable microstrip antenna"*, IET Electronics Letters, Vol.42, No.6, pp.316-318, 2006 in the paper- C.W. Jung, Y.J. Kim, Y.E. Kim and F. De Flaviis, *"Macro-micro frequency tuning antenna for reconfigurable wireless communication systems"*, Vol. 43, No.4, **IET Electronics Letters**

4. Reference to the paper- Shynu S.V., **Gijo Augustin**, C.K. Aanandan, P.Mohanan and K.Vasudevan, *"C-Shaped slot loaded reconfigurable microstrip antenna"*, IET Electronics Letters, Vol.42, No.6, pp.316-318, 2006 in the paper- Giuseppe Ruvio Max.J.Ammann and Zhi Ning Chen, *"Wideband Reconfigurable Rolled Planar Monopole Antenna*, Vol. 55, No.6, **IEE Transactions on Antennas and Propagation.**

RESUME OF THE AUTHOR

GIJO AUGUSTIN

Research Scholar
CREMA, Department of Electronics
Cochin University of Science and Technology
Kochi, India – 682 022.
Tel   : +91 484 2576418
Fax   : +91 484 2575800
Mobile   : +91-9495383242
Email   : gijo@ieee.org

Objective:

To pursue research activities in the field of Multiband Antennas,
Reconfigurable Antennas for communication Systems

Education :

M.Sc. Industrial Electronics
Bharathidasan University, Trichy, India
Duration : 2002-2003
Score :81.86% - First Class and Fourth Rank

B.Sc. Electronics
M.G. University , Kottayam, India
Duration : 1997-2000
Score :77.97% - First Class with Distinction

Participation in National / International Conferences

Participated and presented research paper in XXIX URSI General Assembly, 7-16 August 2008, held at Chicago, Illinois, USA.

Participated and presented research paper in National Symposium on Antennas and Propagation(APSYM), December 2006 held at department of Electronics, CUSAT, India.

Publications:

International Journal   : 13
International Conference   : 16
National Conference   : 7

Academic Honours

Recipient of Young Scientist Award by International Union of Radio Science(URSI) in the year 2008.

Awarded Senior Research Fellowship by Council of Scientific and Industrial Research(CSIR), Government of India in the year 2007.

Recipient of University IIIrd Rank for M.Sc. Industrial Electronics examination conducted by the Bharathidasan University, India.

Teaching Experience:

Six Months of teaching experience for M.Sc. Applied Electronics at College of Applied Science, IHRD, Affiliated to M.G. University, Kottayam, India.

Computer Proficiency:

Programming Languages: Matlab, C, Fortran.
RF CAD Packages   : Ansoft HFSS, Zeland IE3D, CST Microwave-
                          Studio, Flomerics Microstripes.

Membership in Professional Bodies

Student Member- Institute of Electronics and Electrical Engineers (IEEE)

INDEX

A

Agilent E8362B 70
Ansoft HFSS 67, 83, 85, 92, 153, 157
Antenna Classification 7
antenna elements 19, 21, 65, 148, 152
Antenna Fabrication 69
Antenna Gain Measurement 74
antennas
    half wave length dipole 14
    printed sleeve dipole 162

B

boundary, air 134
Broad Classification of Antennas 8
Broadband CPW 62-3
Broadband Planar Antennas 24

C

calibration 74
CDMA 4-5, 46
Compact Antenna for Wireless Access
    Point Fig 159, 161
conformal grids FD-TD method 65
coplanar wave guide 15, 48, 81, 85, 87
Coupling Aperture in CPW-Fed
    Microstrip Antennas 26
CPW 15-17, 33-4, 49-50, 162
CPW-fed compact meandered patch
    antenna 44, 61
CPW Techniques in Antennas 48

D

directivity 10, 35

E

Early History of Radio 23

F

FDTD analysis 52, 66, 135
FEM (Finite Element Method) 83
Finite Element Method (FEM) 83
flared monopole 103-4, 117, 120-3,
    125, 130, 136, 138, 148, 152
flaring length 108, 110
flaring width 108-9, 144
frequency scannability 164, 169, 171

G

gain 7, 19-20, 32-3, 37, 52, 66, 74, 87,
    93, 108, 117, 127, 141
GPS antenna 19
ground plane dimensions 88, 101, 104,
    115, 152
Guglielmo Marconi 3, 5

H

HFSS (High Frequency Structure
    Simulator) 83, 135, 158, 171
Horn antenna 3, 7
HP 8510c 72
Horn Antenna 73

L

Leaky Wave Antenna 163, 169
Luebbers 52

M

Marconi 3